SYNTHESIS AND APPLICATIONS OF CAGED THIOLS FOR STUDYING PROTEIN PRENYLATION

A DISSERTATION

SUBMITTED TO THE FACULTY OF THE GRADUATE SCHOOL

OF THE UNIVERSITY OF MINNESOTA

BY

Daniel Abate Pella

IN PARTIAL FULFILLMENT OF THE REQUIREMENTS

FOR THE DEGREE OF DOCTOR OF PHILOSOPHY

ADVISOR:

Dr. Mark D. Distefano

FEBRUARY 2012

Acknowledgements

What a long, fulfilling journey this has been. When I first started this program I would have never imagined that I would grow this much academically and as a person.

I would like extend my sincere thanks to my advisor Mark Distefano for welcoming me in his group after a distressful period during my second year. His wisdom, knowledge and enthusiasm for science were a guiding light thoughout my graduate school career. I will do my best to emulate his passion and dedication for the field wherever I may head from this point on.

A big thank you goes to MDD group members past and present. Thank you for the scientific help you have provided me all these years as well as being a constant source of support. In particular, Dr. Dan Mullen for his help with peptide synthesis and Josh Ochocki for helping finish the biological experiments regarding caged inhibitors.

Thank you to my fellow organic division classmates, who were amazing friends and an invaluable source of support and laughter all these years and beyond.

I would like to thank my collaborators for all their assistance with regards to my projects. Thank you Dr. Nicholette Zeliadt for being an amazing partner to work with regarding the caged inhibitors project. Thank you Dr. Betsy Wattenberg for her scientific contributions and lab space and materials. Thank you Dr. David Blank and Dr. Benj Fitzpatrick for their help with the two-photon laser.

Finally, thank you so much to my family for being my greatest friends and cheerleaders throughout my journey. I would have never made it this far without your unconditional

love and support. My undying gratitude goes to my dad Sergio and mom Susana, my sister Paola, and my grandparents Marta and Italo.

To my dear family and friends,

My parents, Sergio and Susana

And all those who supported me along the way

My endless gratitude

for I would never made it this far without you

Abstract

Ras proteins are a subfamily of small GTP-binding proteins that are involved in various critical cellular processes including cell growth, survival and nuclear transport. It has been reported that roughly 30% of human cancers are derived from mutations of Ras, and prenylation is a key step that activates their oncogenicity. Commercial inhibitors of prenylation have been successful at arresting Ras activation and can be categorized into two families: farnesyltransferase inhibitors (FTIs) and geranylgeranyltransferase inhibitors (GGTIs). The focus of this thesis is to explore the use of photoremovable protecting groups (caging groups) to better understand the process of prenylation by caging the critical thiol residues of FTIs, GGTIs and peptides.

The caging group bromohydroxy coumarin (bhc) was covalently bound to the thiol of the FTI L-744,832 in order to inactivate the inhibitor. This caged FTI was evaluated with respect to its one- and two-photon uncaging kinetics and ability to release FTI upon photolysis. Analysis shows that bhc photolysis occurs more rapidly compared to the most frequently used family of nitrobenzyl-based cages, and that FTI is produced with good yields upon one- and two-photon excitation. Bhc-FTI was then tested on different cell lines in order to show that upon irradiation FTI is released that inhibits Ras farnesylation (observed via Western blot analysis), Ras membrane localization (detected by confocal microscopy), and downstream signaling (fibroblast morphology).

This same approach was utilized to cage FTI with bromohydroxy quinoline (BHQ). The covalent inactivation of FTI with BHQ was employed to cage the active site thiol (BHQ-FTI) and active site amine (BHQ-FTI urethane). Kinetic evaluation suggests that BHQ-FTI uncages faster than bhc-FTI but it produces little FTI upon photolysis due to the formation of unreactive photoproducts. Despite its poor yield, one photon cell experiments with BHQ-FTI resulted in the inhibition of Ras farnesylation, Ras membrane localization and downstream signaling. Quantitation and biological experiments with BHQ-FTI urethane are ongoing.

Peptides that are substrates of protein farnesyltransferase (PFTase) were caged with bhc and BHQ at their crucial thiol that is targeted for farnesylation. Upon one-photon photolysis peptides caged with BHQ show poor yields of free peptide while bhc-caged ones result in good peptide production. One of these caged peptides was subjected to an *in vitro* farnesylation assay to show that no farnesylation occurs, but upon one- and two-photon irradiation farnesylated peptide can be detected. Application of this caged peptide to study the mechanism of farnesylation via X-ray crystallography is under way.

Certain Ras proteins are alternatively geranylgeranylated and retain full function when farnesylation has been inhibited; as a result, GGTI-286 was caged with bhc to study this phenomenon. The synthesis of this GGTI and the inactivation of its thiol via covalent bonding with bhc is described here. The kinetic analysis of bhc-GGTI as well as its quantitation and biological testing are a work still in progress.

Table of Contents

List of Figures

List of Schemes

List of Tables

List of Abbreviations

ONB: *ortho*-nitrobenzyl, pHP: *para*-hydroxyphenacyl, BHQ: bromohydroxy quinoline, MNI: methoxy nitroindole, NCL: native chemical ligation, CNB: α-carboxy-2-nitrobenzyl, CDMNB: α-carboxy-4,5-dimethoxy-2-nitrobenzyl, PBS: phosphate buffer saline, HEPES: (4-(2-hydroxyethyl)-1-piperazineethanesulfonic acid, PFTase: protein farnesyltransferase, FPP: farnesyl diphosphate, HPLC: high pressure liquid chomatography, PKA: protein kinase, DMNB: 4,5-dimethoxy-2-nitrobenzyl, BCMACMOC: {7-[bis(carboxymethyl)amino]coumarin-4-yl}methoxycarbonyl, BCMCMOC: [7,8-Bis(carboxymethoxy)coumarin-4-yl]methoxycarbonyl, SPPS: solid-phase peptide synthesis, DMB: 3,5-dimethoxybenzoin, GTP: guanosine triphosphate, FTI: farnesyltransferase inhibitor, bhc: bromohydroxy coumarin, TEA: triethylamine, MOM: methoxymethyl, LC-MS: liquid chomatography-mass spectroscopy, EIC: extracted ion current, t_R: retention time, MS/MS: tandem mass spectrometry, SPS-PAGE: sodium dodecyl sulfate polyacrylamide gel electrophoresis, DMSO: dimethylsulfoxide, GFP: green fluorescent protein, DMF: dimethylformamide, CH3CN: acetonitrile, TFA: trifluoroacetic acid, DTT: Dithiotheitol, IAF: iodoacetamido fluorescein, DMAP: 4-dimethylaminopyridine, Fmoc: fluorenylmethyloxycarbonyl, BOP: benzotriazol-1-oxy-tris(demethylamino)phosphonium hexafluorophosphate, DIEA: diisopropylethylamine, PDB: protein data base, GGTase: geranylgeranyltransferase, GGTI: geranylgeranyltransferase inhibitor, HOBt: hydroxybenzotriazole, EDC: 1-ethyl-3-(3-dimethylaminopropyl)carbodiimide hydrochloride, Boc: di-tert-butyl dicarbonate, Trt: trityl, h: hour.

Preface

Please note the following:

Chapter 2: Reproduced in part with permission from D. Abate-Pella, N. A. Zeliadt, J. D. Ochocki, J. K. Warmka, T. M. Dore, D. A. Blank, E. V. Wattenberg, M. D. Distefano, Photochemical Modulation of Ras-Mediated Signal Transduction using Caged Farnesyltransferase Inhibitors: Activation via One- and Two-Photon Excitation. *Angew. Chem., Int. Ed.* **2011** (submitted).

Chapter 4: Reproduced in part with permission from D. Abate-Pella, M. D. Distefano, Photocaged Cysteine Peptides for studying Protein Farnesylation (in preparation).

Chapter 1. Background – Caged Thiols

1.1 Introduction

Photoremovable protecting groups, or caging groups, have been utilized over the last 30 years to study and manipulate biological phenomena[1-5]. This is accomplished by the covalent attachment of a caging moiety to a molecule of interest, thereby changing the reactivity of the functional group to which the covalent bond was attached. This process typically results in the masking or inactivation of the desired functional group; irradiation with light, however, releases the caging group and the original reactivity of the functional group is restored. Thus, caging groups are employed to control the spatiotemporal activity of biomolecules utilizing light as an orthogonal trigger[6-9].

Since the introduction of the *ortho*-nitrobenzyl (ONB) cage in the 1970's[10], the field has grown to include a plethora of protecting groups[11-14] (Fig. **1.1**) and the inactivation of several functional groups of biological relevance. To date, the most frequently used caging group is the aforementioned ONB cage and its derivatives (Fig. **1.1A**). Among their advantages are ease of installment, high sensitivity to one-photon excitation and ability to release product in good yields[15,16], though they are poor chromophores and possess poor sensitivity to two-photon excitation. The second most often employed caging family is the coumarin-4-ylmethyl and its derivatives (Fig **1.1B**). They have much better two-photon sensitivity and absorb light at longer wavelengths compared to

ONB groups, but they have lower quantum yields[17,18]. Other notable groups include phenacyl (pHP, Fig. **1.1C**), quinoline (BHQ, Fig. **1.1D**) and indole (MNI, Fig. **1.1E**), among others.

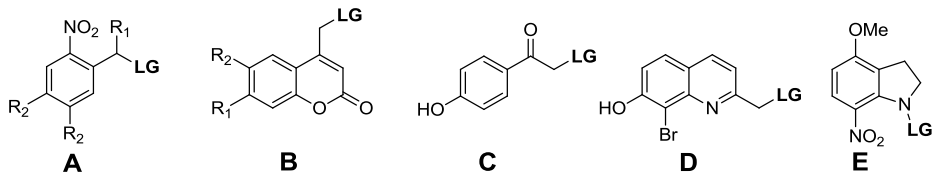

Figure 1.1. An overview of commonly used photoremovable protecting groups and their derivatives. A) *ortho*-nitrobenzyl (ONB) derivatives. B) coumarin derivatives. C) *para*-hydroxyphenacyl (pHP). D) bromohydroxy quinoline (BHQ). E) methoxy nitroindole (MNI). LG denotes leaving group.

Among the functional groups of biological importance most frequently masked are phosphates, carboxylates, alcohols and amines. Recent examples include caged ATP[19,20], caged glutamate[21-22], and caged drugs[23,24] and enzymes[25,26]. Biologically active thiols, chief among them cysteine, have not been studied in such depth compared to the aforementioned functional groups. The objective of this review is to highlight the uses and applications of caging groups for thiols available in literature.

1.2 *ortho*-nitrobenzyl cages for thiols

ONB cages have been employed to cage critical cysteine residues of peptides and proteins [27,28]. In an effort to improve the thiol protecting groups during native chemical

ligation[29] (NCL), Hagen and coworkers[30] applied the ONB-derived α-carboxy-2-nitrobenzyl (CNB) and α-carboxy-4,5-dimethoxy-2-nitrobenzyl (CDMNB) cages to peptides (Fig. **1.2**). Interestingly, it had been previously reported that the presence of amines promotes decarboxylation instead of photorelease[31] so photolysis of was carried out in two different buffers (amine-free PBS or amine-enriched HEPES) and the N-terminus of peptides **2a** and **2b** were acylated to study this process.

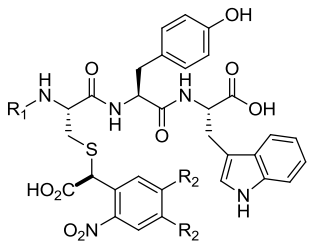

peptide	R1	R2
1a	H	H
1b	H	OMe
2a	Ac	H
2b	Ac	OMe

Figure 1.2. Model cysteine peptides **1** and **2** used for studying NCL caged with CNB and CDMNB groups. Adapted from Hagen et al[30].

Upon irradiation and analysis of the reaction products by HPLC, they found that the compound that produced the most free cysteine was peptide **2b** in PBS. Additionally, no traces of the decarboxylated product were found. In contrast, photolysis of peptide **1b** in HEPES yielded roughly twice as much decarboxylated peptide compared to free cysteine. Overall, CNB peptides **1a** and **2a** were the slowest to uncage while free N-terminus peptides **1a** and **1b** produced the most decarboxylated product. The compound which uncaged the fastest and produced the most free cysteine, **2b**, released cysteine with an efficiency of 74%. This data suggests that CDMNB is a better protecting group than CNB for thiols, but only in the absence of free amines. The reported quantum yields

(ϕ_{chem}) of the cysteine building blocks for peptides **1** and **2** were 0.04 and 0.07, respectively.

Degraw and coworkers also describe the caging of cysteine of peptides that are substrates of the enzyme protein farnesyltransferase (PFTase) with the CNB group[32]. Using ^{3}H-FPP (farnesyl diphosphate) to quantify the extent of reaction, they found that the peptide KKKSKTKC(CNB)VIM (**3**, Fig. **1.3A**) was not processed at all by PFTase while caged. However, upon irradiation with 365 nm light the released peptide behaved normally and was a substrate of the enzyme (Fig. **1.3B**). The quantum yield ϕ_{chem} of peptide **3** (0.16) is higher than that of those reported by Hagen[30], and the extent of reaction suggests a roughly 60% deprotection yield.

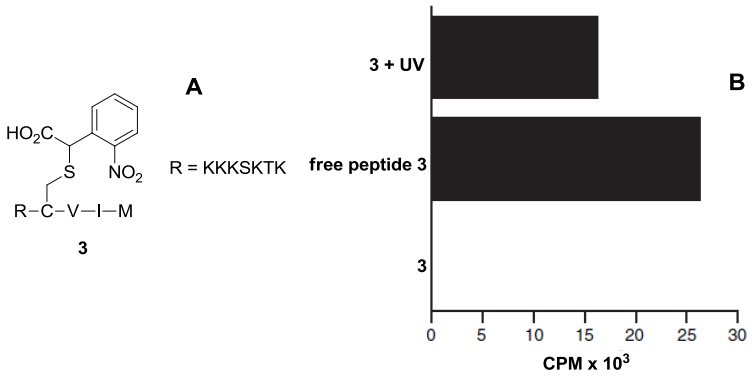

Figure 1.3. Photolysis and farnesylation of CNB-caged peptide **3**. A) Structure of KKKSKTKC(CNB)VIM. B) PFTase-catalyzed farnesylation of **3** before and after photolysis with ^{3}H-FPP. Adapted from Degraw et al[32].

The CNB group was utilized Ghosh and coworkers to cage protein participants in signaling pathways[33]. Cofilin proteins play a critical role in cell motility by

depolymerizing actin filaments. Cofilins are in turn regulated by the phosphorylation of Ser-3; however, Cys-3 mutants of cofilin are unable to be phosphorylated and thus remain constitutively active (**4**, Fig. **1.4A**). The CNB group was used to cage mutant cofilin (**5**) and utilizing an *in vitro* assay they were showed that caged mutant **5** did not depolymerize actin (Fig. **1.4B**). Conversely, irradiation with UV light restored the constitutive activity of mutant cofilin **4** (Fig. **1.4C**). An HPLC assay used to quantify the activity of irradiated caged mutant **5** compared to mutant **4** suggested that most (> 90%) of the activity was restored. The quantum yield of this caged protein is unkown.

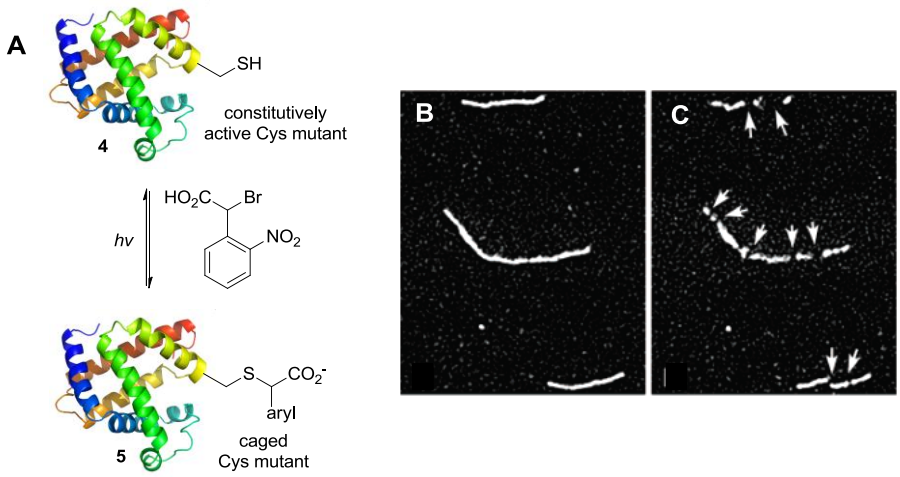

Figure 1.4. Caging of cofilin mutant with CNB. A) Design and synthesis of caged Cys mutant **5**. B) Rhodamine-labeled actin filaments are not cleaved by caged mutant **5**. C) Photolysis of **5** for 15 min restores mutant Cys cofilin activity. Cleavage sites are marked with arrows. Adapted from Gosh et al[33].

A critical cysteine residue in the catalytic subunit of cAMP-dependent protein kinase (PKA) was caged with three different derivatives of nitrobenzyl by Bayley et al[34]. For this study, they utilized the *ortho*-nitrobenzyl (ONB), dimethoxy-nitrobenzyl (DMNB)

and α-carboxy-nitrobenzyl (CNB) cages and analyzed their ability to inactivate PKA as well as their ability to restore activity upon irradiation. In this case, the best cage was ONB. Not only did ONB-caged PKA have the least residual activity in an *in vitro* assay but it also was able to restore the most activity to the protein after irradiation. In order for a caged signaling protein to be useful it must show at least a 10-fold increase in activity upon photolysis, and DMNB- and CNB-caged PKA only increased activity by 2-3 fold compared to 20-30 fold by ONB. Additionally, the effect of pH on uncaging was also tested by Bayley and coworkers. The extent of photolysis at 312 nm irradiation was more efficient at slightly acidic conditions (pH 6) compared to slightly basic ones (pH 8.5), though the specific catalytic activity increase was the same at both pHs. However, the differences in the extent of photolysis led to a much higher quantum yield (ϕ_{chem}) in acidic conditions (0.84) compared to basic ones (0.14).

1.3 Coumarin cages for thiols

The use of coumarins to photoinactivate thiols has only been studied in recent years, and mostly by the Hagen and Distefano groups. The coumarin derivative {7-[bis(carboxymethyl)amino]coumarin-4-yl}methoxycarbonyl (BCMACMOC, Fig. **1.5**) was employed to cage a cysteine residue (**6**) and an aromatic thiol (**7**)[35]. However, this was accomplished by masking them as thiocarbonates rather than thioethers.

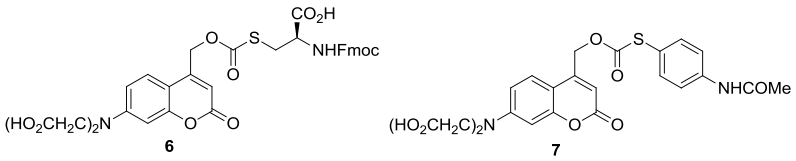

Figure 1.5. Structures of caged cysteine **6** and aromatic thiol **7** with the coumarin BCMACMOC.

Both compounds were found to be highly soluble in buffered solutions (up to 1 mM concentrations) due to the incorporation of carboxylic acids onto the coumarin amine. Unfortunately, caged aromatic thiol **7** was not very stable in aqueous systems and 10% was hydrolyzed in the dark after a 24 h period. Their relevant photochemical properties are listed in Table **1.1**. Upon photolysis, both **6** and **7** uncage via a solvent-assisted heterolysis and are released as thiocarbonates which subsequently undergo decarboxylation. Though the actual photolysis step was estimated to be fast (ns scale) decarboxylation is the rate-limiting step which occurs much more slowly (~100 s), a potential drawback that may limit the applicability of the BCMACMOC group to thiols. On a positive note, both compounds possess low fluorescence, high molar absorptivity (ε), and can be uncaged with wavelengths higher than 430 nm which is non-damaging. This study did not include the yields of the resulting thiols upon photolysis in its scope.

Compound	$\lambda_{max\ abs}$ (nm)	ε_{max} (M^{-1} cm^{-1})	ε_{430} (M^{-1} cm^{-1})	ϕ_{chem}	$\lambda_{max\ f}$ (nm)	ϕ_f
6	383	18,500	2,000	0.06	480	0.052
7	383	18,700	2,700	0.09	497	0.011

Table 1.1. Photochemical properties of caged thiols **6** and **7**. Long-wavelength absorption maxima, λ_{max}, extinction coefficients at the absorption maxima and at 430 nm, ε^{max} and ε^{430}, photochemical quantum yields, ϕ_{chem}, fluorescence maxima, $\lambda_{max\ f}$, and fluorescence quantum yields, ϕ_f. Adapted from Hagen et al[35].

In effort to improve the water solubility of cages, Hagen and coworkers reported the synthesis of a caged cysteine utilizing a different coumarin derivative, [7,8-Bis(carboxymethoxy)coumarin-4-yl]methoxycarbonyl (BCMCMOC), in addition to another cysteine with their previously explored coumarin cage BCMACMOC[36]. Both of these caged cysteines masked thiols as a thiocarbonate rather than a thioether (Fig. **1.6A**) and were utilized as building blocks in solid-phase peptide synthesis (SPPS) to incorporate the photoremovable moieties into peptides. Interestingly BCMCMOC cysteine **8** has a very different absorption spectrum compared to BCMACMOC cysteine **9**, with a λ_{max} of 324 nm and negligible absorptivity past 390 nm while **9** has a λ_{max} of 385 nm and is able to absorb up to 450 nm. These results suggested that these caged cysteines could be deprotected in a wavelength-selective fashion. A solution of a binary mix of caged cysteines **8** and **9** were first irradiated at 402 nm and subsequently at 325 nm and the amount of cysteine produced was quantified (Fig. **1.6B**). As predicted, photolysis at 402 nm deprotected only cysteine **8** while photolysis at 325 deprotected the

remaining cysteine **9**. However, while photolysis of **8** produced cysteine with 60% efficiency uncaging **9** liberated cysteine with a lesser 40% yield.

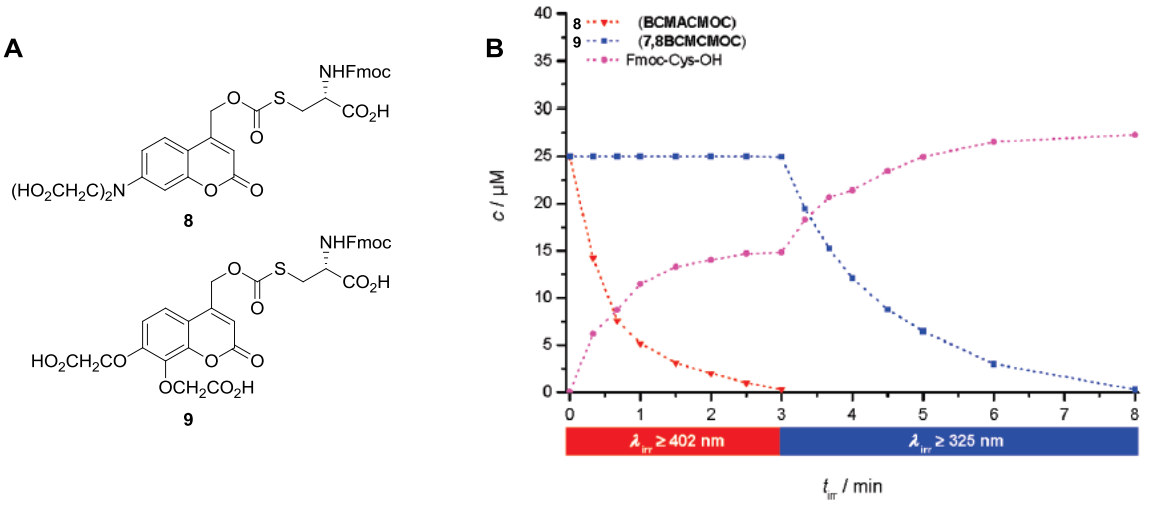

Figure 1.6. Caging of Fmoc-cysteine with the photoremovable coumarins BCMACMOC (**8**) and BCMCMOC (**9**). A) Structures of caged cysteines used in this study. B) Wavelength-selective photolysis of a mixture of **8** and **9**. Adapted from Hagen et al[36].

Caged cysteines **8** and **9** were then used to cage the Cys^1 and Cys^8 residues of the model peptide resact, the sperm attractant in the sea urchin *Arbacia punctulata*. Irradiation at 402 nm removed the BCMACMOC group from Cys^1, but upon deprotection an S-to-S acyl transfer occurred and an equimolar mixture of Cys^1 and Cys^8 BCMCMOC was obtained (Fig. **1.7**). This result limits the applicability of two different photolyzable thiocarbonates for selective deprotection, though further irradiation with 325 nm light removed the remaining BCMCMOC groups.

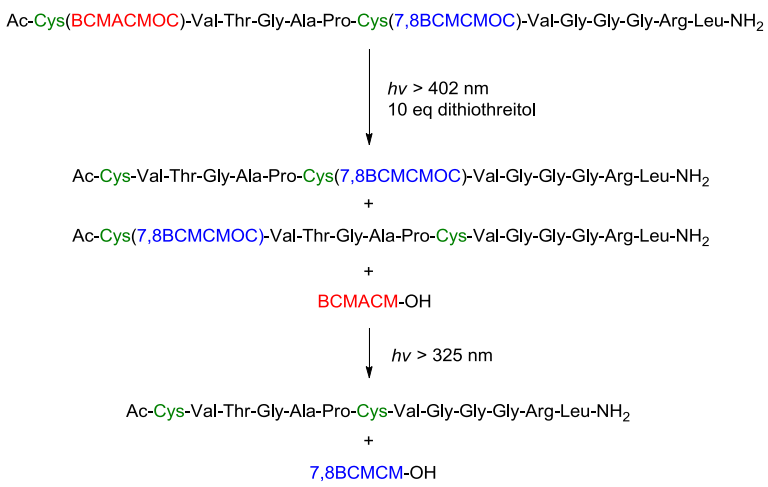

Figure 1.7. Wavelength-selective deprotection of Ac^0-Cys^1(BCMACMOC),Cys^8(7,8BCMCMOC)-resact. Adapted from Hagen et al[36]

1.4. Phenacyl cages for thiols

The first example of a phenacyl cage used to inactivate thiols was reported by Pei and coworkers in 1999 to study tyrosine phosphatases[37]. Among the derivatives utilized to generate caged cysteine residues was *p*-hydroxy phenacyl (pHP, Fig. **1.8A**). A pHP cage was tested for its ability to restore activity to inactivated enzyme **10** after photolysis at 350 nm (Figs. **1.8B, C**). While the activity of the full enzyme (SHP-1) was restored to ~80% the catalytic domain of the protein (SHP-1(ΔSH2)) was only restored to ~30% activity. The other phenacyl derivatives tested resulted in lower % activity recoveries compared to pHP. No further photochemical analyses were conducted in this study.

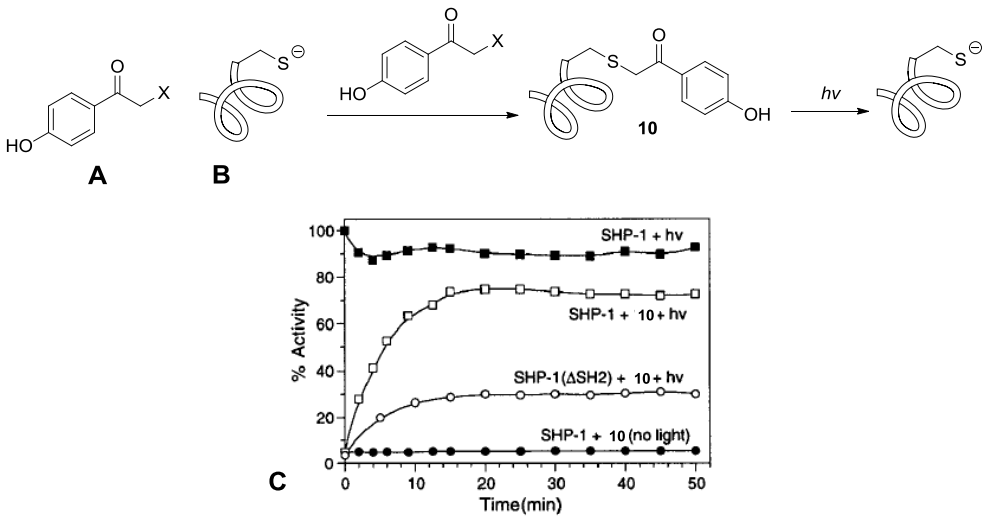

Figure 1.8. Photochemical inactivation of a tyrosine phosphatases. A) Structure of the pHP caging group. B) Inactivation and photorelease of a tyrosine phosphatase by phenacyl derivatives. C) An i*n vitro* assay was used to show that enzyme **10** is inactive (bottom trace), while UV irradiation restores activity to the enzyme (middle traces) with a ~80% efficiency compared to wild type enzyme (top trace). Adapted from Pei et al[37].

A more in-depth study of the properties of pHP as a thiol caging group was conducted by Goeldner et al[38]. pHP was utilized to cage a cysteine derivative (**11**), a thymidine nucleoside derivative (**12**), and the antioxidant glutathione (**13**, Fig. **1.9**). The synthesis of these caged biomolecules was reported with high yields (80-90%) due to the ease of installment of pHP as an α-bromide acetophenone.

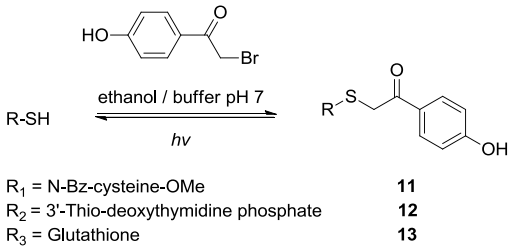

Figure 1.9. Thiol derivatives inactivated with the pHP group. Adapted from Goeldner et al[38].

The photolysis reactions of **11**, **12**, and **13** were carried out at 312 nm and monitored by HPLC and MS. The results of these reactions are summarized in Table **1.2**. In the case of caged coumpounds **11** and **12** the resulting free thiols were recovered in high yields (60-70%). Additionally, three other photolysis products were detected in all three reactions: the expected pHP derived *p*-hydroxyphenyl acetic acid and *p*-hydroxy acetophenone, as well as *p*-hydroxyphenylacetic thioester derived from the biomolecules. These thioesters were produced in 20-30% yield, lowering the efficacy of thiol released. A quantum yield of 0.085 was calculated for thymidine **12**, lower than ones reported for carboxylates and phosphates.

Compound	**11**	**12**	**13**
Photolytic products	%	%	%
RSH (RSSR)	60 (5)	71	ND
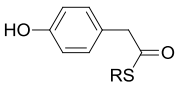	30	29	23

Table 1.2. Products and yields obtained from photolysis of caged thiols **11**, **12** and **13**. Adapted from Goeldner et al[38].

1.5 Benzoyl cages for thiols

The benzoyl group and its derivatives have generally been used to inactivate alcohols, and to date there are only two examples of caged thiols in the literature using this group. As a result, very little is known about the photochemical properties of these thiols. In 1995 Bradley and Pirrung reported the caging of phenylmethylthiol (**14**) with 3,5-dimethoxybenzoin (DMB, Fig. **1.10A**) as a thiocarbonate, resulting in a high deprotection yield (95%) though photolysis was conducted in an organic solvent (benzene)[39]. No further measurements with this caged thiol were performed in this study.

Porter and coworkers reported the synthesis of a caged organic thiol (**15**), masked as a thioester, utilizing 2-benzoylbenzoic acid[40] (Fig. **1.10B**). In order for photolysis to occur

with this moiety, there must be a hydrogen donor (alcohols) or electron donors (amines) present in solution which may not be ideal in all biological setups. Efficiency yields for this compound were high, and 60% of free thiol was recovered as well as 20% of material as a disulfide (according to NMR analysis) when photolyzed in the presence of cyclohexylamine. Additionally, two species related to the 2-benzoylbenzoic acid cage were found: 3-phenylphthalide and diphthalidyl. Overall, more studies must be carried out to determine the applicability of benzoyl groups to cage thiols.

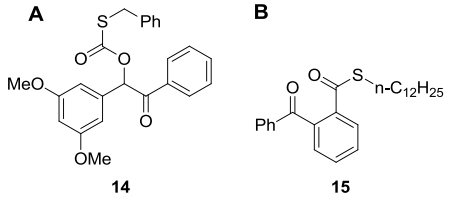

Figure 1.10. Benzoyl-derived caged thiols. A) 3,5-dimethoxybenzoin (DMB) caged phenylmethylthiol (**14**). B) 2-benzoylbenzoic acid caged aliphatic thiol **15**.

1.6 References

1. M. Goard, G. Aakalu, O. D. Fedoryak, C. Quinonez, J. St. Julien, S. J. Poteet, E. M. Schuman, T. M. Dore, *Chem. Biol*. **2005**, *12*, 685.

2. M. E. Vazquez, M. Nitz, J. Stehn, M. B. Yaffe, B. Imperiali, *J. Am. Chem. Soc.* **2003**, *125*, 10150.

3. M. C. Pirrung, S. J. Drabik, J. Ahamed, H. Ali, *Bioconjugate Chem*. **2000**, *11*, 679.

4. R. O. Schonleber, J. Bendig, V. Hagen, B. Giese, *Bioorg. Med. Chem*. **2002**, *10*, 97.

5. J. Gjerstad, E. C. Valen, D. Trotier, K. Doving, *Neuroscience* **2003**, *119*, 193.

6. J. Goedhart, T.W. J. Gadella, Jr., *Biochemistry* **2004**, *43*, 4263.

7. C. P. Salerno, D. Magde, A. P. Patron, *J. Org. Chem*. **2000**, 65, 3971.

8. S. Yagai, T. Karatsu, A. Kitamura, *Chem. Eur. J.* **2005**, *11*, 4054.

9. J. C. Cruz, M. Thomas, E. Wong, N. Ohgami, S. Sugii, T. Curphey, C. C. Y. Chang, T.-Y. Chang, *J. Lipid Res*. **2002**, *43*, 1341.

10. J. H. Kaplan, B. Forbush III, J. F. Hoffman, *Biochemistry* **1978**, *17*, 1929.

11. M. Goeldner, R. Givens, *Dynamic Studies in Biology*, Wiley-VCH, Weinheim, **2005**.

12. G. Marriott, *Methods in Enzymology*, Vol. *291*, Academic Press, San Diego, **1998**.

13. S. R. Adams, R. Y. Tsien, *Annu. Rev. Physiol*. **1993**, *55*, 755.

14. A. P. Pelliccioli, J. Wirz, *Photochem. Photobiol. Sci.* **2002**, *1*, 441.

15. K. R. Gee, R. Wieboldt, G. P. Hess, *Proc. Natl. Acad. Sci. U. S. A.*, **1994**, *91*, 8752.

16. D. D. Young, A. Deiters, *Bioorg. Med. Chem. Lett*., **2006**, *16*, 2658.

17. T. Furuta, M. Iwamura, *Methods Enzymol*. **1998**, *291*, 50.

18. T. Furuta, S. S. H. Wang, J. L. Dantzker, T. M. Dore, W. J. Bybee, E. M. Callaway,W. Denk, R. Y. Tsien, *Proc. Natl. Acad. Sci. USA* **1999**, *96*, 1193.

19. R. S. Givens, C.-H. Park, Tetrahedron Lett. **1997**, *37*, 6259.

20. J. W. Wootton, D. R. Trentham, *NATO ASI Ser., Ser. C* **1989**, *272*, 277.

21. D. L. Pettit, S. S.-H. Wang, K. R. Gee, G. J. Augustine, *Neuron* **1997**, *19*, 465.

22. K. R. Gee, L. W. Kueper, J. Barnes, G. Dudley, R. S. Givens, *J. Org. Chem.* **1996**, *61*, 1228.

23. H. J. Montgomery, B. Perdicakis, D. Fishlock, G. A. Lajoie, E.Jervis, J. G. Guillemette, *Bioorg. Med. Chem*. **2002**, *10*, 1919.

24. B. Perdicakis, H. J. Montgomery, G. L. Abbott, D. Fishlock, G. A. Lajoie, J. G. Guillemette, E. Jervis, *Bioorg. Med. Chem*. **2005**, *13*, 47.

25. F. G. Cruz, J. T. Koh, K. H. Link, *J. Am. Chem. Soc.* **2000**, *122*, 8777.

26. D. D. Young, M. O. Lively, A. Deiters, *J. Am. Chem. Soc.* **2010**, *132* , 6183.

27. A. Blanc, C. G. Bochet, *J. Org. Chem*. **2003**, *68*, 1138 – 1141.

28. S. R. Adams, J. P. Y. J. Kao, R. Y. Tsien, *J. Am. Chem. Soc*. **1989**, *111*, 7957.

29. P. E. Dawson, S. B. H. Kent, *Annu. Rev. Biochem*. **2000**, *69*, 923.

30. N. Kotzur, B. Briand, M. Beyermann, V. Hagen *Chem. Commun*. **2009**, *172*, 3255.

31. A. Barth, S. R. Martin, J. E. T. Corrie, *Photochem. Photobiol. Sci*. **2006**, *5*, 107.

32. A. J. DeGraw, M. A. Hast, J. Xu, D. Mullen, L. S. Beese, G. Barany, M. D. Distefano, *Chem. Biol. Drug. Des*. **2008**, *72*, 171.

33. M. Ghosh, I. Ichetovkin, X. Song, J. S. Condeelis, D. S. Lawrence *J. Am. Chem. Soc.* **2002**, *124*, 2440.

34. C.-Y. Chang, T. Fernandez, R. Panchal, H. Bayley, *J. Am. Chem. Soc*. **1998**, *120*, 7661.

35. V. Hagen, B. Dekowski, N. Kotzur, R. Lechler, B. Wiesner, B. Briand, M. Beyermann *Chem. Eur. J.* **2008**, *14*, 1621.

36. N. Kotzur, B. Briand, M. Beyermann, and V. Hagen, *J. Am. Chem. Soc.* **2009**, *131*, 16927.

37. G. Arabaci, X.-C. Guo, K. D. Beebe, K. M. Coggeshall, D. Pei, *J. Am. Chem. Soc*. **1999**, *121*, 5085.

38. A. Specht, S. Loudwig, L. Peng, M. Goeldner, *Tetrahedron Lett.* **2002**, *43*, 8947.

39. M. C. Pirrung, J.-C. Bradley, *J. Org. Chem*. **1995**, *60*, 1116.

40. P. B. Jones, M. P. Pollastri, N. A. Porter, *J. Org. Chem*. **1996**, *61*, 9455.

Chapter 2. Photochemical Modulation of Ras-Mediated Signal Transduction Using the Farnesyltransferase Inhibitor bhc-L-744,832

2.1 Introduction

The creation of caged molecules involves the attachment of protecting groups to biologically active compounds such as ligands, substrates, and drugs that can be removed under specific conditions. Photoremovable protecting groups are the most commonly utilized due to their ability to be removed with high spatial and temporal resolution[1-7]. Such molecules have been used in a plethora of biochemical studies ranging from probing the mechanisms of enzymatic reactions[8, 9] to controlling cellular activity[10-13]. Ras proteins are small GTP-binding proteins that belong to a superfamily of regulatory polypeptides that participate in key signal transduction pathways and regulate such diverse cellular phenomena as nuclear transport, cytoskeletal structure and cell division[14]. Given the critical roles of Ras proteins, it would be useful to have small molecules that could inhibit Ras-mediated signaling in a controllable manner; such compounds would be useful for a variety of cellular studies and could complement other approaches including antisense and RNAi strategies. For proper function, Ras proteins must be post-translationally modified by the enzyme protein farnesyltransferase (PFTase)[15, 16]. Because of this requirement, the growth of cancer cells that signal via oncogenic forms of Ras can be arrested by inhibiting PFTase[17-19]; as a result, a large number of farnesyltransferase inhibitors (FTIs) have been developed including several that are

available commercially including L-744,832 (**1**)[20-25]. Hence, in principle, caged inhibitors of PFTase could be used to modulate Ras function. To design such compounds, we reasoned that functionalization of the thiol group present in **1** would greatly reduce the affinity of the compound for PFTase. Crystallographic data suggests that the thiol of **1** forms an important interaction with a Zn(II) ion positioned within the active site[26, 27] and binding measurements with related peptides show a significant decrease in affinity upon alkylation of the corresponding thiol[28]; metal substitution experiments are also consistent with this mode of substrate-metal coordination[29]. For the caging moiety, we elected to explore the utility of the thioether-linked bhc group[30]. While bhc has not previously been employed for sulfur protection, it was chosen in lieu of others[31-35] because it has been shown to be useful for both one- and two-photon uncaging processes.

2.2 Research Objectives

We have synthesized a caged inhibitor of PFTase, bhc-FTI (**2**, Fig. **2.1**). This was accomplished by covalently linking bhc to the active site thiol of the FTI. This thioether-caged FTI **2** should be a worse inhibitor of PFTase compared to commercially available **1**. As a result, Ras should remain farnesylated and localized to the cell membrane in the presence of **2** and Ras-related signal transduction pathways should remain active. Irradiation of **2** with light, however, releases active FTI to inhibit the farnesylation of Ras which in turn localizes Ras to the cytoplasm of the cell, unable to carry out its regular

downstream signaling. One-photon irradiation processes are more effective at uncaging molecules compared to two-photon ones, but we are interested in two-photon processes which allow deeper tissue penetration and minimize damage to biological samples. Described here are the photochemical characterization of **2** and its applications to control the activity of Ras in cells via one- and two-photon processes.

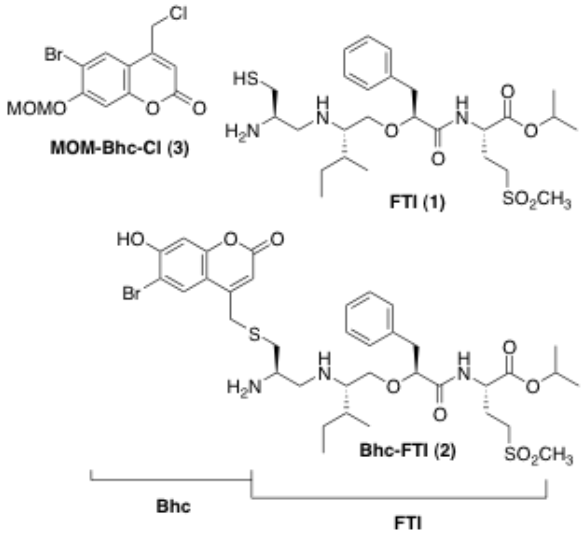

Figure 2.1. The FTI L-744,832 (**1**) was caged using the MOM-protected chloride MOM-bhc-Cl (**3**) to obtain inactivated inhibitor bhc-FTI (**2**).

2.3 Results and Discussion

2.3.1 Synthesis of bhc-FTI

To prepare the caged FTI analogue (**2**), a MOM-protected precursor of the photoremovable bhc protecting group was synthesized (Scheme **2.1**). MOM-bhc-Cl (**3**) was prepared from the known compound bhc-Cl[30] by reacting it with chloromethyl methyl ether in the presence of TEA to afford the desired ether in 86% yield. This protected chloride was then used to alkylate the active site thiol of FTI **1** via zinc acetate and acidic pH conditions to ensure that the thiol is selectively alkylated as well as minimize the formation of FTI disulfide dimer. This reaction was left stirring for 48 hours before purification by HPLC to yield MOM-bhc-FTI (**5**) in 62% yield. The last step in the synthesis is to remove the MOM ether to activate the bhc cage; this was accomplished through acidolytic cleavage by the addition of Reagent K for 2 hours before HPLC purification to afford the caged inhibitor bhc-FTI (**2**) in 95% yield.

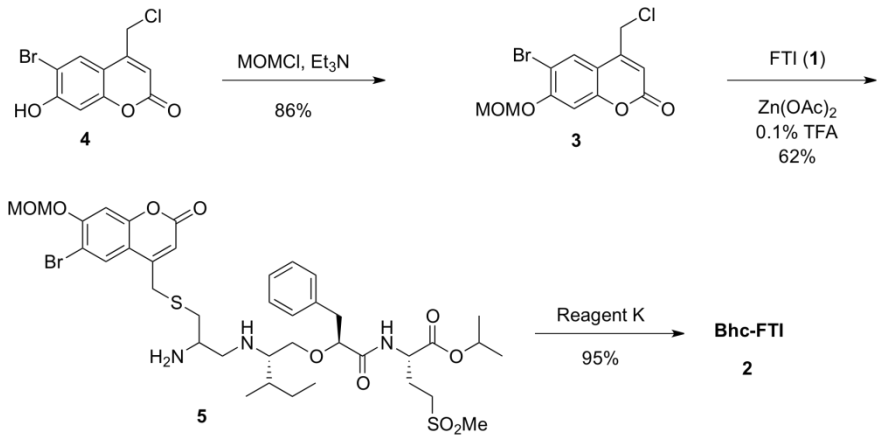

Scheme 2.1. Synthesis of bhc-FTI (**2**).

2.3.2 One-photon properties of bhc-FTI

Initially, the photolysis of the caged drug in buffered aqueous solution was studied by following the disappearance of starting material upon irradiation via HPLC analysis since the FTI product has little UV absorbance. Those experiments yielded a half life for bhc-FTI of approximately 12 seconds in a standard Rayonet photoreactor, indicating that this molecule reacts rapidly compared with *o*-nitrobenzyl protected thiols. A quantum yield of 0.09 for bhc-FTI uncaging was measured, which is typical of other bhc-caged compounds[30-32]. To characterize the products of photolysis, LC-MS experiments were performed (Fig. **2.2**). Analysis of the reaction mixture from the photolysis of bhc-FTI (**2**) revealed the disappearance of starting material **2** (t_R = 19 min, m/z = 812, Fig. **2.2A**) and the production of an ion at m/z = 560.3 (t_R = 16.5 min, Fig. **2.2B**) in the extracted ion current chromatograms consistent with the production of FTI (**1**); this was further substantiated via MS/MS analysis where the fragmentation of the new product was found to be identical with that of FTI (**1**). MS analysis of the photolysis reaction mixture also revealed the presence of a new species with identical mass as **2** (m/z = 812) but with a different retention time (t_R = 20.3 min, Fig. **2.2C**). MS/MS analysis of that compound showed a mass spectrum distinct from that of **2**. We tentatively assign this isomeric species to be one in which the bhc group has undergone S to N migration via a photogenerated carbocationic intermediate.

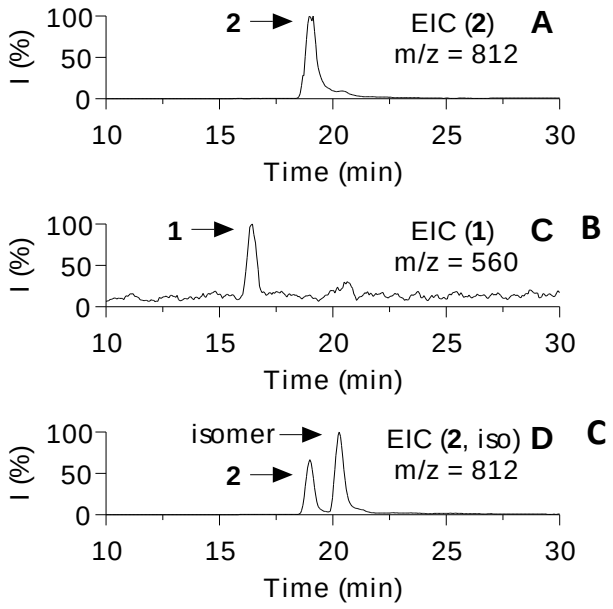

Figure 2.2. Analysis of uncaging of bhc-FTI (**2**) by photolysis at 365 nm. A) LC-ESI-MS of **2** prior to photolysis showing EIC (m/z = 812) of pure **2**. B) LC-ESI-MS of **2** after photolysis showing EIC (m/z = 560) of **1** produced from photolysis of **2**. C) LC-ESI-MS of **2** after photolysis showing EIC (m/z = 812) of **2** and photorearranged **2**.

To quantify the efficiency of photocleavage, an HPLC-based method was developed. The amount of **2** present was evaluated by its UV absorbance while the amount of **1** produced was determined via derivatization with a thiol-reactive fluorescein acetamide reagent. A plot showing the disappearance of **2** and concomitant appearance of **1** as a function of photolysis time (Fig. **2.3**) shows that **2** uncages with an efficiency of greater than 70%. These results indicate that bhc can be used to mask the thiol of FTI **1** and that it can be efficiently removed upon photolysis suggesting that it is suitable for the caging of biologically relevant thiol-containing molecules.

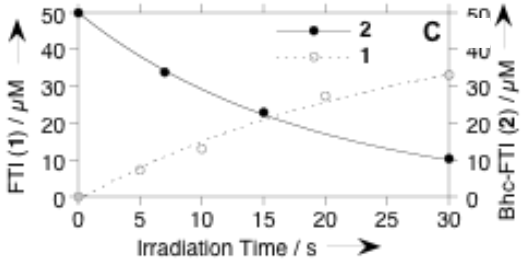

Figure 2.3. Quantitation via HPLC of starting material (**2**) disappearance and product (**1**) formation as a function of irradiation time at 365 nm. Bhc-FTI (**2**) was quantified using its coumarin absorption while FTI (**1**) was quantified by derivatization with a fluorescent maleimide. The data was fit to a simple first order process.

2.3.3 Applications of bhc-FTI to control cellular processes

Next, the biochemical effects of uncaging FTI inside cells were examined. First, the effect of FTI release on Ras processing was studied since it has been previously established that inhibition of PFTase results in blockage of subsequent processing events (proteolysis and methylation) that can be easily detected by Western blot analysis (Fig. **2.4**)[37, 38]. Photolysis at 365 nm of H-Ras MCF10A cells suspended in media in the presence of bhc-FTI (**2**, 2.5 μM) resulted in a significant decrease in the amount of processed Ras and a concomitant increase in the level of unprocessed Ras (Lane 4); these changes were similar to those observed with cells treated directly with FTI (Lane 5). No changes were observed in Ras processing when the cells were not irradiated (Lane 3) or irradiated without bhc-FTI (**2**) (Lane 2). Farnesylation of Ras is required for oncogenic mutants to cause cellular transformation because the lipid modification causes

localization of the enzyme to the plasma membrane where it can interact with additional proteins and stimulate downstream signal transduction pathways. Accordingly, the levels of phosphorylated erk, a known product of activated Ras, were monitored via Western blot analysis[39]. Untreated cells (Fig. **2.4**, Lane 1) or cells exposed to bhc-FTI without irradiation (Lane 3) show significant levels of phosphorylated erk; in contrast, cells irradiated in the presence of bhc-FTI (Lane 4) or those exposed to free FTI (Lane 5) manifested significantly decreased levels of phosphorylated erk. Overall, these results provide biochemical evidence that uncaging of bhc-FTI results in the inhibition of Ras processing and downstream events and suggest that Ras mediated signaling can be modulated with such a caged inhibitor.

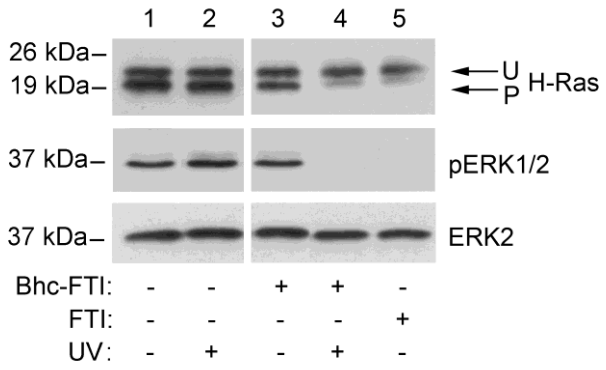

Figure 2.4. Effect of bhc-FTI (**2**) UV-mediated uncaging on H-Ras prenylation and ERK1/2 phosphorylation state in MCF10A cells. H-Ras MCF10A cells were treated with 2.5 μM FTI (**1**) for 120 min or 2.5 μM Bhc-FTI (**2**) for 30 min and exposed to UV as indicated for 4 min in a Rayonet photoreactor. After 24 h, whole cell lysates were prepared. For the H-Ras immunoblot, 40 μg of protein was resolved by 15% SDS-PAGE. For the p-ERK1/2 immunoblot, 30 μg of protein was resolved by 10% SDS-PAGE. Total ERK2 levels were measured as a negative control since they should not change in response to treatment with the FTI. Note the faster mobility of processed Ras (P) compared with unprocessed Ras (U). Lane 1) Vehicle (0.1% DMSO (v/v)). Lane 2)

Vehicle (0.1% DMSO (v/v)) followed by UV. Lane 3) Bhc-FTI (**2**). Lane 4) Bhc-FTI (**2**) followed by UV. Lane 5) FTI (**1**).

Ultimately, the desired application of caged FTIs is to use them to control cellular properties. To assess their utility for this purpose, we first examined the ability of bhc-FTI (**2**) to alter Ras localization in live cells. This was accomplished using a cell line that expresses H-Ras as an N-terminal GFP fusion (GFP-Ras)[40]. Under normal conditions, GFP-Ras is farnesylated and hence localizes to the plasma membrane; in the presence of FTI (**1**), prenylation is inhibited resulting in cytosolic accumulation. Confocal microscope images from such experiments using bhc-FTI (**2**) are shown in Fig. **2.5**. Treatment of MDCK cells expressing GFP-Ras with bhc-FTI without irradiation (Fig **2.5C**) results in membrane localization similar to the untreated control sample (Fig **2.5A**). However, irradiation of the cells treated with bhc-FTI (Fig. **2.5D**) shifts the distribution of GFP-Ras to one that is more cytosolic, similar to what is obtained upon treatment with free FTI (Fig. **2.5B**).

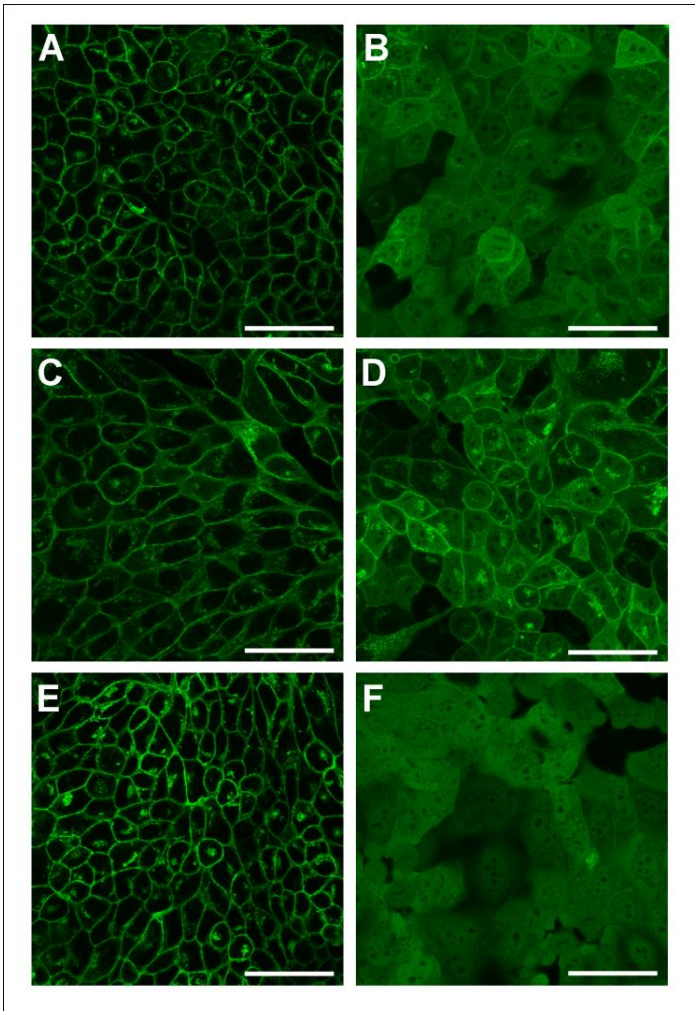

Figure 2.5. GFP-H-Ras localization in MDCK cells treated with bhc-FTI (**2**) after 365 nm irradiation. Treatments were as follows: A) Vehicle (0.2% DMSO (v/v)). B) 1 µM FTI (**1**). C) 10 µM bhc-FTI (**2**), no irradiation. D) 10 µM bhc-FTI (**2**) plus irradiation. E) No treatment plus irradiation. F) 5 µM FTI (**1**). 24 h after treatment with the compounds indicated, cells in panels D and E were then exposed to UV (365 nm) for 15 min. All samples were incubated for an additional 24 h prior to imaging with a confocal microscope, 60x objective. Scale bar = 50 mm. (note that panel B image captured with 40x objective). For these experiments, photolysis reactions were performed using a UV transilluminator.

These results provide direct evidence that caged FTIs can be used to modulate Ras localization in live cells. To observe the downstream effects of FTI release on cellular properties and complement the aforementioned biochemical results, experiments using a fibroblast cell line were conducted (Fig. **2.6**). Ciras-3 cells constitutively express an oncogenic Ras gene resulting in an aberrant smaller, rounded cell morphology (Fig. **2.6A**). Treatment of these cells with free FTI (**1**) (Fig. **2.6B**) results in their conversion to a larger and more spread phenotype. No change in morphology was observed with cells treated with bhc-FTI without irradiation (Fig. **2.6C**). However, upon photolysis in the presence of bhc-FTI (**2**) (Fig. **2.6D**), the cells take on the characteristic spread appearance signaling that the transforming effect of oncogenic Ras has been abrogated.

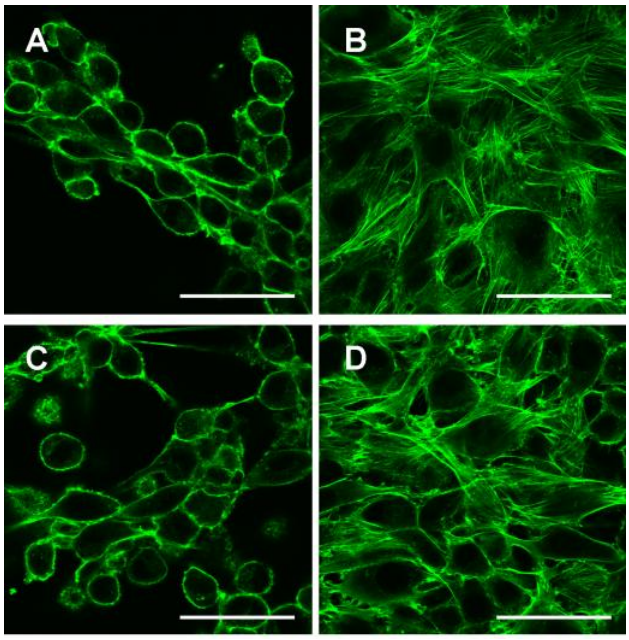

Figure 2.6. Morphology of Ciras-3 fibroblasts treated with bhc-FTI (**2**) after irradiation at 365 nm. Cells were plated in the presence of the treatments noted. After a 24 h incubation, cells were then subjected to UV irradiation (using a 365 nm transilluminator) for 15 min (where indicated) and incubated an additional 24 h prior to imaging. Prior to imaging, the cells were stained with AlexaFluor 488-phalloidin conjugate to stain the

actin in the cell. A) No treatment. B) 2.5 µM FTI (**1**). C) 2.5 µM bhc-FTI (**2**). D) 2.5 µM bhc-FTI (**2**) plus UV. Imaging was performed with an inverted microscope: 20x objective. Scale bar = 50 µm.

2.3.4 Two-photon experiments with bhc-FTI

The aforementioned experiments demonstrate that caged FTIs can be uncaged in living cells and that they can be used to control Ras-mediated signaling pathways. Since it would be useful to employ these molecules for studies in tissues or whole organisms, we next investigated the ability of bhc-FTI (**2**) to be uncaged by long wavelength irradiation via two-photon excitation; such a process would enable greater penetration and decrease potential UV-induced cellular damage. Accordingly, bhc-FTI (**2**) was photolyzed with a Ti:sapphire laser tuned to 800 nm, and the reaction products were analyzed in a manner analogous to that described above for the one-photon experiments employing UV irradiation. The extinction coefficient of the bhc chromophore at 400 nm is 68% of that at λ_{max} (377 nm) thereby enabling two-photon excitation at 800 nm. An extracted ion current chromatogram obtained via LC-MS of the reaction mixture (Fig. **2.7**) and subsequent MS-MS analysis confirmed the formation of FTI (**1**); as was noted in the UV irradiation experiments with bhc-FTI (**2**), an isomer of **2** was also formed upon irradiation at 800 nm (Fig. **2.7D**). The extent of conversion of **2** to **1** via two-photon excitation was also studied. As was described above, the amount of **2** remaining was evaluated by its UV absorbance while the amount of **1** produced was determined via derivatization with a thiol-reactive fluorescein acetamide reagent. A plot showing the disappearance of **2** and

concomitant appearance of **1** as a function of photolysis time (Fig. **2.7E**) shows that approximately 40% of **2** could be converted to **1** after 120 min of irradiation.

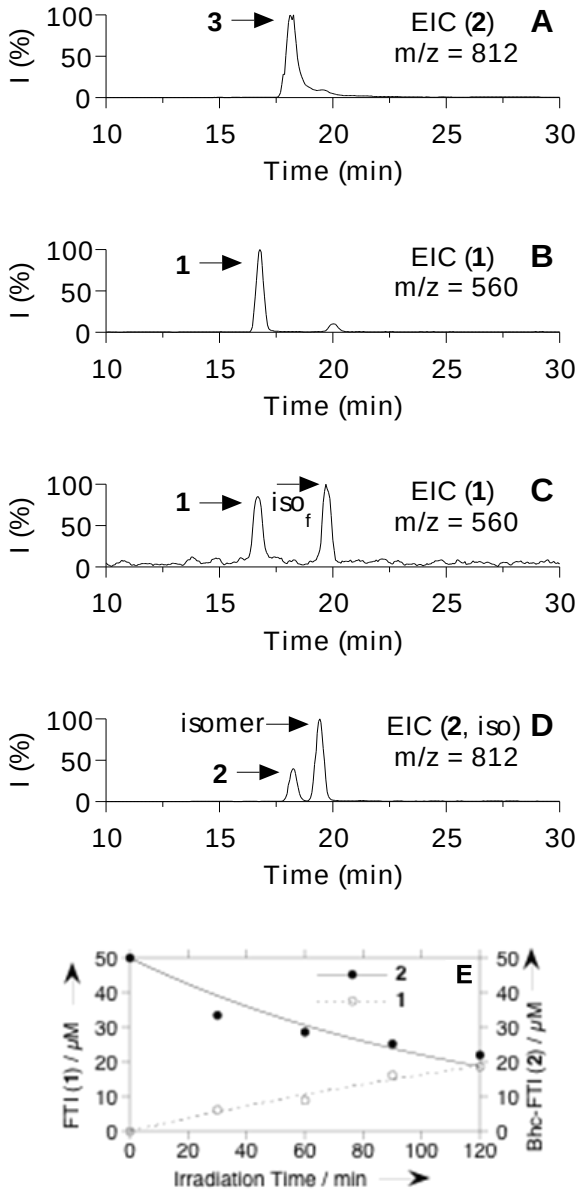

Figure 2.7. Analysis of uncaging of bhc-FTI (**2**) by photolysis at 800 nm. A) Extracted ion current (EIC) chromatogram (m/z = 810 - 815) of a sample of purified **2**. B) EIC chromatogram (m/z = 559 - 561) of a sample of purified **1**. C) EIC chromatogram (m/z = 559 - 561) of a sample of **2** after 120 min of photolysis at 800 nm showing the production of **1**. The peak at 19.5 min labeled (iso_f) probably results from fragmentation of the

isomer of **2**. D) EIC chromatogram (m/z = 810 - 815) of a sample of **2** after 120 min of photolysis showing remaining starting material (**2**) and the formation of an isomeric product (iso). E) Quantitation via HPLC of starting material (**2**) disappearance and product (**1**) formation as a function of irradiation time.

To study whether such levels of conversion would be physiologically useful, samples irradiated as described above were added to the MDCK cells expressing GFP-Ras and the pattern of localization was examined by confocal microscopy (Fig. **2.8**). Cells treated with the irradiated bhc-FTI (Fig. **2.8D**) show significant cytosolic localization of GFP-Ras compared to the untreated cells (Fig. **2.8A**) suggesting that these levels of uncaging are physiologically useful. Finally, we examined the uncaging of bhc-FTI (**2**) via two-photon excitation in the presence of Ciras-3 cells. Upon irradiation at 800 nm in the presence of bhc-FTI (**2**) (Fig. **2.9D**), the Ciras-3 cells take on the characteristic spread appearance signaling that the transforming effect of oncogenic Ras has been suppressed.

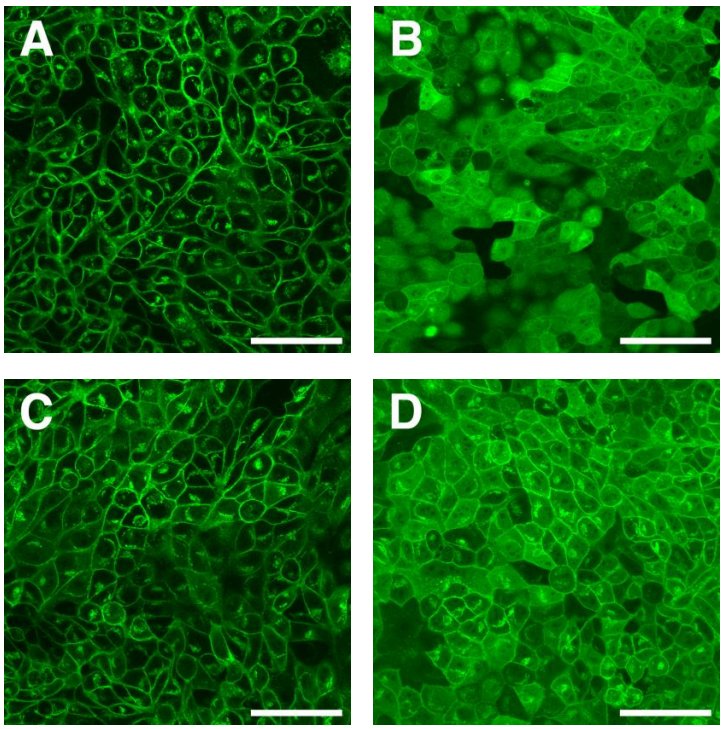

Figure 2.8. GFP-H-Ras localization in MDCK cells treated with Bhc-FTI after 800 nm irradiation. Cells were plated after following treatments: A) Vehicle treated cells (0.1% DMSO (v/v)). B) FTI (**1**, 1 μM). C) Bhc-FTI (**2**, 10 μM) solution without irradiation. D) Bhc-FTI (**2**, 10 μM) solution irradiated for 120 min at 800 nm. Cells were incubated for an additional 24 h prior to imaging with an inverted confocal microscope, 40x objective. Scale bar = 50 μm.

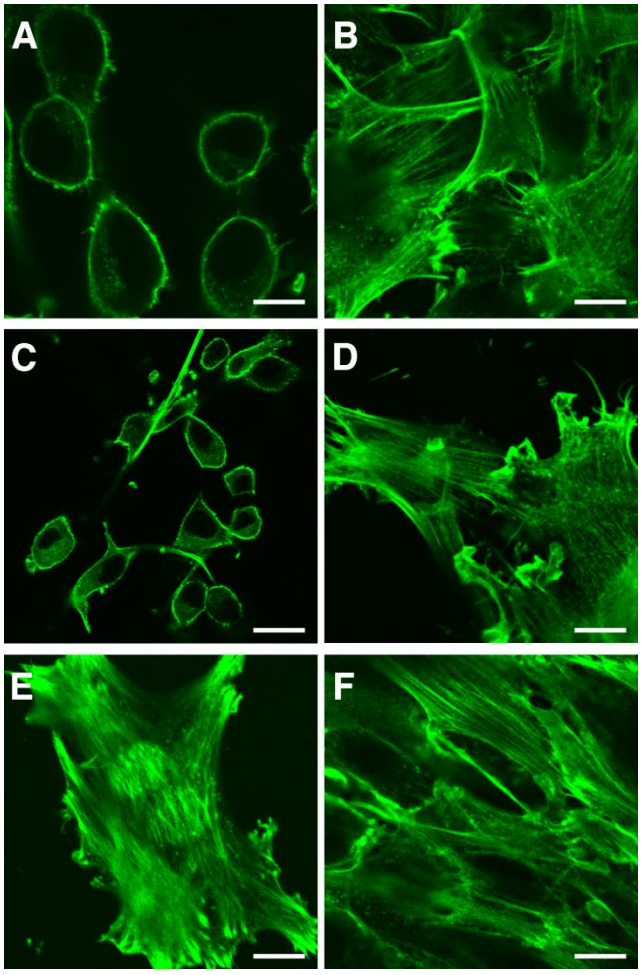

Figure 2.9. Morphology of Ciras-3 fibroblasts treated with bhc-FTI (**2**) after irradiation at 800 nm. Cells were plated in the presence of the treatments noted. Following treatment, the cells were then immediately subjected to two photon irradiation for either 1 or 2 h (where indicated) and incubated an additional 24 h. Images were obtained from cells that were stained with AlexaFluor 488-phalloidin conjugate (after the 24 h incubation) to visualize the actin in the cell (following manufacturers protocols). A) Vehicle (0.2% DMSO (v/v)). B) 5 µM FTI (**1**). C) 2.5 µM bhc-FTI (**2**). D) 2.5 µM bhc-FTI (**2**) + 1 h two photon irradiation. E) 5 µM bhc-FTI (**2**) + 2 h two photon irradiation. F) 2.5 µM bhc-FTI (**2**) + 2 h two photon irradiation. Imaging was performed with an inverted microscope: 40x objective. Scale bar = 20 µm.

2.4 Conclusions and Future Directions

In summary, we have prepared a caged inhibitor of PFTase that liberates FTI (**1**) upon one- and two-photon excitation. The FTI produced inhibits farnesylation, membrane localization of Ras and downstream signaling. While the use of bhc-based thioethers to mask a mercaptan renders uncaging slightly less efficient (compared with phosphates and carboxylates), such thioethers are inert to background cleavage in the absence of photolysis; this property is advantageous for biological experiments that require extended incubation times. The ability to uncage FTI via both one- and two-photon processes opens up the possibility of performing such experiments in tissue samples and perhaps even whole organisms where light penetration and phototoxicity are relevant concerns. The current challenge is to see whether physiologically useful levels of FTI can be uncaged in those more complex systems; experiments to address that are currently in progress.

2.5 Experimental

Compound **4**[1] was prepared as previously reported. All other reagents and solvents were purchased from commercial sources and used without further purification. ^{1}H NMR spectra were recorded at 300 or 500 MHz on Varian instruments at 25 °C. HRMS was performed with a Bruker BioTOF II instrument from Bruker Daltonics, Inc. (Fremont,

CA). UV spectra were performed with a Cary 50 Bio UV-Visible Spectrophotometer (Palo Alto, CA). HPLC analysis (analytical and preparative) was performed using a Beckman model 125/166 instrument, equipped with a UV detector and C18 columns (Varian Microsorb-MV, 5 µm, 4.6 x 250 mm and Phenomenex Luna, 10 µm, 10 x 250 mm respectively). LC/MS analysis was performed employing a Thermo LCQ Deca ion trap mass spectrometer (Thermo Scientific, San Jose, CA) interfaced with an Agilent 1100 Capillary HPLC equipped with an Agilent Zorbax 300SB-C18, 5 µm, 0.5 x 150 mm column. MDCK cells stably expressing GFP-H-Ras were the generous gift of Dr. Mark Philips (NYU School of Medicine). 10T1/2 and Ciras-3 mouse fibroblasts were the generous gift of Dr. Jim R. Davie (Department of Biochemistry and Molecular Biology, University of Manitoba). MCF10A and H-Ras MCF10A cells were the generous gifts of Dr. Aree Moon (College of Pharmacy, Duksung Women's University, Seoul, Korea). Dulbecco's Modified Eagle Medium (DMEM), DMEM/F12, a-Minimum Essential Medium (a–MEM), heat-inactivated horse serum, L-glutamine, fetal bovine serum (FBS) and AlexaFluor488-phalloidin conjugate were from Invitrogen Corporation (Carlsbad, CA). Cholera toxin, insulin, and epidermal growth factor (EGF) were purchased from Sigma (St. Louis, MO). Glass-bottomed culture dishes (35 mm and 96 well plate) fitted with microwells (14 mm and 5 mm diameter for the 35 mm dishes and 96 well plate, respectively) and a No. 1.5 glass coverslip were from MatTek Corporation (Ashland, MA).

2.5.1 Synthesis of Bhc-FTI

MOM-Bhc-Cl (3). Bhc-Cl (**4**) (200 mg, 0.69 mmol) was dissolved in THF under a nitrogen atmosphere. Triethylamine (211 µL, 1.5 mmol) was then added, followed by drop wise addition of chloromethyl methyl ether (105 µL, 1.4 mmol). The reaction was then left stirring overnight. The THF was removed *in vacuo* and the reaction rediluted with $CHCl_3$ (50 mL), washed with H_2O (3 x 20 mL) and brine (3 x 20 mL), dried and evaporated. The crude material was then purified via column chromatography (2:1 hexane/EtOAc) to give a yellow powder in 86% yield. ^{1}H NMR ($CDCl_3$) δ 7.83 (1H, s) 7.17 (1H, s), 6.45 (1H, s), 5.32 (2H, s), 4.60 (2H, s), 3.52 (3H, s). HR-MS (ESI) *m/z* calcd for $[C_{12}H_{10}BrClO_4 + H]^+$ 332.9524 (^{79}Br, ^{35}Cl), 334.9502 (^{81}Br, ^{35}Cl) and 336.9479 (^{81}Br, ^{37}Cl); found 332.9531 (^{79}Br, ^{35}Cl), 334.9522 (^{81}Br, ^{35}Cl) and 336.9492 (^{81}Br, ^{37}Cl).

MOM-Bhc-FTI (5). Compound **3** (5 mg, 16.8 µmol) and FTI (**1**) (5 mg, 7.9 µmol) were dissolved in 1 mL of a solution of 2:1:1 DMF/CH_3CN/H_2O containing 0.1% TFA under a N_2 atmosphere. $Zn(OAc)_2$ was then added (5 mg, 24 µmol) and the reaction monitored by analytical HPLC. After 2 d, the solvents were removed and the reaction purified via HPLC using a semi-preparative method (flow rate: 5 mL/min, gradient: 0% solvent B, 5 min; 0-55% B in 10 min; 55-70% B in 15 min; 70-100% B in 10 min; solvent A: H_2O and 0.1% TFA, solvent B: CH_3CN and TFA). The product eluted at 57% B and was then lyophilized to give 4.5 mg of a fluffy white solid in 62% yield. ^{1}H NMR (DMSO) δ 8.61 (1H, s) 8.13 (1H, s), 8.03 (1H, s), 7.23 (8H, m), 7.10 (1H, s), 7.00 (1H, s), 6.90 (1H, s), 6.42 (1H, s), 6.33 (1H, s), 5.42 (3H, s), 4.88 (1H, m), 4.38 (1H, m), 4.01 (3H, s), 3.98 (1H, s), 2.98 (3H, s), 2.85 (1H, m), 2.72 (1H, m), 2.18 (2H, m), 2.05 (2H, m), 1.35 (2H, m), 1.16 (6H, d), 0.80 (4H, m), 0.71 (3H, m). HR-MS (ESI) *m/z* calcd for

$[C_{38}H_{54}BrN_3O_{10}S_2 + H]^+$ 856.2507 (^{79}Br) and 858.2493 (^{81}Br); found 856.2565 (^{79}Br) and 858.2541 (^{81}Br).

Bhc-FTI (2). Compound **5** (5 mg, 5.9 µmol) was dissolved in 1 mL Reagent K (825 µL TFA, 25µL H_2O, 25 µL ethanedithiol, 50 µL thioanisole, 50 mg phenol) and stirred for 2 h while monitoring by analytical HPLC. After 2 h the excess TFA was removed by rotary evaporation and purified via HPLC using a semi-preparative method (flow rate: 5mL/min, gradient: 0% solvent B for 2 min; 0-50% B in 5 min; 50-80% B in 30 min; 80-100% B in 5 min; solvent A: H_2O and 0.1% TFA, solvent B: CH_3CN and 0.1 % TFA). The desired product eluted at 54% B and was then lyophilized to give 4.2 mg of a yellow solid in 92% yield. ^{1}H NMR (DMSO) δ 8.61 (1H, s) 8.02 (1H, s), 7.24 (8H, m), 7.10 (1H, s), 7.00 (3H, s), 6.90 (1H, s), 6.36 (1H, s), 4.88 (1H, m), 4.37 (1H, m), 4.11 (2H, s), 3.99 (2H, s), 2.98 (3H, s), 2.88 (1H, m), 2.72 (1H, m), 2.18 (2H, m), 2.06 (2H, m), 1.35 (4H, m), 1.22 (3H, s), 1.16 (6H, d), 0.82 (4H, m), 0.75 (3H, m). HR-MS (ESI) *m/z* calcd for $[C_{36}H_{50}BrN_3O_9S_2 + H]^+$ 812.2245 (^{79}Br) and 814.2230 (^{81}Br); found 812.2252 (^{79}Br) and 814.2242 (^{81}Br).

2.5.2 Kinetic analysis of uncaging of bhc-FTI

Solutions of compound **2** dissolved in PBS buffer (1 mL, 100 µM) and 1 mM DTT were placed in quartz tubes (10 x 50 mm) and irradiated with 365 nm UV light from a Rayonet reactor (16 x 14 W bulbs). Each sample was irradiated for a period ranging from 8 to 60 s. After each irradiation period, 100 µL aliquots were withdrawn and analyzed by RP-

HPLC. The compounds were eluted with a gradient of 0.1% TFA in H_2O and 0.1% TFA in CH_3CN (Gradient 3%/mL, flow rate 1 mL/min) and monitored at 245 nm. Decay curves were plotted using Kaleidagraph 3.0 software and analyzed by non-linear regression analysis.

2.5.3 LC-MS analysis of bhc-FTI

Samples containing **3** (10 µM, in PBS buffer containing 1 mM DTT) before and after irradiation for 2 min with 365 nm UV light from a Rayonet reactor were analyzed via LC-MS for the production of **1**. A solution of 10 µM **1** was also analyzed as a standard. The method utilized was as follows: flow rate: 10 µL/min, gradient: 0 % solvent B in 2 min; 0-45% solvent B in 10 min; 45-80% solvent B in 20 min; 80-100% solvent B in 5 min; solvent A: 0.1 % TFA in H_2O, solvent B: 0.1% TFA in CH_3CN).

2.5.4 Quantitative HPLC analysis of the extent of uncaging of bhc-FTI and the production of FTI upon photolysis

Solutions of 0-50 µM FTI (**1**) were reacted with 200 µM 5-iodoacetamido fluorescein (IAF) in PBS buffer pH 7.2 and allowed to react for 60 minutes before analysis by RP-HPLC. The compounds were eluted using a C8 column with a gradient of 0.1% TFA in H_2O and 0.1% TFA in MeOH (flow rate 1 mL/min, gradient: 0-40% solvent B in 20 min, 40-55% B in 15 min, 55-100% B in 5 min) and monitored by fluorescence (ex: 488, em:

510 nm). These data were used to construct a calibration curve for the compound IAF-FTI.

Solutions of 50 µM bhc-FTI (**2**) in PBS buffer pH 7.2 and 500 mM DTT were irradiated for times ranging from 0-30 seconds (one-photon, 365 nm, Rayonet reactor) or 0-120 minutes (two-photon, 800 nm, Ti:sapphire laser) and reacted with 700 µM IAF for 60 minutes before analysis by RP-HPLC. The reactions were analyzed by the aforementioned method. IAF elutes at 45% B while IAF-FTI elutes at 46% B. IAF-DTT adducts elute between 40 and 44% B.

2.5.5 Cell photolysis for western blot experiments using a Rayonet reactor

Aliquots of cells (3 mL) suspended in cell media (DMEM-F12) were incubated with **2** (5 µM) overnight and then placed in borosilicate glass tubes (10 x 75 mm) and irradiated with 365 nm UV light from a Rayonet reactor (16 x 14 W bulbs). Each sample was irradiated for a period ranging from 1 to 5 minutes. After each irradiation, the cells were re-plated in 35 mm glass bottom microwell dishes and allowed to incubate for 24 h prior to subsequent analysis.

2.5.6 Photolysis of MDCK and Ciras-3 cells using a transilluminator

MDCK or Ciras-3 cells were plated in 35 mm glass bottom microwell dishes and treated as noted, followed by immediate irradiation with 365 nm UV light from a handheld lamp (UVP model UVL-56, Upland, CA). Cells were irradiated for time intervals ranging

from 0 to 15 minutes. After irradiation the cells were allowed to incubate for 24 hours before being visualized by microscopy. For actin staining, the cells were stained according to manufacturers protocols.

2.5.7 Two-photon irradiation of bhc-FTI for analysis of GFP-Ras localization

A 100 µL solution of 1 mM **3** in PBS buffer and 1 mM DTT was placed in a quartz cuvette (2 x 2 x 10 mm, 100 µL volume) and irradiated using a homebuilt, regeneratively amplified Ti:sapphire laser system[43]. Samples were irradiated for 30 – 120 minutes at 1 kHz with 15 µJ pulses focused to a diameter of ~1 mm and centered at a wavelength of 800 nm. The laser pulses had a Gaussian full width at half maximum of ~70 fs. Aliquots were removed at selected times and stored in -20 °C prior to subsequent analysis. LC-MS experiments with these samples were performed as described above. For biological experiments, an aliquot of the irradiated solution was added to MDCK cells suspended in cell media (DMEM-F12) so that the concentration of **3** (without irradiation) would be 10 µM. These cells were then incubated for 24 hours before visualization via confocal microscopy.

2.5.8 Two-photon irradiation Ciras-3 cells in the presence of bhc-FTI (2)

Ciras-3 cells were plated in a glass-bottomed 96 well plate and treated as noted. The cells were then immediately subjected to two-photon irradiation using 800 nm light from a fs-pulsed and mode-locked Ti:sapphire laser[43] (120 mW) for 60 or 120 minutes. Following

irradiation, the cells were incubated an additional 24 h prior to imaging. For actin staining, the cells were stained according to manufacturers protocols.

2.5.9 Cell Culture and Microscopy

MDCK cells were grown in DMEM supplemented with 10% FBS. 10T1/2 and Ciras-3 cells were grown in α–MEM supplemented with 10% FBS. MCF10A and H-Ras cells were grown in DMEM/F12 supplemented with 5% horse serum, 0.5 mg/mL hydrocortisone, 10 mg /mL insulin, 20 ng/mL EGF, 0.1 mg/mL cholera toxin, and 2 mM L-glutamine. All cells were grown at 37 °C with 5.0% CO_2. For experiments, cells were seeded in culture dishes at the following densities: MDCK, 1.7 x 10^4 cells/cm^2; 10T1/2, 8.3 x 10^3 cells/cm^2; Ciras-3, 2.5 x 10^4 cells/cm^2, MCF10A and H-Ras MCF10A, 3.3 x 10^4 cells/cm^2. For microscopy, cells were seeded in 35 mm glass bottom microwell dishes (or glass–bottomed 96 well plates, depending on the experiment). Cells were treated as indicated in the figure legends, and live cells were imaged with an Olympus FluoView IX2 Inverted Confocal microscope, using a 40x or 60x objective, or with an Olympus Inverted scope, using a 20x objective.

2.5.10 Antibodies and Immunoblotting

Cell lysates were prepared using the following buffer: 50 mM Tris-HCl, pH 7.4, 1% NP-40, 0.25% Na-deoxycholate, 150 mM NaCl, 1 mM EDTA, 1 mM PMSF, 1 mg/mL aprotinin, 1 mg/mL leupeptin, 1 mM Na_3VO_4, 1 mM NaF, 20 mM glycerophosphate.

Lysates were cleared by centrifugation (16,000 x g, 10 min, 4 °C). 30-40 μg of protein was resolved using 10% or 15% SDS-polyacrylamide minigels, and then transferred to Immobilon-P PVDF membranes (Millipore, Bedford, MA). After blocking in a TBST/5% milk solution, immunoblots were incubated overnight at 4 °C using the following primary antibodies and dilutions: phospho-p44/42 MAPK (Thr-202/Tyr-204) (E10) (mouse monoclonal) (1:2000) from Cell Signaling (Beverly, MA), and H-Ras (C-20) (rabbit polyclonal) (1:500) from Santa Cruz Biotechnology (Santa Cruz, CA). The following secondary antibodies were used: anti-mouse IgG horseradish peroxidase-linked antibody and anti-rabbit IgG horseradish peroxidase-linked antibody from Cell Signaling. Immunoblots were visualized using the Pierce SuperSignal West Pico substrate (ThermoFisher Scientific, Waltham, MA).

2.6 References

1. A. P. Pelliccioli, J. Wirz, *Photochem. Photobiol. Sci.* **2002**, *1*, 441.
2. R. S. Givens, P. G. Conrad, II, A. L. Yousef, J.-I. Lee, *CRC Handb. Org. Photochem. Photobiol. (2nd Ed.)* **2004**, 691.
3. G. Mayer, A. Heckel, *Angew. Chem., Int. Ed.* **2006**, *45*, 4900.
4. G. C. R. Ellis-Davies, *Nat. Methods* **2007**, *4*, 619.
5. H.-M. Lee, D. R. Larson, D. S. Lawrence, *ACS Chem. Biol.* **2009**, *4*, 409.
6. A. Specht, F. Bolze, Z. Omran, J.-F. Nicoud, M. Goeldner, *HFSP J.* **2009**, *3*, 255.
7. C. W. Riggsbee, A. Deiters, *Trends Biotechnol.* **2010**, *28*, 468.
8. S. Loudwig, H. Bayley, in *Dynamic Studies in Biology* (Eds.: M. Goeldner, R. Givens), Wiley-VCH, Weinheim, **2005**, pp. 253.

9. I. Schlichting, S. C. Almo, G. Rapp, K. Wilson, K. Petratos, A. Lentfer, A. Wittinghofer, W. Kabsch, E. F. Pai, et al., *Nature* **1990**, *345*, 309.
10. V. Hagen, J. Bendig, S. Frings, B. Wiesner, B. Schade, S. Helm, D. Lorenz, U. B. Kaupp, *J. Photochem. Photobiol., B* **1999**, *53*, 91.
11. V. Hagen, K. Benndorf, U. B. Kaupp, in *Dynamic Studies in Biology* (Eds.: M. Goeldner, R. Givens), Wiley-VCH, Weinheim, **2005**, pp. 155.
12. D. D. Young, A. Deiters, *Angew. Chem., Int. Ed.* **2007**, *46*, 4290.
13. H. Li, J.-M. Hah, D. S. Lawrence, *J. Am. Chem. Soc.* **2008**, *130*, 10474.
14. A. Hall, *Current Opinion in Cell Biology* **1993**, *5*, 265.
15. P. J. Casey, P. A. Solski, C. J. Der, J. E. Buss, *Proc. Nat. Acad. Sci. U.S.A.* **1989**, *86*, 8323.
16. F. L. Zhang, P. J. Casey, *Annu. Rev. Biochem.* **1996**, *65*, 241.
17. N. E. Kohl, C. A. Omer, M. W. Conner, N. J. Anthony, J. P. Davide, S. J. deSolms, E. A. Giuliani, R. P. Gomez, S. L. Graham, K. Hamilton, *Nat Med* **1995**, *1*, 792.
18. L. Sepp-Lorenzino, Z. Ma, E. Rands, N. E. Kohl, J. B. Gibbs, A. Oliff, N. Rosen, *Cancer Res.* **1995**, *55*, 5302.
19. M. H. Gelb, L. Brunsveld, C. A. Hrycyna, S. Michaelis, F. Tamanoi, W. C. Van Voorhis, H. Waldmann, *Nat. Chem. Biol.* **2006**, *2*, 518.
20. J. B. Gibbs, A. Oliff, N. E. Kohl, *Cell* **1994**, *77*, 175.
21. R. A. Gibbs, *Curr. Opin. Drug Discovery Dev.* **2000**, *3*, 585.
22. M. Schlitzer, M. Bohm, I. Sattler, H. M. Dahse, *Bioorg. Med. Chem.* **2000**, *8*, 1991.
23. S. M. Sebti, A. D. Hamilton, *Oncogene* **2000**, *19*, 6584.
24. R. J. Doll, P. Kirschmeier, W. R. Bishop, *Curr. Opin. Drug. Disc. Devel.* **2004**, *7*, 478.
25. S. F. Sousa, P. A. Fernandes, M. J. Ramos, *Curr. Med. Chem.* **2008**, *15*, 1478.
26. C. L. Strickland, W. T. Windsor, R. Syto, L. Wang, R. Bond, Z. Wu, J. Schwartz, H. V. Le, L. S. Beese, P. C. Weber, *Biochemistry* **1998**, *37*, 16601.
27. S. B. Long, P. J. Hancock, A. M. Kral, H. W. Hellinga, L. S. Beese, *Proc. Nat. Acad. Sci. USA* **2001**, *98*, 12948.

28. D. B. Rozema, S. T. Phillips, C. D. Poulter, *Org. Lett.* **1999**, *1*, 815.
29. C.-C. Huang, P. J. Casey, C. A. Fierke, *J. Biol. Chem.* **1997**, *272*, 20.
30. T. Furuta, S. S. H. Wang, J. L. Dantzker, T. M. Dore, W. J. Bybee, E. M. Callaway, W. Denk, R. Y. Tsien, *Proc. Nat. Acad. Sci. USA* **1999**, *96*, 1193.
31. O. D. Fedoryak, T. M. Dore, *Org. Lett.* **2002**, *4*, 3419.
32. Y. Zhu, C. M. Pavlos, J. P. Toscano, T. M. Dore, *J. Am. Chem. Soc.* **2006**, *128*, 4267.
33. A. J. DeGraw, M. A. Hast, J. Xu, D. Mullen, L. S. Beese, G. Barany, M. D. Distefano, *Chem. Biol. Drug Des.* **2008**, *72*, 171.
34. V. Hagen, B. Dekowski, N. Kotzur, R. Lechler, B. Wiesner, B. Briand, M. Beyermann, *Chem.--Eur. J.* **2008**, *14*, 1621.
35. N. Kotzur, B. Briand, M. Beyermann, V. Hagen, *J. Am. Chem. Soc.* **2009**, *131*, 16927.
36. W. M. Kwok, H.-Y. An, C. Ma, A. C. Rea, J. L. Nganga, Y. Zhu, T. M. Dore, D. L. Phillips, *J. Phys. Chem. B* **2010**, Submitted.
37 J. B. Gibbs, D. L. Pompliano, S. D. Mosser, E. Rands, R. B. Lingham, S. B. Singh, E. M. Scolnick, N. E. Kohl, A. Oliff, *J. Biol. Chem.* **1993**, *268*, 7617.
38. N. E. Kohl, K. S. Koblan, C. A. Omer, A. Oliff, J. B. Gibbs, *Methods Mol. Biol.* **1998**, *84*, 283.
39. S. Kraus, R. Seger, *Methods Mol. Biol.* **2004**, *250*, 29.
40. E. Choy, V. K. Chiu, J. Silletti, M. Feoktistov, T. Morimoto, D. Michaelson, I. E. Ivanov, M. R. Philips, *Cell* **1999**, *98*, 69.
41. D. P. Walsh, Y.-T. Chang, *Chem. Rev.* **2006**, *106*, 2476.
42. X. Ouyang, J. K. Chen, *Chem. Biol.* **2010**, *17*, 590.
43. D. F. Underwood, D. A. Blank, *J. Phys. Chem. A* **2003**, *107*, 956.

Chapter 3. Photochemical Modulation of Ras-Mediated Signal Transduction using BHQ-based caged farnesyltransferase inhibitors

3.1 Introduction

The term 'caging' was first coined in 1978[1], giving rise to photoremovable protecting group chemistry with the advent of the *ortho*-nitrobenzyl cage. Since then the scope of caging groups has expanded from organic synthesis protecting groups[2] to include the inactivation of biologically important molecules such as enzymes, substrates and drugs[3-5]. A critical advantage of caging groups over other molecules is that they can be orthogonally removed by simple exposure to light in a spatiotemporal manner[6-9]. This feature has been exploited to manipulate and affect biological processes in *in vivo* samples such as cells and embryos[10-12]. The Ras superfamily of proteins includes over 150 small GTPases that are involved in several signal transduction pathways which have effects on cellular growth and regulation[13]. Importantly, mutation of Ras proteins has been liked in approximately 30% of human cancers[14] so it would be useful to manipulate their activity in cells. In order for Ras proteins to work properly they must be processed by the enzyme protein farnesyltransferase (PFTase)[15,16]. This enzyme can in turn be disrupted by small molecules known as farnesyltransferase inhibitors (FTIs) such as L-744,832[17-20] (**1**, Fig. **3.1**). We have previously employed a thiol caged FTI using the bhc photoremovable group to manipulate Ras behavior in cells; we rationalized that a cousin of bhc, the bromohydroxy quinoline (BHQ) group, could be employed in a similar

fashion. The BHQ group has been chiefly employed to inactivate alcohols, phosphates and carboxylic acids[21,22] but it has shown good one-photon uncaging properties due to a high quantum yield compared to other groups[23,24] as well as good affinity for two-photon deprotection. Activated versions of BHQ such as MOM-BHQ chloride (**2**) were utilized to mask the reactivity of the thiol of FTI **1** as a thioether (BHQ-FTI, **3**) and amine as a urethane (BHQ-FTI urethane, **4**).

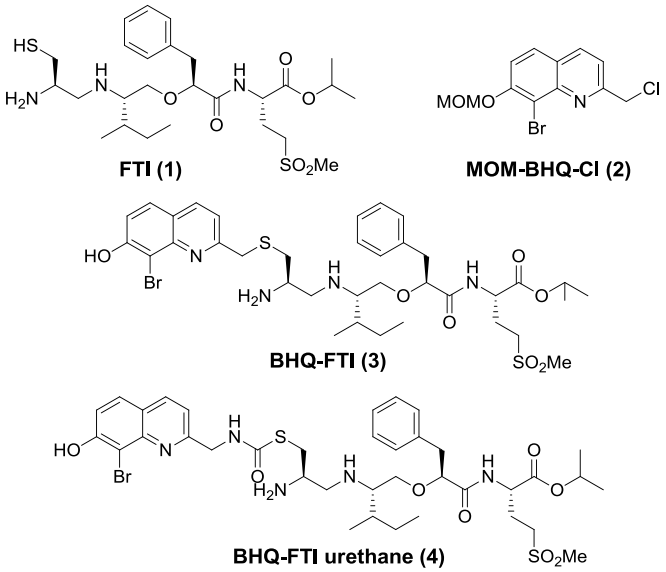

Figure 3.1. Caging of the FTI L-744,832 (**1**) with BHQ derivatives such as MOM-BHQ-Cl (**2**) to give inactivated thioether BHQ-FTI (**3**) and BHQ-FTI urethane (**4**).

3.2 Research Objectives

We have expanded on our strategy to cage FTI **1** and employed the BHQ group to inactivate FTI via a thioether mask (BHQ-FTI, **3**) and a urethane mask (BHQ-FTI

urethane, **4**). We are interested in these new BHQ caged FTIs in order to explore and improve upon the photolysis kinetics and efficacy of FTI release compared to our previous efforts using a bhc cage; and in the case of caged urethane **4**, explore the reactivity of a previously unreported BHQ-caged functional group. With regards to the biological significance of these caged FTIs both should be worse inhibitors of PFTase compared to **1**, and a result Ras should remain farnesylated and localized to the cell membrane. Conversely, irradiation of **3** or **4** with light releases FTI that inhibits Ras farnesylation and disrupts its downstream signaling pathways. Reported here are the synthesis, photochemical characterization and biological applications of caged PFTase inhibitors **3** and **4**.

3.3 Results and Discussion

3.3.1 Synthesis, photochemical characterization and biological applications of BHQ-FTI

3.3.1.1 Synthesis of BHQ-FTI

A MOM-protected chloride derivative of BHQ (**2**) was utilized to cage FTI **1** (Scheme **3.1**). MOM-BHQ alcohol[25] (**5**) was reacted with tosyl chloride and DMAP to yield protected chloride **2**. This chloride was then utilized to cage the thiol of FTI **1** under

zinc acetate and acidic pH conditions. Purification of this reaction by semipreparative HPLC afforded MOM-protected caged FTI **6** in 57% yield. The MOM ether was subsequently removed using excess Reagent K and purified via HPLC in order to yield BHQ-FTI (**3**) in 95%.

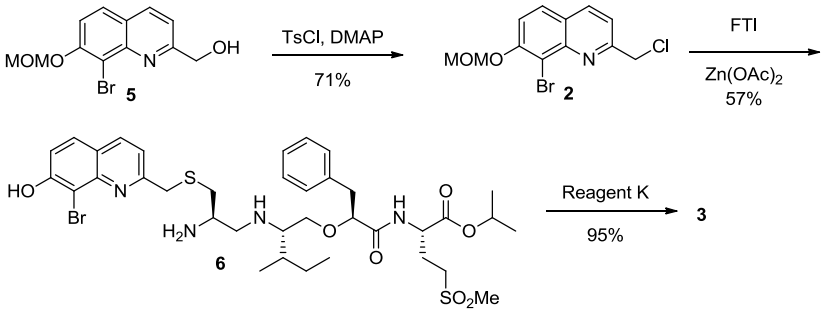

Scheme 3.1. Synthesis of BHQ-FTI (**2**).

3.3.1.2 Photochemical characterization of BHQ-FTI

The photolysis of **3** was carried out in a buffered aqueous solution (pH 7.2) using 365 nm and was monitored by HPLC UV absorbance. The disappearance of BHQ-FTI (**3**) can be observed as a function of irradiation time in Fig. **3.2**, though since FTI **1** has poor UV absorbance it was not observed. A quantum yield of 0.11 mol•ein^{-1} was calculated based on these results, comparable to other BHQ analogues[21,22].

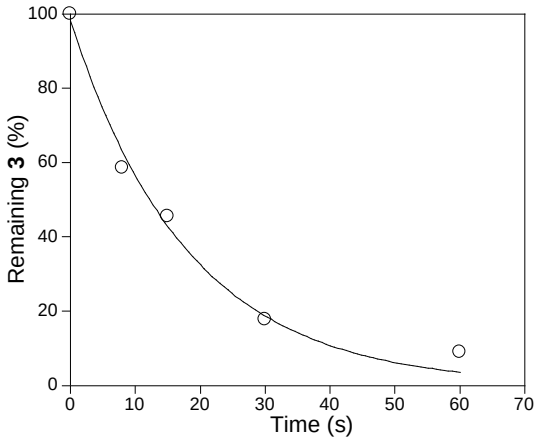

Figure 3.2. Kinetic analysis of uncaging of BHQ-FTI (**3)** by irradiation at 365 nm.

Next, the amount of FTI produced from photolysis of **3** was quantified via LC-MS extracted ion current (EIC) analysis. A photolyzed solution of **3** revealed the presence of an ion at m/z = 650.3 with a retention time of 22.4 min (Fig. **3.3C**), matching the EIC chromatogram of FTI (Fig. **3.3B**). However, a second, more abundant product with m/z = 715.3 that eluted at 24.2 min was also observed (Fig. **3.3D**). That mass corresponds to a product that has lost HBr that we tentatively assign as dehydrobrominated starting material. Comparison of the relative intensities of the two photolysis products in the mass spectrum suggests that **3** produces FTI with a yield of approximately 10% (Fig **3.3E**).

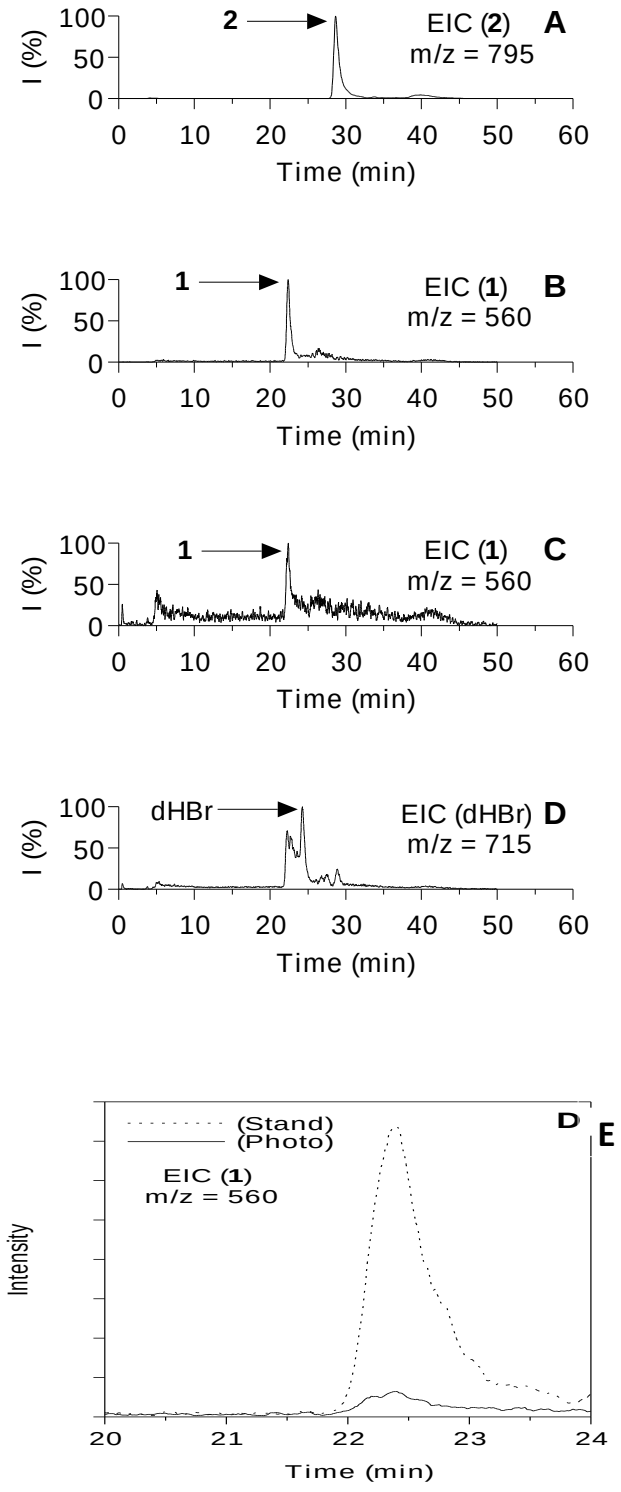

Figure 3.3. Analysis of BHQ-FTI (**3**) photolysis via LC-MS. A) Extracted ion current (EIC) chromatogram (m/z = 794.5 – 795.5) of a sample of purified **2**. B) EIC

chromatogram (m/z = 559.5 – 560.5) of a sample of purified **1**. C) EIC chromatogram (m/z = 559.5 – 560.5) of a sample of **2** after 120 sec of photolysis showing the production of **1**. D) EIC chromatogram (m/z = 714.5 – 715.5) of a sample of **2** after 120 sec of photolysis showing the production of a dehydrobrominated (dHBr) product. E) EIC chromatograms (m/z = 559.5 – 560.5) monitoring the amount of **1** produced upon photolysis of a 10 µM solution of **2** (solid line) compared with a 10 µM standard of **1** that would represent 100% conversion (dashed line). Integration of this data indicates a yield of 9.4%.

3.3.1.3 Applications of BHQ-FTI to control cellular processes

The ability of BHQ-FTI to release biologically relevant levels of FTI to block Ras processing upon irradiation was examined via Western blotting[26,27]. MCF10A cells were irradiated with 365 nm light after incubation with BHQ-FTI (Lane 4), resulting in a significant decrease in the amount of processed Ras and a substantial increase in unprocessed Ras. These results are comparable to cells incubated with FTI **1** (Lane 5). Cells that were treated with **3** without irradiation had similar levels of processed and unprocessed Ras (Lane 3) compared to cells that were only irradiated (Lane 2) or untreated (Lane 1). Additional testing for phosphorylated erk, a product of active Ras[28], showed significantly decreased levels of the compound present in cells treated with FTI **1** (Fig. **3.4**, Lane 5) or BHQ-FTI **3** plus irradiation (Lane 4). Untreated cells, cells exposed to UV light only or exposed to BHQ-FTI **3** only (Lanes 1, 2 and 3, respectively) show increased levels of phosphorylated erk, indicating that more Ras remains active in those samples. Overall, these results show that BHQ-FTI **3** photolysis results in the production of FTI with sufficient levels to affect Ras processing and downstream signaling in cells.

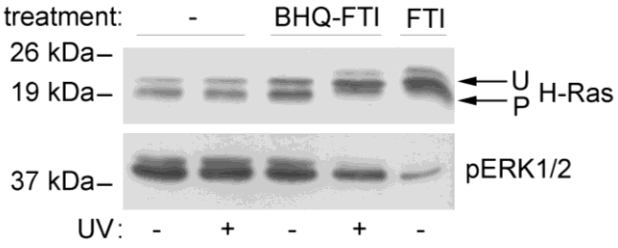

Figure 3.4. Effect of BHQ-FTI (**2**) UV-mediated uncaging on H-Ras prenylation and ERK1/2 phosphorylation state in MCF10A cells. H-Ras MCF10A cells were treated with 5 μM FTI (**1**) for 120 min or 5 μM BHQ-FTI (**2**) for 30 min and exposed to UV as indicated for 4 min in a Rayonet photoreactor. After 24 h, whole cell lysates were prepared. For the H-Ras immunoblot, 40 mg of protein was resolved by 15% SDS-PAGE. For the p-ERK1/2 immunoblot, 30 mg of protein was resolved by 10% SDS-PAGE. Note the faster mobility of processed Ras (P) compared with unprocessed Ras (U). Lane 1) Vehicle (0.1% DMSO (v/v)). Lane 2) Vehicle (0.1% DMSO (v/v)) followed by UV. Lane 3) BHQ-FTI (**2**). Lane 4) BHQ-FTI (**2**) followed by UV. Lane 5) FTI (**1**).

Next, we evaluated the ability of BHQ-FTI **3** to change the localization of Ras in cells. For this purpose the MDCK cell line, which expresses a GFP-Ras fusion protein[29], was utilized. When GFP-Ras is farnesylated it accumulates in the cell's plasma membrane; however, inhibition of farnesylation by FTI results in localization in the cytosol. The localization of GFP-Ras in cells, and thus its corresponding farnesylation status, was probed using confocal microscopy (Fig. **3.5**). Untreated cells (Fig. **3.5A**) show GFP-Ras is mostly only occurs in the plasma membrane. Cells treated with FTI only (Fig. **3.5B** and **3.5F**, respectively) as well as cells treated with BHQ-FTI (**3**) plus UV (Fig. **3.5D**) show that Ras has accumulated in the cytoplasm, indicating that BHQ-FTI (**3**) can be

used to modulate Ras localization. Additionally, treatment of cells with UV only or BHQ-FTI (**3**) only (Fig. **3.5E** and **3.5C**, respectively) result in similar accumulation of Ras in the cell membrane compared to untreated cells.

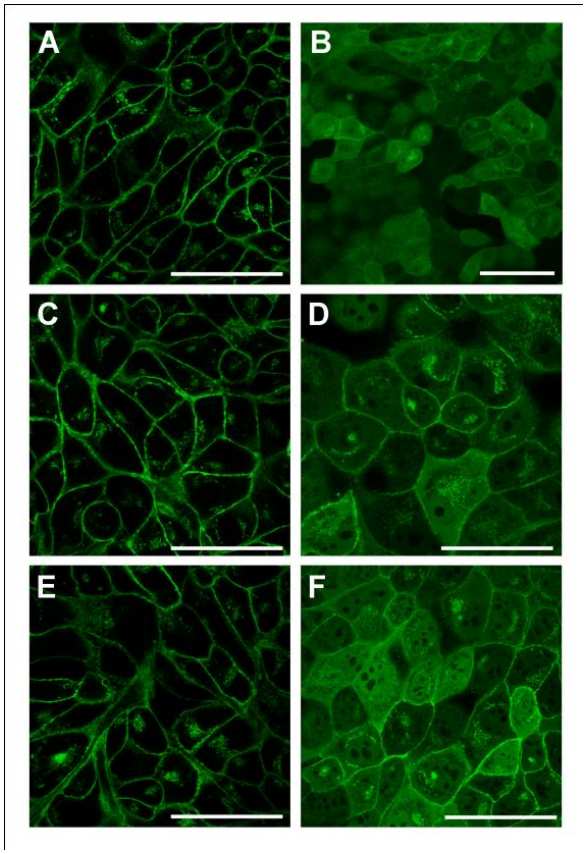

Figure 3.5. GFP-H-Ras localization in MDCK cells treated with BHQ-FTI (**3**) after 365 nm irradiation. A) Vehicle (0.2% DMSO (v/v)). B) 1 µM FTI (**1**). C) 10 µM BHQ-FTI (**3**), no irradiation. D) 10 µM BHQ-FTI (**3**) plus irradiation. E) No treatment plus irradiation. F) 5 µM FTI (**1**). 24 h after treatment with the compounds indicated, cells in panels D and E were then exposed to UV (365 nm) for 15 min. All samples were incubated for an additional 24 h prior to imaging with a confocal microscope, 60x objective. Scale bar = 50 mm. (note that panel B image captured with 40x objective). For these experiments, photolysis reactions were performed using a UV transilluminator.

Ciras-3 cells, which express an oncogenic Ras gene, were employed to test the ability of BHQ-FTI (**3**) to modulate the downstream signaling of Ras (Fig. **3.6**). These cells have a characteristic rounded, small morphology (Fig. **3.6A**) but treatment with FTI results in their conversion to a larger and more spread appearance (Fig. **3.6B**). Treatment with BHQ-FTI (**3**) only did not result in cell morphology change (Fig **3.6C**). Cells incubated with **3** and irradiated with UV light (Fig. **3.6D**) showed the larger and more spread out morphology similar to cells treated with FTI, indicating the transforming effects of oncogenic Ras has been suppressed.

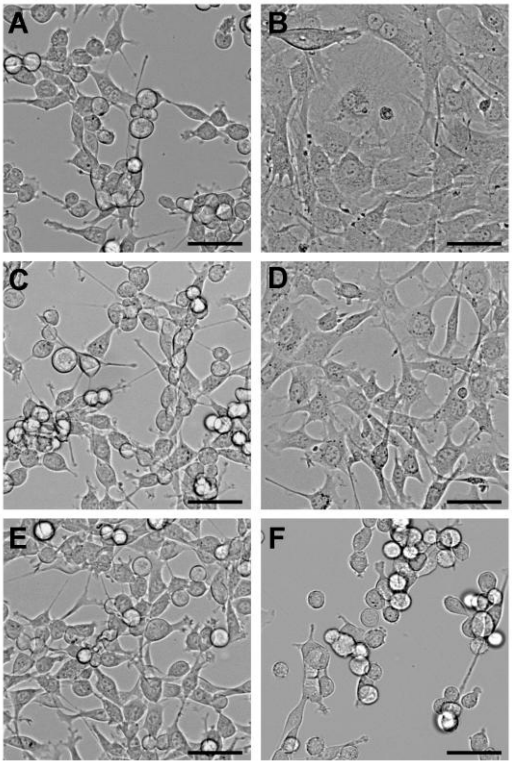

Figure 3.6. Morphology of Ciras-3 fibroblasts treated with BHQ-FTI. Cells were plated in the presence of the treatments noted. After a 24 h incubation, cells were subjected to UV irradiation (using a 365 nm transilluminator) for 15 min (where indicated) and

incubated an additional 24 h prior to imaging. A) No treatment. B) 10 µM FTI (**1**). C) 10 µM BHQ-FTI (**2**). D) 10 µM BHQ-FTI (**2**) plus UV. E) No treatment, plus UV. F) Vehicle (0.2% DMSO (v/v)). Imaging was performed with an inverted microscope: 20x objective. Scale bar = 50 mm.

3.3.2 Synthesis, photochemical characterization and biological applications of BHQ-FTI urethane

3.3.2.1 Synthesis of BHQ-FTI urethane

In an effort to improve the amount of FTI (**1**) produced from photolysis of BHQ-FTI (**3**), we decided to alter the functionality of the BHQ cage. It has been reported that BHQ releases carboxylic acids and carbonates in good yields[21,22], so we originally set to install a thiocarbonate cage instead of a thioether one.

MOM-BHQ alcohol (**5**) was reacted with nitrobenzyl chloroformate and DMAP before the addition of FTI **1**. However, upon purification by HPLC and analysis of collected fractions by MS it was discovered that there were two peaks with the mass of the desired caged FTI; upon further inspection we rationalized that the close proximity of a primary amine to the thiocarbonate moiety resulted in an S- to N- shift similar to the process of native chemical ligation[30]. A small amount of the desired MOM-BHQ thiocarbonate was obtained, but since this compound would rearrange over time via S- to N- shift we

decided to continue our work with this rearrangement product, MOM-BHQ-FTI urethane (**7**). The MOM ether of protected urethane **7** was removed via Reagent K and HPLC purification yielded BHQ-FTI urethane (**4**) in 85% yield.

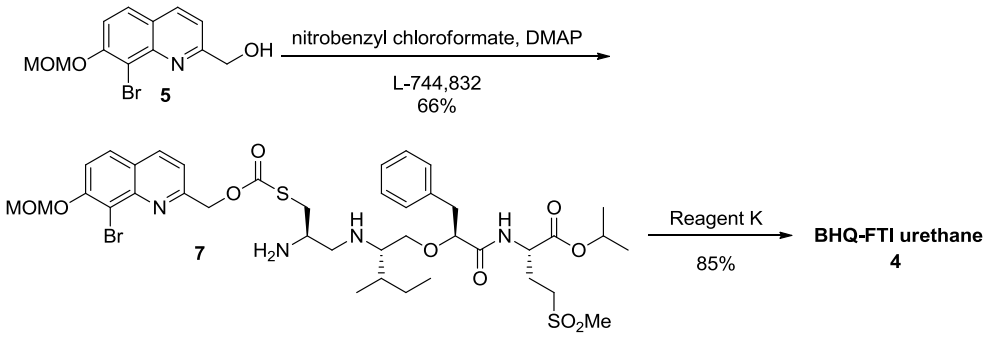

Scheme 3.2. Synthesis of BHQ-FTI urethane.

3.3.2.2 Photochemical characterization of BHQ-FTI urethane

A photolysis decay time course was obtained for caged FTI urethane **4** (Fig. **3.7**). This compound was photolyzed in aqueous buffer (pH 7.2) using 365 nm light and monitored by HPLC UV absorbance. Its disappearance is observed as a function of irradiation time, though production of FTI **1** cannot be quantified by HPLC due to poor UV absorption. These results indicate that urethane **4** photolyzes more slowly compared to BHQ-FTI **3** as well as our bhc- caged FTI.

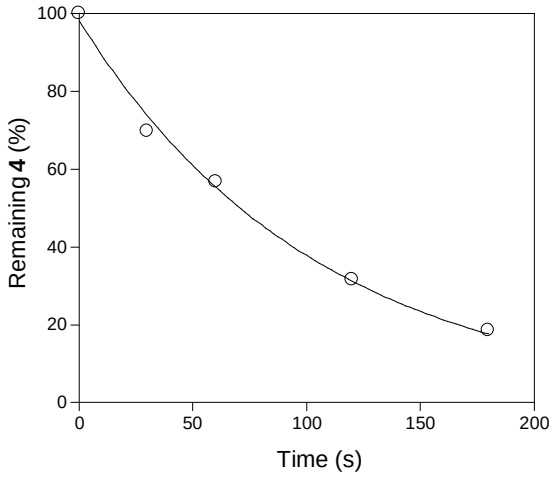

Figure 3.7. Kinetic analysis of uncaging of BHQ-FTI urethane (**4)** by irradiation at 365 nm.

3.3.2.3 Applications of BHQ-FTI urethane to control cellular processes

We evaluated the ability of BHQ-FTI urethane **4** to change the localization of Ras in cells. As in the case of BHQ-FTI 3, the GFP-Ras[29] expressing MDCK cell line was employed for this purpose. Confocal microscopy was used to identify the farnesylation status of GFP-Ras (Fig. **3.8**); naturally farnesylated Ras accumulates in the cell membrane whereas inhibition by FTI localizes Ras to the cytoplasm. Treatment of cells with 5 μM caged urethane **4** (Fig. **3.8D**) does not result in relocation of GFP-Ras from the cell membrane, similar to what is observed in untreated cells (Fig. **3.8A**). Addition of caged urethane **4** plus UV for 10 min (Fig. **3.8B**) results in migration of GFP-Ras to the cytosol, though slightly less compared to addition of FTI **1** (Fig. **3.8C**). These results

indicate that caged urethane **4** can be used to control cellular processes, though further tests must be carried out to fully study its properties.

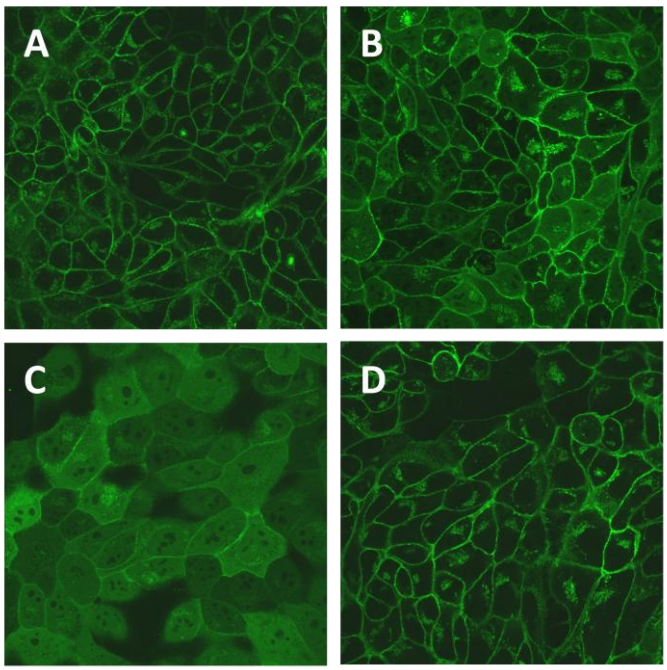

Figure 3.8. GFP-H-Ras localization in MDCK cells treated with BHQ-FTI urethane (**4**) after 365 nm irradiation. A) Vehicle (0.2% DMSO (v/v)). B) 5 µM BHQ-FTI urethane (**4**) plus irradiation. C) 5 µM FTI (**1**). D) 5 µM BHQ-FTI urethane (**4**). 24 h after treatment with the compounds indicated, cells in panels B were then exposed to UV (365 nm) for 10 min. All samples were incubated for an additional 24 h prior to imaging with a confocal microscope, 40x objective. For these experiments, photolysis reactions were performed using a UV transilluminator.

3.4 Conclusion and Future Directions

In conclusion, two new caged inhibitors of PFTase have been synthesized and their ability to release FTI (**1**) upon irradiation has been studied. Our thioether-masked BHQ-

FTI (**3**) photolyzes at a very similar rate compared to bhc-caged FTI, while BHQ-FTI urethane (**4**) is significantly slower to uncage. Additionally, BHQ-FTI (**3**) produces FTI (**1**) with an efficiency of about 10% due to the appearance of non-productive photoproducts. Despite this modest yield, BHQ-FTI (**3**) inhibits farnesylation, membrane localization and downstream signaling of Ras when irradiated in cells. Preliminary studies suggest that BHQ-FTI urethane (**4**) also inhibits membrane localization of Ras in a similar fashion. An advantage of using the BHQ group to inactivate thioethers and urethanes is that such compounds do not undergo background cleavage, which is an important feature for biological experiments that require long incubation times such as those described here. Experiments to investigate the two-photon properties of thioether **3** and urethane **4** are under way.

3.5 Experimental

Compound **5** was prepared from its respective literature procedure[25]. All other reagents and solvents were purchased from commercial sources and used without further purification. ^{1}H NMR spectra were recorded at 300 or 500 MHz on Varian instruments at 25 °C. H-MS was performed with a Bruker BioTOF II instrument from Bruker Daltonics, Inc. (Fremont, CA). HPLC analysis (analytical and preparative) was performed using a Beckman model 125/166 instrument, equipped with a UV detector and C18 columns (Varian Microsorb-MV, 5 µm, 4.6 x 250 mm and Phenomenex Luna, 10 µm, 10 x 250 mm respectively). LC-MS analysis was performed employing a Thermo

LCQ Deca ion trap mass spectrometer (Thermo Scientific, San Jose, CA) interfaced with an Agilent 1100 Capillary HPLC equipped with an Agilent Zorbax 300SB-C18, 5 µm, 0.5 x 150 mm column. MDCK cells stably expressing GFP-H-Ras were the generous gift of Dr. Mark Philips (NYU School of Medicine). Ciras-3 mouse fibroblasts were the generous gift of Dr. Jim R. Davie (Department of Biochemistry and Molecular Biology, University of Manitoba). MCF10A and H-Ras MCF10A cells were the generous gifts of Dr. Aree Moon (College of Pharmacy, Duksung Women's University, Seoul, Korea). Dulbecco's Modified Eagle Medium (DMEM), DMEM/F12, a-Minimum Essential Medium (a–MEM), heat-inactivated horse serum, L-glutamine and fetal bovine serum (FBS) were from Invitrogen Corporation (Carlsbad, CA). Cholera toxin, insulin, and epidermal growth factor (EGF) were purchased from Sigma (St. Louis, MO). Petri dishes (35 mm) fitted with microwells (14 mm) and a No. 1.5 coverglass were from MatTek Corporation (Ashland, MA).

3.5.1 Synthesis of BHQ-FTI

MOM-BHQ chloride (2). Dimethylamino pyridine (22.5 mg, 0.185 mmol) and tosyl chloride (31 mg, 0.162 mmol) were dissolved in dichloromethane and stirred for 5 min. MOM-BHQ alcohol **7** (46 mg, 0.154 mmol) was then added and the reaction left stirring overnight. The reaction was then diluted with dichloromethane and washed with H_2O (2 x 10 mL). The organic layer was dried over $MgSO_4$, the solvent removed, and purified via flash column (100% dichloromethane). A yellow solid was obtained (30 mg, 0.0946 mmol, 71% yield). ^{1}H NMR ($CDCl_3$) δ 8.16 (1H, d, J=8.5 Hz), 7.76 (1H, d, J=9.0 Hz),

7.60 (1H, d, J=8.5 Hz), 7.53 (1H, d, J=9.0 Hz), 5.42 (2H, s), 4.91 (2H, s), 3.58 (3H, s). H-MS (ESI) *m/z* calcd for $(C_{12}H_{11}BrClNO_2 + H)^+$ 315.9734 (^{79}Br) and 317.9711 (^{81}Br), found 315.9765 (^{79}Br) and 317.9722 (^{81}Br).

MOM-BHQ-FTI (6). MOM-BHQ-Cl (**2**) (12.5 mg, 40 µmol), $Zn(OAc)_2$ (8.7 mg, 0. 40 µmol) and FTI (**1**) (5 mg, 8 µmol) were dissolved in a solvent mixture of 2:1:1 DMF/CH_3CN/H_2O (1.6 mL) and TFA (0.1%) under a N_2 atmosphere. The reaction was protected from light and its progress was monitored by HPLC. After the reaction was judged complete (3 days), the solvents were removed *in vacuo* and the remaining oil was purified via reversed-phase HPLC (flow rate: 5 mL/min, gradient: 0-70 % solvent B in 70 min; 70-100% solvent B in 10 min; solvent A: H_2O and 0.1 % TFA, solvent B: CH_3CN and 0.1% TFA). The desired product eluted at 45% B and was then lyophilized to give 3.5 mg of a fluffy white solid in 57% yield. H-MS (ESI) *m/z* calcd for $[C_{38}H_{55}BrN_4O_8S_2 + H]^+$ 839.2717 (^{79}Br) and 841.2702 (^{81}Br); found 839.2738 (^{79}Br) and 841.2718 (^{81}Br).

BHQ-FTI (3). MOM-BHQ-FTI (**6**) (1.5 mg, 2 µmol mmol) was dissolved in 1 mL Reagent K (825µL TFA, 25µL H_2O, 25 µL ethanedithiol, 50 µL thioanisole, 50 mg phenol) under a N_2 atmosphere and stirred for 3 h. The solvent was then removed *in vacuo* and the remaining oil was rediluted with 5 mL H_2O and purified via reversed-phase HPLC (flow rate: 5 mL/min, gradient: 0-70 % solvent B in 70 min; 70-100% solvent B in 10 min; solvent A: H_2O and 0.1 % TFA, solvent B: CH_3CN and 0.1% TFA). The desired product eluted at 40% B and was then lyophilized to give 1.25 mg of a fluffy

yellow solid in 95% yield. ^{1}H NMR (DMSO) δ 10.95 (1H, s) 8.91 (1H, s), 8.60 (1H, s), 8.33 (1H, s), 8.27 (1H, d), 7.82 (1H, d), 7.45 (1H, d), 7.33 (1H, d) 7.21 (3H, m), 7.18 (2H, m), 4.88 (1H, m), 4.39 (2H, m), 4.11 (2H, q), 3.64 (2H, d) 3.55 (2H, m), 3.46 (2H, m), 3.24 (1H, m), 3.10 (1H, m), 3.00 (3H, s), 2.86 (6H, m), 2.19 (1H, m), 2.04 (1H, m), 1.73 (1H, m), 1.37 (2H, m), 1.15 (6H, d), 1.11 (2H, m), 0.83 (3H, t), 0.73 (3H, d). H-MS (ESI) *m/z* calcd for $[C_{36}H_{51}BrN_4O_7S_2 + H]^+$ 795.2455 (^{79}Br) and 797.2440 (^{81}Br); found 795.2501 (^{79}Br) and 797.2485 (^{81}Br).

3.5.2 Synthesis of BHQ-FTI urethane

MOM-BHQ-L-744,832 urethane (7). MOM-BHQ alcohol (**5**, 1.3 mg, 4.3 μM) was dissolved in 250 μL dichloromethane, to which dimethylamino pyridine (0.7 mg, 2.7 μM) and nitrophenyl chloroformate (1.1 mg, 5.4 μM) were added. The reaction was monitored by TLC and stirred until all alcohol had been reacted. A solution of FTI (**1**, 3 mg, 5.4 μM) and dimethylamino pyridine (0.7 mg, 2.7 μM) in 250 μL dichloromethane was then added to the first reaction and left stirring for 2 h. This crude reaction mixture was purified via RP-HPLC (Solvent A: H_2O in 0.1% TFA, Solvent B: CH_3CN in 0.1% TFA, Gradient: 0% B over 5 min, 0-40% B over 10 min, 40-80% B over 30 min, 80-100% B over 10 min). Urethane **7** elutes at 58% B and was subsequently lyophilized to give a white powder (2.5 mg, 66 % yield). H-MS (ESI) *m/z* calcd for $[C_{39}H_{55}BrN_4O_{10}S_2 + H]^+$ 884.2616 (^{79}Br) and 886.2606 (^{81}Br); found 884.2656 (^{79}Br) and 886.2646 (^{81}Br).

BHQ-L-744,832 urethane (4). MOM-protected urethane **6** (2.2 mg, 2.6 μM) was dissolved in 1 mL Reagent K (TFA/H_2O/thioanisole/phenol/ethanedithiol 82.5:5:5:5:2.5) for 2 h. Excess TFA was removed via rotary evaporation and the crude mixture purified via RP-HPLC (Solvent A: H_2O in 0.1% TFA, Solvent B: CH_3CN in 0.1% TFA, Gradient: 0% B over 5 min, 0-40% B over 10 min, 40-80% B over 30 min, 80-100% B over 10 min). Urethane **4** elutes at 50% B and was subsequently lyophilized to give a white powder (2 mg, 91% yield). H-MS (ESI) *m/z* calcd for $[C_{74}H_{102}Br_2N_8O_{18}S_4 + 2H]^{2+}$ (dimer) 839.2275 (^{79}Br) and 840.2275 (^{81}Br); found 839.2301 (^{79}Br) and 840.2276 (^{81}Br).

3.5.3 Kinetic analysis of uncaging of BHQ-FTI and BHQ-FTI urethane

Solutions of compound **3** or **4** dissolved in PBS buffer (1 mL, 100 μM) and 1 mM DTT were placed in quartz tubes (10 x 50 mm) and irradiated with 365 nm UV light from a Rayonet reactor (16 x 14 W bulbs). Each sample was irradiated for a period ranging from 8 to 60 s (**3**) or 30 to 180 s (**4**). After each irradiation period, 100 μL aliquots were withdrawn and analyzed by RP-HPLC. The compounds were eluted with a gradient of 0.1% TFA in H_2O and 0.1% TFA in CH_3CN (Gradient 3%/mL, flow rate 1 mL/min) and monitored at 245 nm. Decay time courses were plotted using Kaleidagraph 3.0 software and analyzed by non-linear regression analysis.

3.5.4 Cell photolysis for western blot experiments using a Rayonet reactor

Aliquots of cells (3 mL) suspended in cell media (DMEM-F12) were incubated with **3** (5 μM) overnight and then placed in borosilicate glass tubes (10 x 75 mm) and irradiated with 365 nm UV light from a Rayonet reactor (16 x 14 W bulbs). Each sample was irradiated for a period ranging from 1 to 5 minutes. After each irradiation, the cells were replated in 35 mm glass bottom microwell dishes and allowed to incubate for 24 h prior to subsequent analysis.

3.5.5 Photolysis of MDCK and Ciras-3 cells using a transilluminator

Aliquots of 3 mL of Ciras-3 or MDCK cells suspended in cell media (DMEM-F12) and previously incubated with 10 μM **3** or 5 μM **4** were placed in 35 mm glass bottom microwell dishes and irradiated with 365 nm UV light from a handheld lamp (UVP model UVL-56, Upland, CA). Cells were irradiated for time intervals ranging from 0 to 10 minutes. After irradiation the cells were allowed to incubate for 24 hours before being visualized by microscopy.

3.5.6 LC-MS analysis of BHQ-FTI

Samples containing **3** (10 μM, in PBS buffer containing 1 mM DTT) before and after irradiation for 2 min with 365 nm UV light from a Rayonet reactor were analyzed via LC-MS for the production of **1**. A solution of 10 μM **1** was also analyzed as a standard. The method utilized was as follows: flow rate: 10 μL/min, gradient: 0 % solvent B in 5

min; 0-45% solvent B in 10 min; 45-80% solvent B in 20 min; 80-100% solvent B in 5 min; solvent A: 0.1 % TFA in H_2O, solvent B: 0.1% TFA in CH_3CN).

3.5.7 Cell Culture

MDCK cells were grown in DMEM supplemented with 10% FBS. 10T1/2 and Ciras-3 cells were grown in a–MEM supplemented with 10% FBS. MCF10A and H-Ras cells were grown in DMEM/F12 supplemented with 5% horse serum, 0.5 mg/mL hydrocortisone, 10 mg /mL insulin, 20 ng/mL EGF, 0.1 mg/mL cholera toxin, and 2 mM L-glutamine. All cells were grown at 37 °C with 5.0% CO_2. For experiments, cells were seeded in culture dishes at the following densities: MDCK, 1.7 x 10^4 cells/cm^2; 10T1/2, 8.3 x 10^3 cells/cm^2; Ciras-3, 2.5 x 10^4 cells/cm^2, MCF10A and H-Ras MCF10A, 3.3 x 10^4 cells/cm^2.

3.5.8 Microscopy

Cells were seeded in 35 mm glass bottom microwell dishes. Cells were treated as indicated in the figure legends, and live cells were imaged with an Olympus FluoView IX2 Inverted Confocal microscope, using a 40x or 60x objective, or with an Olympus Inverted scope, using a 20x objective.

3.5.9 Antibodies and Imunoblotting

Cell lysates were prepared using the following buffer: 50 mM Tris-HCl, pH 7.4, 1% NP-40, 0.25% Na-deoxycholate, 150 mM NaCl, 1 mM EDTA, 1 mM PMSF, 1 mg/mL aprotinin, 1 mg/mL leupeptin, 1 mM Na_3VO_4, 1 mM NaF, 20 mM glycerophosphate. Lysates were cleared by centrifugation (16,000 x g, 10 min, 4 °C). 30-40 mg of protein was resolved using 10% or 15% SDS-polyacrylamide minigels, and then transferred to Immobilon-P PVDF membranes (Millipore, Bedford, MA). After blocking in a TBST/5% milk solution, immunoblots were incubated overnight at 4 °C using the following primary antibodies and dilutions: phospho-p44/42 MAPK (Th-202/Tyr-204) (E10) (mouse monoclonal) (1:2000) from Cell Signaling (Beverly, MA), and H-ras (C-20) (rabbit polyclonal) (1:500) from Santa Cruz Biotechnology (Santa Cruz, CA). The following secondary antibodies were used: anti-mouse IgG horseradish peroxidase-linked antibody and anti-rabbit IgG horseradish peroxidase-linked antibody from Cell Signaling. Immunoblots were visualized using the Pierce SuperSignal West Pico substrate (ThermoFisher Scientific, Waltham, MA).

3.6 References

1. J. H. Kaplan, B. Forbush III, J. F. Hoffman, *Biochemistry* **1978**, *17*, 1929.
2. A. Patchornik, B. Amit, R. B. Woodward, *J. Am. Chem. Soc*. **1970**, *92*, 6333.
3. G. Mayer, A. Heckel *Angew. Chem. Int. Ed*. **2006**, *45*, 4900.
4. S. R. Adams, R. Y. Tsien, *Annu. Rev. Physiol*. **1993**, *55*, 755.
5. K. Curley, D. S. Lawrence, *Pharmacol. Ther*. **1999**, *82*, 347.

6. G. Dorman, G. D. Prestwich, *Trends Biotechnol*. **2000**, *18*, 64.

7. C. G. J. Bochet, *J. Chem. Soc., Perkin Trans*. **2002**, *1*, 125.

8. M. Goeldner, R. Givens, *Dynamic Studies in Biology*, Wiley-VCH, Weinheim, **2005**.

9. A. P. Pelliccioli, J. Wirz, *Photochem. Photobiol. Sci.* **2002**, *1*, 441.

10. C. Chou, D. D. Young, A. Deiters, *ChemBioChem* **2010**, *11*, 972.

11. E. Fino, R. Araya, D. S. Peterka, M. Salierno, R. Etchenique, R. Yuste, *Frontiers in Neural Circuits* **2009**, *3*, 1.

12. D. D. Young, M. O. Lively, A. Deiters, *J. Am. Chem. Soc.* **2010**, *132*, 6183.

13. A. Hall, *Current Opinion in Cell Biology* **1993**, *5*, 265.

14. J. Downward, *Nat. Rev. Cancer* **2003**, *1*, 11.

15. P. J. Casey, P. A. Solski, C. J. Der, J. E. Buss, *Proc. Nat. Acad. Sci. U.S.A.* **1989**, *86*, 8323.

16. F. L. Zhang, P. J. Casey, *Annu. Rev. Biochem.* **1996**, *65*, 241.

17. J. B. Gibbs, A. Oliff, N. E. Kohl, *Cell* **1994**, *77*, 175.

18. R. A. Gibbs, *Curr. Opin. Drug Discovery Dev.* **2000**, *3*, 585.

19. M. Schlitzer, M. Bohm, I. Sattler, H. M. Dahse, *Bioorg. Med. Chem.* **2000**, *8*, 1991.

20. S. M. Sebti, A. D. Hamilton, *Oncogene* **2000**, *19*, 6584.

21. O. D. Fedoryak, T. M. Dore, *Org. Lett.* **2002**, *4*, 3419.

22. Y. Zhu, C. M. Pavlos, J. P. Toscano, T. M. Dore, *J. Am. Chem. Soc.* **2006**, *128*, 4267.

23. A. J. DeGraw, M. A. Hast, J. Xu, D. Mullen, L. S. Beese, G. Barany, M. D. Distefano, *Chem. Biol. Drug Des.* **2008**, *72*, 171.

24. V. Hagen, B. Dekowski, N. Kotzur, R. Lechler, B. Wiesner, B. Briand, M. Beyermann, *Chem.--Eur. J.* **2008**, *14*, 1621.

25. T. M. Dore, Y. Zhu, K. G. Reddie, J. D. Lauderdale, (University of Georgia Research Foundation, Inc., USA). Application: US, **2010**, p. 46pp.

26. J. B. Gibbs, D. L. Pompliano, S. D. Mosser, E. Rands, R. B. Lingham, S. B. Singh, E. M. Scolnick, N. E. Kohl, A. Oliff, *J. Biol. Chem.* **1993**, *268*, 7617.
27. N. E. Kohl, K. S. Koblan, C. A. Omer, A. Oliff, J. B. Gibbs, *Methods Mol. Biol.* **1998**, *84*, 283.
28. S. Kraus, R. Seger, *Methods Mol. Biol.* **2004**, *250*, 29.
29. E. Choy, V. K. Chiu, J. Silletti, M. Feoktistov, T. Morimoto, D. Michaelson, I. E. Ivanov, M. R. Philips, *Cell* **1999**, *98*, 69.
30. P. E. Dawson, S. B. H. Kent, *Annu. Rev. Biochem*. **2000**, *69*, 923.

Chapter 4. Caged Cysteine Peptides for Studying Protein Farnesylation

4.1 Introduction

Photolabile protecting groups have become important tools in numerous areas of chemistry[1] due to their ability to be removed in a time-dependent and localized manner. They also are particularly attractive to the study of molecules of biological relevance and biological systems[2] because the light utilized to remove these groups is noninvasive. Examples of these caged biomolecules include DNA[3], cyclic nucleosides[4], and various enzymes[5] and enzyme substrates[6].

Protein prenylation is a biological process where a farnesyl or geranylgeranyl group is attached to a cysteine residue of certain proteins[7]. In order to be targeted for prenylation the protein must possess a CAAX box motif in its C-terminus, where C is cysteine, A an aliphatic amino acid, and X any amino acid. Among these proteins is the Ras family, which upon farnesylation by the enzyme protein farnesyltransferase (PFTase) become anchored to the cell membrane and participate in signal transduction pathways that regulate key aspects of cell division[8]. Mutations of Ras proteins have been linked to various types of cancer[9] and several PFTase inhibitors[10,11] have been employed to prevent the farnesylation, and hence activation, of Ras proteins.

Alkylation of the CAAX box cysteine of a PFTase substrate with a caging group should in principle prevent its farnesylation by the enzyme. This alkylation would reduce the

coordination of the thiol of cysteine with a key Zn(II) within the active site[12], reduce the nucleophilicity of cysteine as well as introduce a sterically demanding caging group in the active site. We decided to use utilize the caging groups BHQ and bhc to form thioether linkages to cysteine; bhc coumarin derivatives have been utilized to cage thiols[13] and while BHQ has not been employed to cage thiols it has been an effective group for alcohols and one- and two-photon processes[14].

4.2 Research Objectives

Here are described the synthesis of four caged peptide substrates of PFTase and the characterization of the one-photon uncaging products of these peptides. We then conduct an *in vitro* farnesylation assay to show that a caged peptide is not a substrate for PFTase but once irradiated via one- and two-photon processes the peptide becomes a viable PFTase substrate again. In addition, we conduct computational experiments that show a caged peptide bound to PFTase.

4.3 Results and Discussion

4.3.1 Synthesis of caged cysteine residues

Caged peptides **1-4** (Fig. **4.1**) were synthesized utilizing cysteine analogues Fmoc-cys(MOM-BHQ)-OH (**5**) or Fmoc-cys(MOM-bhc)-OH (**6**) as amino acid building blocks for SPPS.

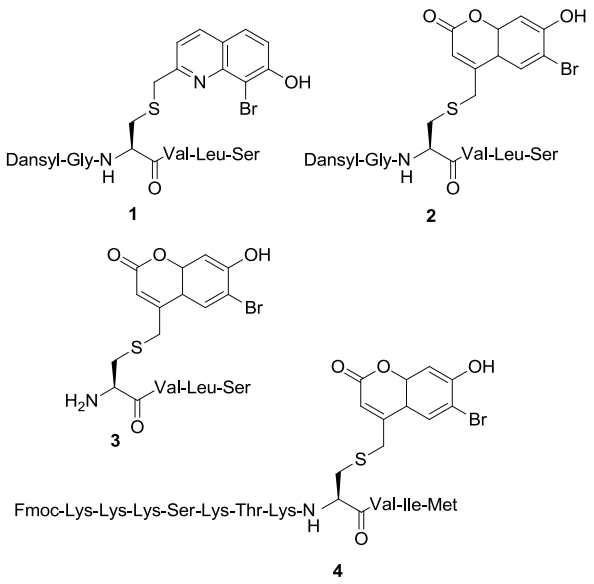

Figure 4.1. Cysteine-modified peptides using the BHQ and bhc caging groups.

BHQ-protected cysteine was prepared from the known compound MOM-BHQ-OH[15] (Scheme **4.1**). This alcohol was converted into a chloride utilizing tosyl chloride and dimethylaminopyridine. Normally, these conditions lead to tosylation but once this benzyl tosylate is formed it is reactive enough to allow the chloride anion to displace it giving MOM-BHQ chloride **8** in 71% yield. Chloride **8** was used to alkylate Fmoc-cysteine methyl ester in the presence of zinc acetate in order to give BHQ-caged cysteine methyl ester **9** in 50% yield. Removal of the methyl ester of **9** was accomplished by refluxing with trimethyl tin hydroxide to give free acid **5** in 91% yield.

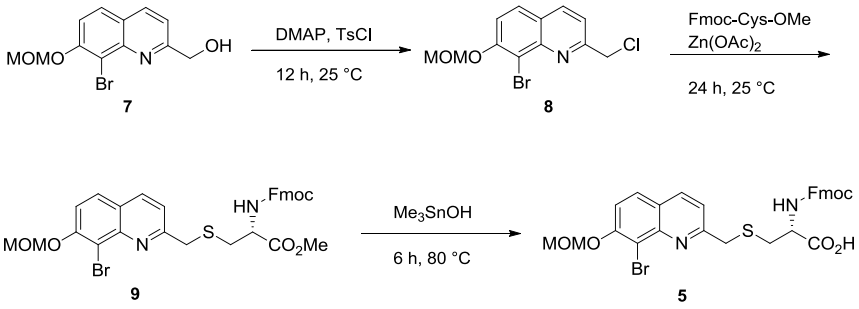

Scheme 4.1. Synthesis of BHQ-caged Fmoc-cysteine **5**.

Bhc-caged cysteine **6** was prepared in a similar fashion from the known compound bhc chloride[16] (Scheme **4.2**). The phenol of bhc-chloride **10** was protected as a MOM ether utilizing chloromethyl methyl ether and triethylamine to give MOM-protected chloride **11** in 87% yield. This chloride was subsequently used to alkylate Fmoc-cysteine methyl ester in order to give **12** in 81% yield, and trimethyl tin hydroxide was used to obtain free acid caged cysteine **6** in 90% yield.

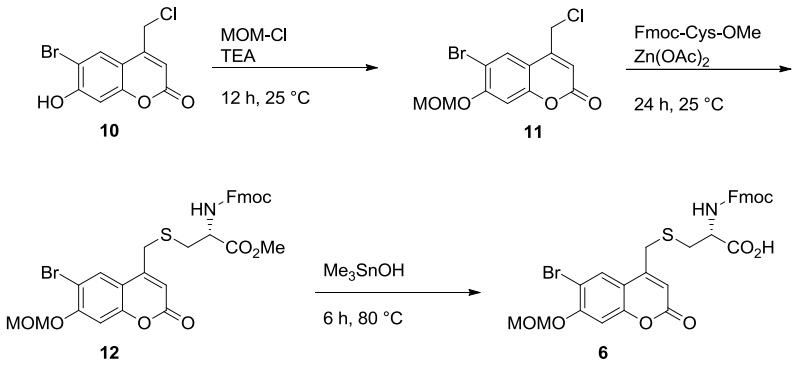

Scheme 4.2. Synthesis of bhc-caged Fmoc-cysteine **6.**

4.3.2 Synthesis of caged peptides

The general strategy for the synthesis of the caged peptides consisted of solid-phase coupling of amino acids in order to incorporate caged cysteines **5** and **6** (Scheme **4.3**), which was accomplished via manual Fmoc chemistry on a Wang resin. The only exception was the coupling of **5** and **6** to the peptide sequence. The aforementioned caged cysteines and resin were reacted with BOP and DIEA and allowed to stir overnight in order to afford resin-bound caged cysteines **13** and **14**. Finally, treatment of the resins with Reagent K removed the amino acid protecting groups as well as the MOM protecting group to afford the desired deprotected caged peptides **1-4**. The Fmoc, dansyl, BHQ and bhc groups were found to be stable to long treatments of TFA required for the deprotections.

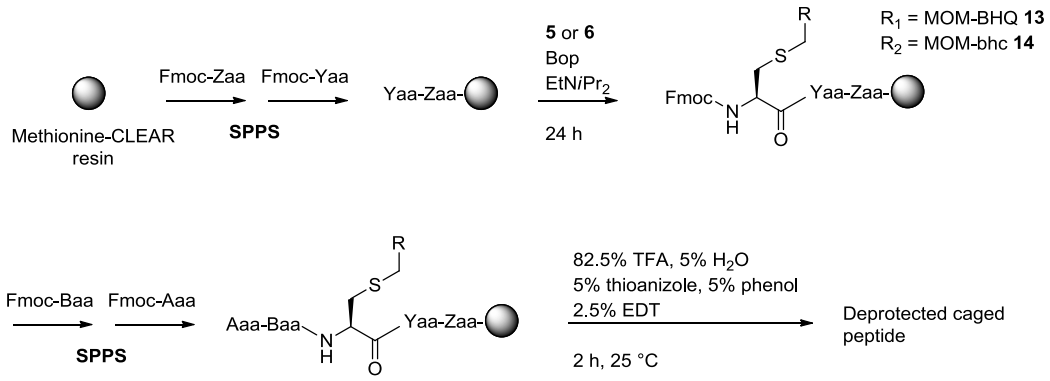

Scheme 4.3. Solid phase synthesis of caged peptides **1-4.**

4.3.3 Analysis of one-photon photolysis products

Compounds **1-3** were subjected to one-photon irradiation conditions in order to evaluate their uncaging kinetics. Solutions of 100 μM of **1-3** in PBS buffer containing 1mM DTT (pH = 7.2) were irradiated using a 365 nm light from a photoreactor for varying amounts

of time. These solutions were then monitored by HPLC in order to generate decay time courses as well as analyzed via LC-MS to confirm the formation of the corresponding free peptides. A comparison of decay times for the photolysis caged peptides **1-3** is shown in Figure **4.2**.

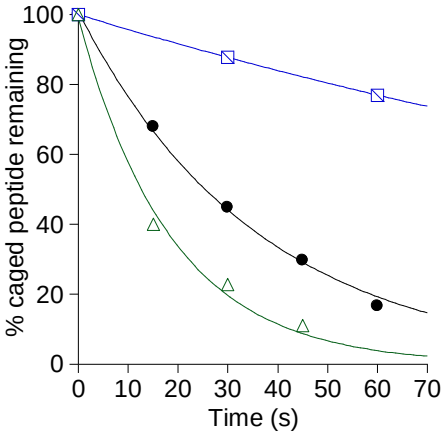

Figure 4.2. Photolysis time courses of caged compounds **1**-**3**. Peptides **1** and **3** (filled circle and open triangle, respectively) undergo photolysis very quickly compared to peptide **2** (crossed square), which is much slower to photolyze.

In the case for BHQ-caged peptide **1**, LC-MS analysis of photolyzed material revealed that ds-GCVLS (**15**, Fig. **4.3**) is only a minor photolysis product. Instead, a compound with a mass that corresponds to a dehydrobrominated version of **1** was the major product. We speculate that when the caging group gets into an excited state it undergoes a pathway that leads to the loss of HBr , rendering BHQ unable to be cleaved from the thiol moiety.

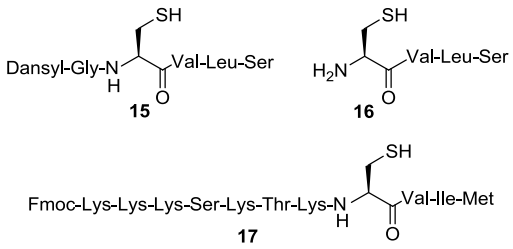

Figure 4.3. Peptides produced from the photolysis of caged peptides **1-4.**

We then conducted the photolysis of bhc-caged peptide **2** and analyzed its reaction products. Upon analysis by LC-MS we discovered that the ds-GCVLS (**15**) generated by this photolysis is only a minor reaction product with a retention time of 24.1 min. The major photolysis product corresponds to an isomer of **2**, having the same molecular weight but slightly longer retention time (t_R = 25.6 min). It is possible that upon photolysis the bhc cation that is formed is quickly captured by the nearby electron-rich dansyl group forming a stable molecule that does not undergo further photolysis.

To confirm this hypothesis bhc-caged peptide **3** was synthesized, which has the same amino acid sequence as **2** but without dansyl glycine fluorophore. Upon photolysis and further inspection by LC-MS, CVLS (**16**) was confirmed as the major product of this photolysis reaction, indicating that indeed the dansyl group was responsible for the formation of an isomer upon photolysis of **2**.

Caged peptide **4** was synthesized with the expectation that its uncaging behavior would be similar to **3**, and the Fmoc chromophore was left attached to the N-terminus to facilitate HPLC UV analysis. LC-MS analysis of photolyzed **4** revealed the disappearance of starting material **4** (t_R = 19.9 min, m/z = 1544, Fig. **4.4A**) and the

production of an ion of m/z = 1294 (t_R = 18.2 min, Fig. **4.4C**) in the extracted ion current chromatogram that corresponds to free peptide Fmoc-KKKSKTKCVIM (**17**, t_R = 18.2 min, m/z = 1294, Fig. **4.4B**). Inspection of the MS/MS reveals that the fragmentation of **17** used as a standard (Fig. **4.4D**) is identical to that of the peptide obtained from the photolysis of **4** (Fig. **4.4E**). No isomers or other photoproducts were detected in this case.

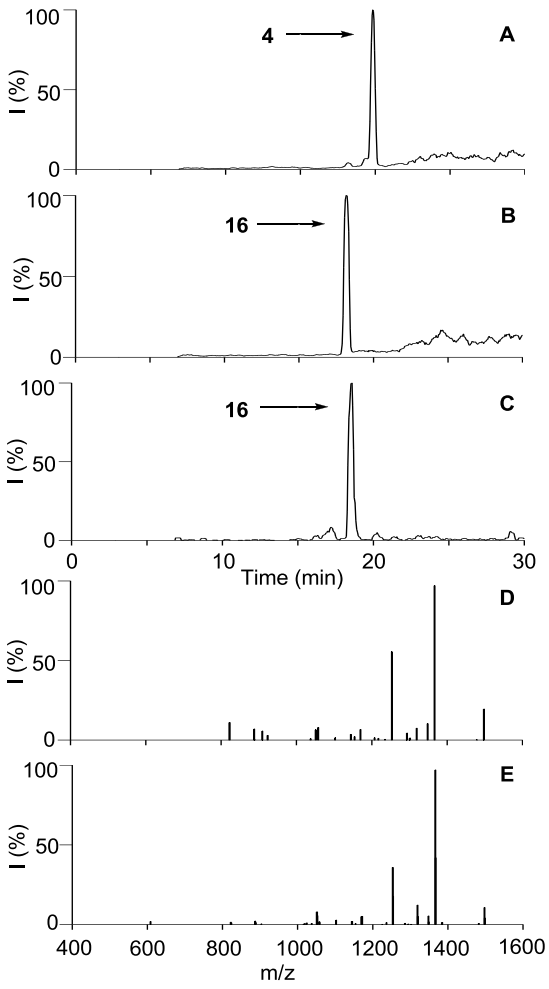

Figure 4.4. LC-MS analysis of the photolysis of caged peptide **4**. A) Extracted ion current (EIC) chromatogram (m/z = 1760-1780) of **4**. B) EIC chromatogram (m/z = 1510-1520) of **17**. C) EIC chromatogram (m/z = 1510-1520) of **4** photolyzed for 60 sec

showing the formation of **17**. D) MS/MS of **17**. E) MS/MS of **17** produced from the photolysis of **4**.

The efficiency of **17** released upon irradiation of **4** was determined via an HPLC assay using a synthesized standard of **17** to determine the amount produced from photolysis (Fig. **4.5**). The amount of **4** and **17** present before and after photolysis were determined by their UV absorbance. Caged peptide **4** photolyzes more slowly compared to compounds **1** and **3**, but it is efficiently converted to **17** with a 70-80% yield. This indicates that the bhc group is also useful for inactivating the thiol of peptides.

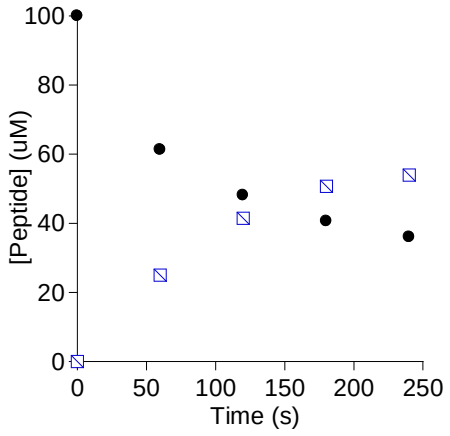

Figure 4.5. Quantitation of peptide **17** production upon photolysis of caged peptide **4**. As peptide **4** (filled circle) is photolyzed the appearance of peptide **17** (crossed square) is observed by HPLC. The overall efficiency of conversion is 70-80%.

4.3.4 One-photon enzymatic studies

Caged peptide **4** should not be a substrate for the PFTase enzyme while caged, but once irradiated it should behave as regular peptide and become farnesylated by the enzyme

(Fig. **4.6**). To test this hypothesis we set up an *in vitro* farnesylation assay using farnesyldiphosphate (FPP) and rat PFTase and synthesized Fmoc-KKKSKTKC(farnesyl)VIM (**18**) as a standard to facilitate analysis.

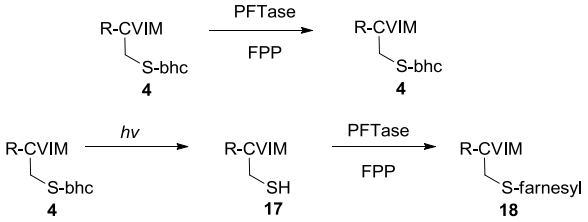

Figure 4.6. Enzymatic studies with caged peptide **4**. When the bhc group is present, PFTase is unable to process a peptide substrate. After photolysis of **4** the bhc group is unmasked, releasing peptide substrate **17** which is then processed by PFTase to farnesylated peptide **18.**

As predicted, caged peptide **4** was not farnesylated when treated with our assay conditions. HPLC analysis of the farnesylation reaction with caged peptide **4** did not result in the formation of a peak that matches the retention time of **18** (t_R = 22.6 min). Caged peptide **4** was then subjected to 10 minutes of photolysis in the presence of Tris buffer and DTT, and this photolyzed solution was analyzed by HPLC. Starting material **4** (Fig. **4.7A**, t_R = 20.5 min) has almost complete been uncaged and a new peak with a retention time of 19.4 min appears (Fig **4.7B**). This photolyzed material was then reacted with the same enzymatic farnesylation conditions and HPLC analysis of this reaction resulted in the formation of a peak with the same retention time as **18** (Fig. **4.7C**, t_R = 22.6 min). Subsequent MS/MS analysis of this peak (Fig. **4.7E**) matched the MS/MS spectrum of our standard farnesylated peptide as well (Fig. **4.7D**).

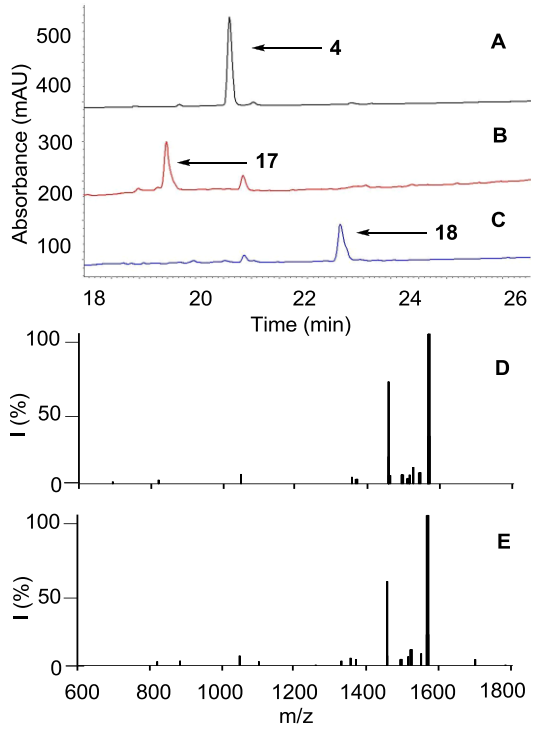

Figure 4.7. Photolysis and farnesylation of caged peptide **4**. A) UV chromatogram of pure **4**. B) UV chromatogram of **4** photolyzed for 10 min shows the elution of free peptide **17** at 19.4 min. C) UV chromatogram of photolyzed **4** subjected to an *in vitro* farnesylation assay shows the elution of farnesylated peptide **18** at 22.6 min. D) MS/MS of farnesylated **18** standard. E) MS/MS of farnesylated **18** obtained from the photolysis and farnesylation of **4**.

4.3.5 Two-photon enzymatic studies

Since it would be useful to employ these molecules for studies in more complex systems where phototoxicity is a relevant concern, caged farnesylation sequence **4** was also subjected to two-photon uncaging conditions aiming to replicate our one-photon enzymatic results. A solution of 1 mM **4** in PBS buffer and 1 mM DTT was irradiated using 800 nm light from a fs-pulsed and mode-locked Ti:sapphire laser[17] (15 mW) for 2

hours. HPLC analysis of the photolyzed solution reveals a small amount of uncaging of **4** and elution of a peak that matches the retention time of **17** of 19.4 min (Figure **4.8A**). Analysis of this peak by MS/MS revealed a mass of 1294 m/z and a fragmentation pattern (Fig. **4.8D**) that matches that of standard peptide **17** (Fig. **4.8C**). An aliquot of this irradiated solution was then treated with farnesylation assay conditions and allowed to react for 2 hours. The elution of a peak with the same retention time as our standard farnesylated peptide **18** (t_R = 22.6) was detected by HPLC (Figure **4.10B**).

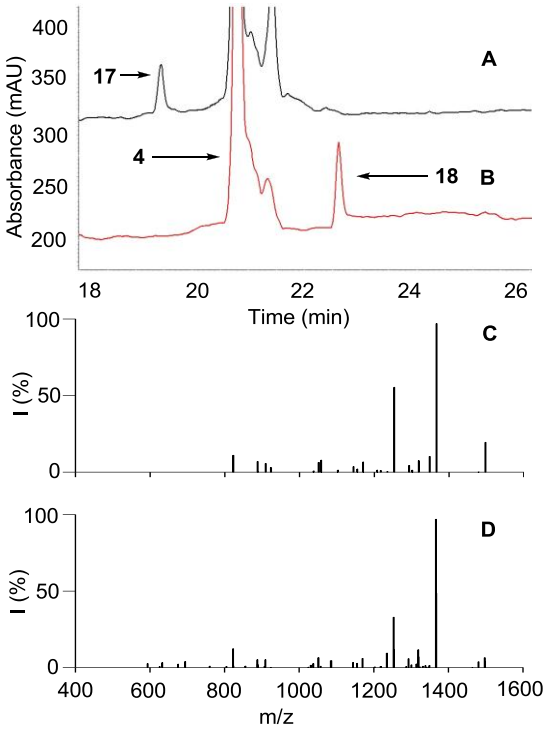

Figure 4.8. Two-photon photolysis and farnesylation of caged peptide **4**. A) UV chromatogram of caged peptide **4** subjected to two-photon irradiation for 2 hours, peptide **4** elutes at 20.7 min and a small amount of **17** is observed at 19.4 min. B) UV chromatogram of **4** subjected to two-photon irradiation for 2 hours and subsequently applied to an *in vitro* farnesylation assay shows the elution of farnesylated **18** at 22.6 min. C) MS/MS of pure **17**. D) MS/MS of **17** produced from the two-photon photolysis of caged peptide **4**.

4.3.6 Computational studies with Fmoc-KKKSKTKC(bhc)VIM

We were interested in obtaining a crystal structure of **4** bound to PFTase for x-ray crystallographic analysis. Unfortunately, we were unable to see any convincing density for **4** in the active site of the enzyme despite high soaking concentrations and lengthy soak periods during the crystallization (Mike Haast, unpublished). This led us to wonder if the coumarin group of bhc is too sterically demanding to fit in the active site of PFTase.

In order to find this out a computational search with Maestro software was carried out utilizing a crystal structure of rat PFTase bound with the substrate peptide sequence TKCVFM and a non-reactive analogue of FPP (PBD ID: 1JCS, Fig. **4.9A**). In this conformational search the caged peptide TKC(bhc)VIM (**19**) was built into the active site of PFTase to replace TKCVFM. To simplify calculations the peptide was not allowed to move and force field OPLS_2005 was applied before minimizing the energy of **19**. From these calculations we obtained 5 hits with a lowest potential energy of -5.41×10^6 for **19**. The interaction between the surface of the enzyme and **19** (Fig. **4.9B**) suggests that the bhc group does indeed fit into the active site of PFTase. In light of these results it is likely that during our crystallization experiments caged peptide **4** did not bind strongly enough to the enzyme to form crystal structures.

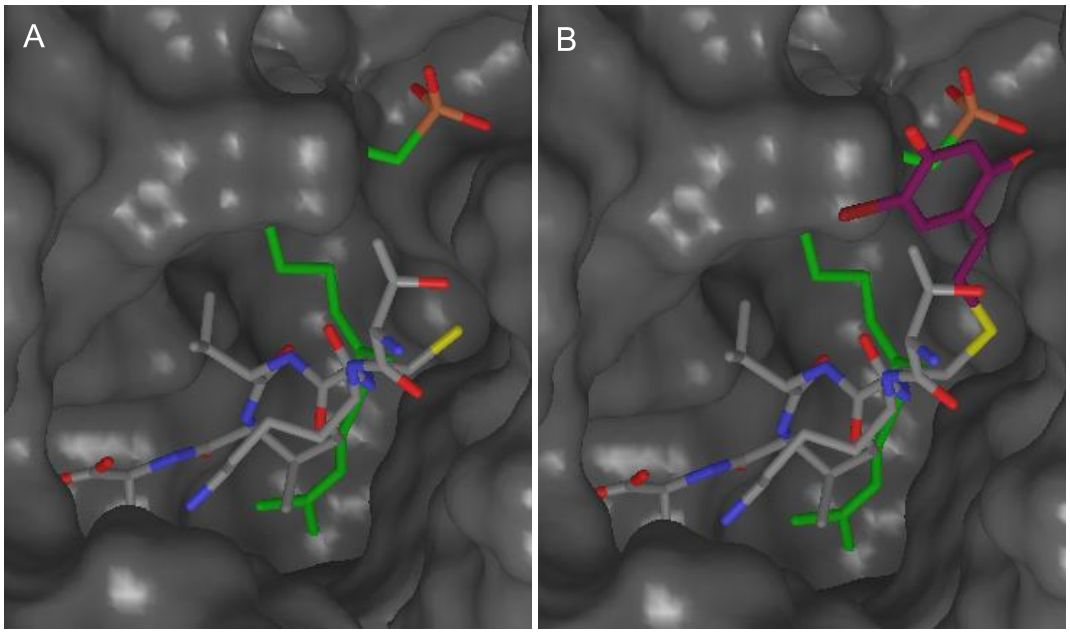

Figure 4.9. Conformational search fitting caged peptide **19** into the active site of the enzyme PFTase. A) Surface of active site of PFTase with TKCVIM (gray) and FPP (green). The free cysteine residue is colored yellow. B) Superimposition of a conformational search hit using caged peptide **19**. The bhc group (magenta) fits in the active site pocket.

4.4 Conclusions and Future Directions

We have synthesized four peptides with a caged cysteine moiety utilizing the BHQ or bhc photolabile protecting groups and studied their release under one-photon irradiation conditions. Analysis of the released photoproducts of peptide **1** indicates that the BHQ group is not a suitable protecting group for thiols, as it produces trace amounts of desired thiol and instead generates a debrominated product that does not undergo further photolysis. On the other hand, the bhc group is a useful protecting group for thiols. With

the exception of peptide **2**, where the electron-rich dansyl group appears to capture the bhc cation upon release, peptides **3** and **4** uncaged without incident and released their corresponding free thiols as the major photolysis product. The bhc group disrupted the ability of the enzyme PFTase to process a peptide that would normally be a substrate, while irradiation with one and two photon conditions allowed the farnesylation of the aforementioned peptide. Finally, a conformational search revealed that the bhc group is able to fit inside the active site of PFTase but also weakens the ability of a peptide to bind to the enzyme itself. These findings suggest it may be possible to regulate and study the farnesylation of peptides in cells by incorporating the bhc group.

4.5 Experimental

Compounds **7**[15] and **10**[16] were prepared from their respective literature procedures. All other reagents and solvents were purchased from commercial sources and used without further purification. ^{1}H NMR was recorded at 300 or 500 MHz on Varian instruments at 25 °C. HR-MS was performed on a Bruker BioTOF II instrument from Bruker Daltonics, Inc. (Fremont, CA). HPLC analysis (analytical and preparative) was performed on a Beckman model 125/166 instrument, equipped with a UV detector and C18 columns (Varian Microsorb-MV, 5 µm, 4.6 x 250 mm and Phenomenex Luna, 10 µm, 10 x 250 mm respectively). LC-MS analysis was performed on a Thermo LCQ Deca ion trap mass spectrometer (Thermo Scientific, San Jose, CA) interfaced with an Agilent 1100 Capillary HPLC. The column utilized was an Agilent Zorbax 300SB-C18, 5 µm,

0.5 x 150 mm. PBS buffer consisted of 137 mM NaCl, 2.7 mM KCl, 10 mM Na_2HPO_4 and 1.76 mM KH_2PO_4 adjusted to pH 7.4 with HCl.

4.5.1 Synthesis of BHQ-caged residues

MOM-BHQ chloride (8). Dimethylamino pyridine (22.5 mg, 0.185 mmol) and tosyl chloride (31 mg, 0.162 mmol) were dissolved in dichloromethane and stirred for 5 min. MOM-BHQ alcohol **7** (46 mg, 0.154 mmol) was then added and the reaction left stirring overnight. The reaction was then diluted with dichloromethane and washed with H_2O (2 x 10 mL). The organic layer was dried over $MgSO_4$, the solvent removed, and purified via flash column (100% dichloromethane). A yellow solid was obtained (30 mg, 0.0946 mmol, 71% yield). ^{1}H NMR ($CDCl_3$) δ 8.16 (1H, d, J=8.5 Hz), 7.76 (1H, d, J=9.0 Hz), 7.60 (1H, d, J=8.5 Hz), 7.53 (1H, d, J=9.0 Hz), 5.42 (2H, s), 4.91 (2H, s), 3.58 (3H, s). HR-MS (ESI) *m/z* calcd for $(C_{12}H_{11}BrClNO_2 + H)^+$ 315.9734 (^{79}Br) and 317.9711 (^{81}Br), found 315.9765 (^{79}Br) and 317.9722 (^{81}Br).

Fmoc-cysteine(MOM-BHQ) methyl ester (9). Chloride **8** (25 mg, 0.079mmol) and Fmoc-cysteine methyl ester (70 mg, 0.20mmol) were dissolved in 3 mL of a solution of 2:1:1 dimethylformamide/CH_3CN/ H_2O/0.1% TFA. Zinc acetate was then added (65 mg, 0.30 mmol) and the reaction monitored by TLC (1:1 hexane/ethyl acetate). After two days the solvent was removed and the reaction purified via column chromatography to give 25 mg of **9** as white powder (50% yield). ^{1}H NMR ($CDCl_3$) δ 8.12 (1H, d, J=8.4 Hz) 7.72 (5H, m), 7.50 (1H, d, J=8.7 Hz), 7.41 (5H, m), 5.40 (3H, s), 4.75 (1H, m), 4.44

(2H, m), 4.29 (3H, m), 3.95 (1H, d, J=13.5), 3.74 (3H, s), 3.58 (3H, s), 3.01 (2H, m). HR-MS (ESI) *m/z* calcd for $(C_{31}H_{29}BrN_2O_6S + H)^+$ 637.1002 (^{79}Br) and 639.0987 (^{81}Br), found 637.1055 (^{79}Br) and 639.1038 (^{81}Br).

Fmoc-cysteine(MOM-BHQ) acid (5). Ester **9** (37 mg, 0.058 mmol) was dissolved in dichloroethane (3 mL) and Me_3SnOH (47 mg, 0.26 mmol) was added to the solution. The reaction was then refluxed and monitored by TLC (1:1 hexane/ethyl acetate). After 6 hours the reaction was judged complete, the solvent was removed, and the resulting oil redissolved ethyl acetate (20 mL). The organic layer was washed with 5% HCl (10 mL) and brine (10 mL), dried and evaporated to give 36 mg of **5** as a brittle brown powder in 91% yield. ^{1}H NMR ($CDCl_3$) δ 8.14 (1H, d, J=8.1 Hz) 7.5 (11H, m), 6.95 (1H, d, J=8.4 Hz), 5.38 (3H, s), 4.75 (1H, m), 4.44 (2H, m), 4.29 (3H, m), 3.95 (1H, d, J=11.2 Hz), 3.55 (3H, s), 3.01 (2H, m). HR-MS (ESI) *m/z* calcd for $(C_{30}H_{27}BrN_2O_6S + H)^+$ 623.0863 (^{79}Br) and 625.0865 (^{81}Br), found 623.0846 (^{79}Br) and 625.0830 (^{81}Br).

4.5.2 Synthesis of bhc-caged residues

MOM-bhc chloride (11). Bhc-Cl (**10**) (200 mg, 0.69 mmol) was dissolved in 20 mL THF under a nitrogen atmosphere. Triethylamine (211 µL, 1.5 mmol) was then added, followed by drop wise addition of chloromethyl methyl ether (105 µL, 1.4 mmol). The reaction was then left stirring overnight. The THF was removed *in vacuo* and the reaction rediluted with $CHCl_3$ (50 mL), washed with H_2O (3 x 20 mL) and brine (3 x 20 mL), dried and evaporated. The crude material was then purified via column

chromatography (2:1 hexane/EtOAc) to give a yellow powder in 86% yield. ^{1}H NMR ($CDCl_3$) δ 7.83 (1H, s) 7.17 (1H, s), 6.45 (1H, s), 5.32 (2H, s), 4.60 (2H, s), 3.52 (3H, s). HR-MS (ESI) *m/z* calcd for $[C_{12}H_{10}BrClO_4 + H]^+$ 332.9524 (^{79}Br, ^{35}Cl), 334.9502 (^{81}Br, ^{35}Cl) and 336.9479 (^{81}Br, ^{37}Cl); found 332.9531 (^{79}Br, ^{35}Cl), 334.9522 (^{81}Br, ^{35}Cl) and 336.9492 (^{81}Br, ^{37}Cl).

Fmoc-cysteine(MOM-bhc) methyl ester (12). Chloride **11** (93 mg, 0.28 mmol) and Fmoc-cysteine methyl ester (200 mg, 0.56 mmol) were dissolved in 3 mL of a solution of 2:1:1 dimethylformamide/CH_3CN/H_2O/0.1% TFA. Zinc acetate was then added (154 mg, 0.70 mmol) and the reaction monitored by TLC (1:1 hexane/ethyl acetate). After two days the solvent was removed and the reaction purified via column chromatography (1:1 hexane/ethyl acetate) to give 149 mg of **5** as yellow powder (81% yield). ^{1}H NMR ($CDCl_3$) δ 7.83 (1H, s) 7.76 (2H, d, J = 7.5), 7.6 (2H, d, J=7.5 Hz), 7.39 (2H, m), 7.31 (2H, m), 7.14 (1H, s), 6.28 (1H, s), 5.29 (2H, s), 4.65 (1H, m), 4.49 (2H, m), 4.22 (1H, t), 3.78 (3H, s), 3.50 (3H, s). HR-MS (ESI) *m/z* calcd for $(C_{31}H_{28}BrNO_8S + Na)^+$ 676.0611 (^{79}Br) and 678.0596 (^{81}Br), found 676.0639 (^{79}Br) and 678.0636 (^{81}Br).

Fmoc-cysteine(MOM-bhc) acid (6). Ester **12** (100 mg, 0.15 mmol) was dissolved in dichloroethane (5 mL) and Me_3SnOH (69 mg, 0.38 mmol) was added to the solution. The reaction was then refluxed and monitored by TLC (1:1 hexane/ethyl acetate). After 7 hours the reaction was judged complete, the solvent removed *in vacuo* and the resulting oil redissolved ethyl acetate (20 mL). The organic layer was washed with 5% HCl (3 x

10 mL) and brine (3 x 10 mL), dried and evaporated to give 92 mg of **1** as a yellow powder (90% yield). ^{1}H NMR (d-acetone) δ 8.12 (1H, s), 7.86 (2H, d, J=7.5), 7.73 (2H, t, J=7), 7.41 (2H, t, J=7.5), 7.33 (2H, m), 7.16 (1H, s), 6.36 (1H, s), 5.73 (1H, d, J=7.5), 5.29 (2H, s), 4.43 (2H, dd, J=7, 20), 4.21 (1H, t, J=6.5), 3.74 (2H, q, J=10.5), 3.50 (3H, s), 2.94 (1H, dd, J=6, 14.5). HR-MS (ESI) *m/z* calcd for $(C_{30}H_{26}BrNO_8S + Na)^+$ 662.0455 (^{79}Br) and 664.0439 (^{81}Br), found 662.0472 (^{79}Br) and 664.0428 (^{81}Br).

4.5.3 General synthesis of caged peptides

The linear peptide sequences were assembled by manual Fmoc chemistry on a methionine-Wang resin (0.25 mmol) with 4 mmol equivalents of amino acid at each step. The only exception was the coupling of **5** and **6**. Caged cysteines **5** or **6**, Bop and diisopropylethyl amine in DMF were added to the peptide resin and allowed to react. The resin was then washed with DMF and dichloromethane and utilized in the next step without characterization.

Ds-GC(BHQ)VLS (**1**). Caged cysteine **5** (198 mg, 0.3 mmol), Bop (44 mg, 0.1 mmol) and DIEA (35 µL, 0.2 mmol) in DMF were added to the peptide resin (0.1 mmol) and allowed to stir overnight. HR-MS (ESI) *m/z* calcd for $(C_{41}H_{52}BrN_7O_{10}S_2 + H)^+$ 946.2473 (^{79}Br) and 948.2460 (^{81}Br), found 946.2404 (^{79}Br) and 948.2390 (^{81}Br).

Ds-GC(bhc)VLS (**2**). Caged cysteine **6** (192 mg, 0.3 mmol), Bop (44 mg, 0.1 mmol) and DIEA (35 µL, 0.2 mmol) in DMF were added to the peptide resin (0.1 mmol) and allowed to stir overnight. HR-MS (ESI) *m/z* calcd for $(C_{41}H_{51}BrN_6O_{12}S_2 + H)^+$ 963.2363 (^{79}Br) and 965.2250 (^{81}Br), found 963.2302 (^{79}Br) and 965.2311 (^{81}Br).

C(bhc)VLS (**3**). Caged cysteine **6** (192 mg, 0.3 mmol), Bop (44 mg, 0.1 mmol) and DIEA (35 µL, 0.2 mmol) in DMF were added to the peptide resin (0.1 mmol) and allowed to stir overnight. HR-MS (ESI) *m/z* calcd for $(C_{27}H_{37}BrN_4O_9S + H)^+$ 673.1537 (^{79}Br) and 675.1521 (^{81}Br), found 673.1575 (^{79}Br) and 675.1548 (^{81}Br).

Fmoc-KKKSKTKC(bhc)VIM (**4**). Caged cysteine **6** (192 mg, 0.3 mmol), Bop (44 mg, 0.1 mmol) and DIEA (35 µL, 0.2 mmol) in DMF were added to the peptide resin (0.1 mmol) and allowed to stir overnight. HR-MS (ESI) *m/z* calcd for $(C_{81}H_{123}BrN_{16}O1_9S_2 + 2H)^{2+}$ 884.3960 (^{79}Br) and 885.3962 (^{81}Br), found 884.4007 (^{79}Br) and 885.4096 (^{81}Br).

4.5.4 General procedure for photolysis of caged peptides

One mL solutions of 100 µM of **1-4** were dissolved in PBS buffer and 1 mM DTT, placed in a quartz cuvette (10 x 50 mm) and irradiated with 365 nm UV light from a Rayonet reactor (16 x 14 watt bulbs). Each sample was irradiated for differing amounts of time. After each irradiation period 100 µL were analyzed by RP-HPLC. The compounds were eluted with 0.1% TFA in H_2O and 0.1% TFA in CH_3CN (gradient

3%/mL, flow rate 1 mL/min) and absorbance was recorded at 245 nm. Decay time courses were plotted using Kaleidagraph 3.0 software and analyzed by non-linear regressional analysis.

4.5.5 LC-MS analysis of caged peptides

Aliquots of 100 µL consisting of PBS buffer, 1 mM DTT and 10 µM caged peptides **1-4** previously irradiated with 365 nm UV light from a Rayonet reactor were analyzed via LC-MS. Solutions of 10 µM **15-17** were also analyzed as standards. The methods utilized are as follows: Compound **1**: flow rate: 10 µL/min, gradient: 0 % solvent B in 2 min, 0-40 % solvent B in 10 min, 40-60% solvent B in 20 min, 80-100% solvent B in 8 min, solvent A: H_2O and 0.1 % TFA, solvent B: CH_3CN and 0.1% TFA. Compound **2**: flow rate: 10 µL/min, gradient: 0 % solvent B in 2 min, 0-100 % solvent B in 30 min, solvent A: H_2O and 0.1 % TFA, solvent B: CH_3CN and 0.1% TFA. Compounds **3** and **4**: flow rate: 10 µL/min, gradient: 0-100 % solvent B in 30 min, solvent A: H_2O and 0.1 % TFA, solvent B: CH_3CN and 0.1% TFA.

4.5.6 Farnesylation of one-photon irradiated Fmoc-KKKSKTKC(bhc)VIM

A solution of **4** (1.25 µL, 2 mM) and DTT (12.5 µL, 0.5 M) in Tris buffer (125 µL, pH = 7.5) was irradiated for 10 min and was added to a farnesylation reaction cocktail solution ($MgCl_2$ (12.5 µL, 1 M), $ZnCl_2$ (6.3 µL, 2 mM), FPP (2.1 µL, 6.07 mM) and H_2O (339 µL)). This cocktail was incubated for 30 min before the addition of 1.5 µL rat

PFTase in 500 µL reaction buffer (Tris buffer (50 mL, 0.5 M), $ZnCl_2$ (12.5 µL, 2Mm), $MgCl_2$ (2.5 µL, 1M), KCl (20 µL, 0.5 M), DTT (1 µL, 0.5 M), BSA (50 µL, 10mg/mL) and H_2O (364 mL)). This new mixture was allowed to react for 1 h before analysis by HPLC at 245 nm. Solvent A: H_2O in 0.1% TFA, Solvent B: CH_3CN in 0.1% TFA, Gradient: 0% B over 2 min, 0-100% B over 30 min, 100% B over 2 min.

4.5.7 Farnesylation of two-photon irradiated Fmoc-KKKSKTKC(bhc)VIM

A solution of **4** (1 mM) and DTT (1 mM) in Tris buffer (100 µL, pH = 7.5) was irradiated for 2 h using 800 nm light from homebuilt, regeneratively amplified Ti:sapphire laser system[17] at 1 kHz with 15 µJ pulses focused to a diameter of ~1 mm and centered at a wavelength of 800 nm. The laser pulses had a Gaussian full width at half maximum of ~70 fs. A 15 µL aliquot of this solution was then added to a farnesylation reaction cocktail solution ($MgCl_2$ (75 µL, 1 M), $ZnCl_2$ (37.5 µL, 2 mM), FPP (12.4 µL, 6.07 mM) and H_2O (2035 µL)). This cocktail was incubated for 30 min before the addition of 4 µL rat PFTase in 2 mL reaction buffer. This new mixture was allowed to react for 1 h before analysis by HPLC at 245 nm. Solvent A: H_2O in 0.1% TFA, Solvent B: CH_3CN in 0.1% TFA, Gradient: 0% B over 2 min, 0-100% B over 30 min, 100% B over 2 min.

4.5.8 Conformational search using TKC(bhc)VIM

For modeling of the PFTase and **19**, the bhc moiety in **19** was built by modifying the existing peptide present in the crystal structure of the enzyme (1JCS). Once modified, a

5000 step mixed torsional/low-mode conformational search was conducted with MacroModel (Schrodinger, version 9.6) using the force field OPLS_2005. The rotatable bonds of the caged cysteine and bhc were chosen for rotational sampling, and the protein was frozen throughout the search. The resulting conformation with the lowest potential energy was chosen for display.

4.6 References

1. (a) M. C. Pirrung, *Chem. Rev.* **1997**, *97*, 473-488. (b) S. Singh-Gasson, R. D. Green, Y. Yue, C. Nelson, F. Blattner, M. R. Sussman, F. Cerrina, *Nature Biotech*. **1999**, *17*, 974-978. (c) F. Guillier, D. Orain, M. Bradley, *Chem. Rev.* **2000**, *100*, 2091-2157.
2. (a) S. R. Adams, R. Y. Tsien, *Annu. Rev. Physiol*. **1993**, *55*, 755-784. (b) G. Dorman, G. D. Prestwich, *Trends Biotechnol.* **2000**, *18*, 64-77. (c) G. Marriott, Ed. *Caged Compounds*; Academic Press: New York, 1998; Vol. 291. (d) J. E. T. Corrie, D. R. Trentham, In *Biological Applications of Photochemical Switches*; H. Morrison, Ed.; John Wiley & Sons: New York, 1993; pp 243-305. (d) J. M. Nerbonne, *Curr. Op. Neurobiol.* **1996**, *6*, 379-386.
3. W. T. Monroe, M. M. McQuain, M. S. Chang, J. S. Alexander, F. R. Haselton, *J. Biol. Chem.* **1999**, *274*, 20895-20900.
4. T. Furuta, H. Takeuchi, M. Isozaki, Y. Takahashi, M. Kanehara, M. Sugimoto, T. Watanabe, K. Noguchi, T. M. Dore, T. Kurahashi, M. Iwamura, R. Y. Tsien, *ChemBioChem* **2004**, *5*, 1119-1128.
5. C. Chungjung, D. D. Young, A. Deiters, *ChemBioChem* **2010**, *11*, 972-977.
6. S. Kantevari, M. Matsuzaki, Y. Kanemoto, H. Kasai, G. C. R. Ellis-Davies, *Nature Methods* **2009**, *7*, 123-125.
7. F. L. Zhang, P. J. Casey, *Annu Rev Biochem*, **1996**, *65*, 241-269.

8. A. Hall, *Current Opinion in Cell Biology*, **1993**, *5*, 265-268.

9. J. Ohkanda, D. B. Knowles, M. A. Blaskovich, S. M. Sebti, A. D. Hamilton, *Curr Top Med Chem* **2002**, *2*, 303-323.

10. M. Schlitzer, M. Bohm, I. Sattler, H. M. Dahse, *Bioorg. Med. Chem.* **2000**, *8*, 1991.

11. S. M. Sebti, A. D. Hamilton, *Oncogene* **2000**, *19*, 6584.

12. C. L. Strickland, W. T. Windsor, R. Syto, L. Wang, R. Bond, Z. Wu, J. Schwartz, H. V. L. Le, L. S. Beese, P. C. Weber, Biochemistry **1998**, *37*, 16601-16611.

13. (a) J. H. Wosnick, M. S. Shoichet, *Chem. Matter.* **2008**, *20*, 55-60. (b) N. Kotzur, B. Briand, M. Beyermann, V. J. Hagen, *J. Am. Chem. Soc.* **2009**, *131*, 16927-16931.

14. Y. Zhu, C. M. Pavlos, J. P. Toscano, T. M. Dore, *J. Am. Chem. Soc.* **2006**, *128*, 4267-4276.

15. T. M. Dore, Y. Zhu, K. G. Reddie, J. D. Lauderdale, (University of Georgia Research Foundation, Inc., USA). Application: US, **2010**, p. 46pp.

16. T. Furuta, S. S.-H. Wang, J. L. Dantzker, T. M. Dore, W. J. Bybee, E. M. Callaway, D. Winfried, R. Y. Tsien, *Proc. Natl. Acad. Sci. USA* **1999**, *96*, 1193-1200.

17. D. F. Underwood, D. A. Blank, *J. Phys. Chem. A* **2003**, *107*, 9

Chapter 5. Synthesis of a caged geranylgeranyltransferase inhibitor: bhc-GGTI-286

5.1 Introduction

Mutations in the Ras superfamily, proteins that bind GTP and are involved in cell regulatory pathways, have been linked to roughly 30% of human cancers[1]. Among the subfamily of proteins mostly responsible for such oncogenicity are H-Ras, K-Ras and N-Ras[2]. In order for these proteins to function properly they must be processed by protein farnesyltransferase (PFTase)[3,4]. However, both K- and N-Ras can be alternatively post-translationally modified by the enzyme geranylgeranyltransferase (GGTase)[5] if PFTase has been inhibited; once geranylgeranylated these proteins localize to the cell membrane and remain fully functional. As a result of this pathway, treatment with molecules designed to inhibit Ras farnesylation, farnesyltransferase inhibitors (FTIs)[6,7], does not lead to inactivation in the case of K- and N-Ras[8]. Geranylgeranyltransferase inhibitors (GGTIs) block the processing of Ras by GGTase[9], but simultaneous treatment with FTI and GGTI leads to pronounced system wide toxicity and apoptosis[10]. We would like to study the process of K- and N-Ras prenylation by applying the photoremovable protecting group bromohydroxy coumarin (bhc) to inactivate a GGTI, GGTI-236[11] (**1**, Fig. **5.1**). The thiol of GGTI **1** forms an important interaction with a Zn(II) ion positioned within the active site of GGTase[11] and alkylation of such thiol should considerably weaken this interaction. We have chosen the bhc group due to its efficacy to release thiols via one- and two-photon excitation processes (Chapter 2).

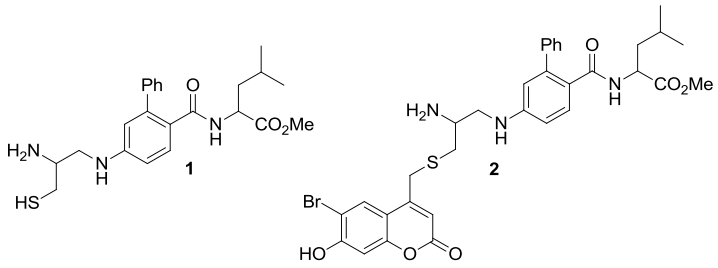

Figure 5.1. GGTI-286 (**1**) and caged inhibitor bhc-GGTI (**2**).

5.2 Research Objectives

We have synthesized a caged inhibitor of GGTase, bhc-GGTI (**2**). This was accomplished by covalently linking bhc to the active site thiol of the GGTI. This thioether-caged GGTI **2** should be a worse inhibitor of GGTase compared to commercially available **1**. Irradiation of **2** with light, however, releases active GGTI to inhibit the geranylgeranylation of K- and N-Ras. Described here is the synthesis and spectroscopic characterization of **2**.

5.3 Results and Discussion

5.3.1 Synthesis of bhc-GGTI

Synthesis of GGTI-286 (**1**) was followed according to literature procedure[11] with one modification (Scheme **5.2**). 2-bromo-1-methyl-4nitrobenzene (**3**) was reacted with phenylboronic acid to afford Suzuki-coupling product 2-methyl-5-nitro-1,1'-biphenyl (**4**) in 66% yield. The methyl group of this biphenyl was then oxidized to a carboxylic acid to afford benzoic acid (**5**) in 64% yield, which was subsequently coupled to leucine methyl ester using HOBt and EDC as the coupling reagents. This coupled leucine methyl ester (**6**) was then reacted with $SnCl_2$ to reduce the nitro group of the biphenyl core in order to yield amine **7** in 96%. This resulting free amine was coupled to N-Boc S-Trt cysteinal (**8**) under reductive amination conditions to afford N-Boc S-Trt protected GGTI (**9**) in 43%. The deprotection of this intermediate was carried in an alternate fashion compared to literature procedure; protected GGTI **9** was reacted with Reagent K over 6 h and subsequently purified by semipreparative HPLC to afford GGTI-286 (**1**).

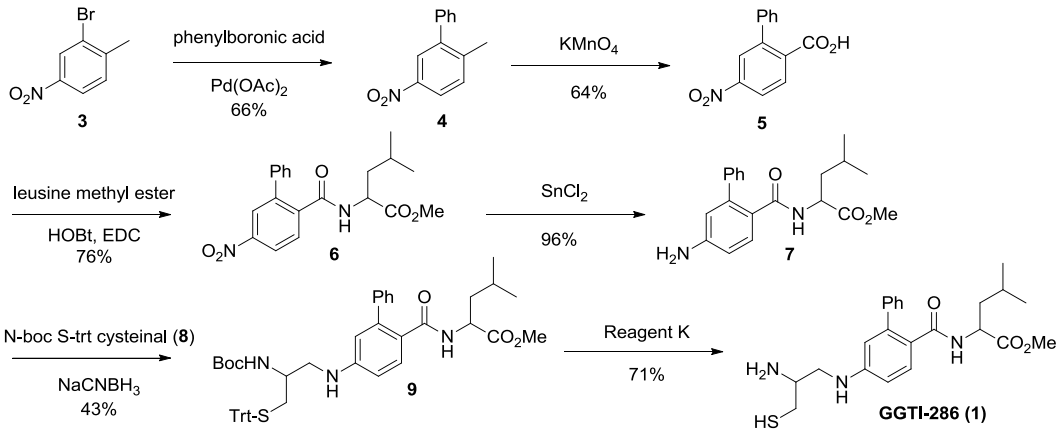

Scheme 5.1. Synthesis of GGTI-286 (**1**).

Upon synthesis of GGTI-286, the next step was to mask its active site thiol with the bhc caging group (Scheme **5.2**). This was accomplished using the same method as the inactivation of the FTI thiol with bhc and BHQ. GGTI (**1**) was reacted with MOM-bhc-Cl (**9**) and $Zn(OAc)_2$ under acidic pH conditions in order to give MOM-protected bhc-GGTI (**10**) in 79% yield after HPLC purification. The MOM ether was subsequently removed by addition of Reagent K for 2 h before HPLC purification to give caged inhibitor bhc-GGTI (**2**) in 94% yield.

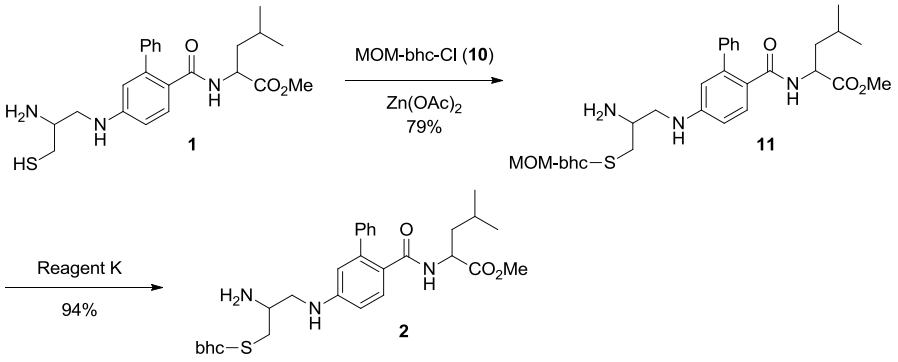

Scheme 5.2. Synthesis of caged inhibitor bhc-GGTI (**2**).

5.4 Conclusion and Future Directions

The synthesis of a thiol-caged GGTI with bhc has been completed. It remains to be seen whether caged GGTI **2** photolyzes at a similar rate and efficiency via one- and two-photon excitation as bhc-FTI. Additionally, biological experiments must be performed in order to assess the reduced reactivity of caged GGTI **2** towards inhibiting the geranylgeranylation of Ras and whether one- and two-photon excitation processes can

produce biologically relevant concentrations of free GGTI **1**. Experiments to address these features are ongoing.

5.5 Experimental

5.4.1 Synthesis of bhc-GGTI

4-Nitro-2-phenyltoluene (4). 4-Nitro-2-bromotoluene (**3**, 6.48 g, 30 mmol) and phenyl boronic acid (3.84 g, 31.5 mmol) were dissolved in 70 mL of acetone. To this mixture was added 85mL of water, potassium carbon-ate hydrate (12.4 g, 75 mmol, 2.5 equiv) and $Pd(OAc)_2$ (0.33 g, 5%equiv). The mixture was refluxed for 10 h and then cooled. The deep black solution was extracted with ether and 3 N HCl. The ether fraction was passed though a layer of Celite. After evaporating solvents, the residue was dried and then recrystallized from methanol to give flake crystals (4.60 g, 88%). ^{1}H NMR ($CDCl_3$) 8.13 (m, 2H), 7.45 (m, 4H), 7.32 (m, 2H), 2.38 (s, 3H).

4-Nitro-2-phenylbenzoic acid (5). 4-Nitro-2-phenyltoluene (**4**, 3.20 g, 15 mmol) was dissolved in 15mL of pyridine and 30mL of water. The mixture was heated to 90 ˚C and then $KMnO_4$ (14.2 g, 90 mmol) was added in portions. The mixture was refluxed for 5 h. The black solid was filtered and the filtrate was acidified with 6 N HCl. The mixture was cooled in an ice bath and the white precipitate was collected (3.1 g, 85%). ^{1}H NMR ($CDCl_3$) 8.26 (m, 2H), 8.07 (d, 1H), 7.45 (m, 3H), 7.38 (m, 2H).

N-[4-Nitro-2-phenylbenzoyl]-leusine methyl ester (6). Compound **5** (2.43 g, 10 mmol) was suspended in 50 mL of DCM. To this solution in an ice bath was added (l)-leusine methyl ester hydrochloride (2.0 g, 10 mmol), triethylamine (1.38mL, 10 mmol), EDCI (2.01 g, 10.5 mmol) and HOBT (1.35 g, 10 mmol). The mixture was stirred at room temperature for 10 h and then extracted with DCM and 1 N HCl. The organic layer was washed with concentrated sodium bicarbonate and dried. After evaporating solvents, the residue was recrystallized from EtOAc and hexane to give 19 (3.22 g, 83%). ^{1}H NMR ($CDCl_3$) 8.25 (m, 2H), 7.86 (m, 1H), 7.45 (m, 5H), 5.72 (d, 1H), 4.56 (m, 1H), 3.67 (s, 3H), 1.40 (m, 1H), 1.25 (m, 1H), 1.16 (m, 1H), 0.80 (d, 6H).

N-[4-Amino-2-phenylbenzoyl]-leusine methyl ester (7). Compound **7** (3.04 g, 7.83mmol) was dissolved in 100 mL of EtOAc. Stannous chloride hydrate (8.84 g, 39mmol) was added and the mixture was refluxed for 2 h. This solution was poured into 200 mL of concentrated sodium bicarbonate and extracted with EtOAc. After evaporating solvents, the residue was dissolved in 10 mL of DCM and 15mL of 3 N HCl in ether was added. Solvents were evaporated and a hydrochloride salt was obtained (2.97 g, 96%). ^{1}H NMR ($CDCl_3$) 7.69 (d, 1H), 7.39 (m, 5H), 6.70 (d, 1H), 6.55 (s, 1H), 5.43 (d, 1H), 4.47 (m, 1H), 3.65 (s, 3H), 1.35 (m, 1H), 1.15 (m, 2H), 0.80 (d, 6H).

N-[4-[N-[2(R)-(tert-Butoxycarbonyl)amino-3-(triphenyl-methyl)thio]propyl]amino-2-phenylbenzoyl]-methionine methyl ester (9). Amine **7** (1.27 g, 3.22 mmol) was dissolved in 10 mL of MeOH and N-Boc-S-Trt cysteinal (**8**, 1.0 equiv) was added. After stirring for 10 min, sodium cyanoborohydride (305 mg, 1.5 equiv) was added and the

mixture was stirred for 12 h at room temperature. After evaporating solvents, the residue was extracted with EtOAc and concentrated sodium bicarbonate. Solvents were evaporated and the residue was purified by flash column chomatography (1:1 hexane/EtOAc) to give **9** as a fluffy foam (1.84 g, 74%). ^{1}H NMR ($CDCl_3$) 7.69 (d, 1H), 7.39 (m, 9H), 7.25 (m, 7H), 6.51 (d, 1H), 6.33 (s, 1H), 5.41 (d, 1H), 4.55 (s, 1H), 4.45 (m, 1H), 4.17 (s, 1H), 3,80 (s, 1H), 3.64 (s, 3H), 3.10 (m, 2H), 2.44 (m, 2H), 1.56 (s, 9H), 1.30 (m, 1H), 1.15 (m, 2H), 0.80 (d, 6H).

GGTI-286 (1). N-Boc and S-Trt-protected GGTI **9** (50 mg, 65 μmol) was dissolved in 20 mL Reagent K (TFA/H_2O/thioanisole/phenol/ethanedithiol 82.5:5:5:5:2.5) for 6 h. Excess TFA was removed via rotary evaporation and the crude mixture purified via RP-HPLC (Solvent A: H_2O in 0.1% TFA, Solvent B: CH_3CN in 0.1% TFA, Gradient: 0% B over 5 min, 0-50% B over 15 min, 50-70% B over 20 min, 70-100% B over 10 min). Caged GGTI **2** elutes at 63% B and was subsequently lyophilized to give a white powder (36 mg, 71% yield). ^{1}H NMR ($CDCl_3$) 7.46 (m, 1H), 7.29 (broad m, 6H), 6.53 (d, 1H), 6.33 (s, 1H), 6.41 (s, 1H), 5.81 (d, 1H), 4.39 (m, 1H), 4.1 (s, 1H), 3.64 (s, 3H), 3.51 (d, 1H), 3.4 (m, 2H), 2.78 (m, 2H), 1.56 (s, 9H), 1.35 (m, 1H), 1.24 (m, 1H), 1.16 (m, 1H), 0.78 (d, 6H). H-MS (ESI) *m/z* calcd for $[C_{23}H_{31}N_3O_3S + H]^+$ 429.9501, found 429.9538.

MOM-bhc-GGTI (11). MOM-bhc-Cl (**10**) (12.5 mg, 40 μmol), $Zn(OAc)_2$ (8.7 mg, 0. 40 μmol) and GGTI (**1**) (5 mg, 8 μmol) were dissolved in a solvent mixture of 2:1:1 DMF/CH_3CN/H_2O (1.6 mL) and TFA (0.1%) under a N_2 atmosphere. The reaction was protected from light and its progress was monitored by HPLC. After the reaction was

judged complete (2 days), the solvents were removed *in vacuo* and the remaining oil was purified via reversed-phase HPLC (flow rate: 5 mL/min, gradient: 0-70 % solvent B in 70 min; 70-100% solvent B in 10 min; solvent A: H_2O and 0.1 % TFA, solvent B: CH_3CN and 0.1% TFA). The desired product eluted at 47% B and was then lyophilized to give 3.5 mg of a fluffy white solid in 57% yield. ^{1}H NMR ($CDCl_3$) 7.84 (s, 2H), 7.77 (s, 1H), 7.42 (d, 1H), 7.3 (m, 2H), 7.26 (m, 4H), 7.17 (s, 1H), 7.07 (1H, s), 6.46 (s, 2H), 6.41 (s, 1H), 6.23 (s, 1H), 5.86 (d, 1H), 5.33 (s, 3H), 5.27 (s, 1H), 4.6 (s, 3H), 4.38 (m, 1H), 3.62 (s, 3H), 3.52 (s, 3H), 3.49 (s, 2H), 2.8 (m, 1H), 1.33 (m, 1H), 1.16 (m, 2H), 0.76 (d, 6H). H-MS (ESI) *m/z* calcd for $[C_{35}H_{40Br}N_3O_7S + H]^+$ 726.1896 (^{79}Br) and 728.1877 (^{81}Br); found 726.1843 (^{79}Br) and 728.1829 (^{81}Br).

bhc-GGTI (2). MOM-protected GGTI **11** (5 mg, 7.3 μM) was dissolved in 1 mL Reagent K (TFA/H_2O/thioanisole/phenol/ethanedithiol 82.5:5:5:5:2.5) for 2 h. Excess TFA was removed via rotary evaporation and the crude mixture purified via RP-HPLC (Solvent A: H_2O in 0.1% TFA, Solvent B: CH_3CN in 0.1% TFA, Gradient: 0-40% B over 15 min, 40-60% B over 20 min, 60-100% B over 10 min). Caged GGTI **2** elutes at 42% B and was subsequently lyophilized to give a white powder (4.5 mg, 94% yield). ^{1}H NMR (DMSO) 8.41 (2H, d), 8.04 (s, 2H), 7.98 (m, 3H), 7.77 (d, 1H), 7.31 (broad m, 6H), 6.89 (1H, s), 6.62 (d, 1H), 6.57 (1H, s), 6.19 (1H, s), 4.47 (m, 1H), 4.2 (m, 2H), 4.02 (s, 1H), 3.98 (2H, s), 3.6 (s, 3H), 2.83 (m, 1H), 2.81 (m, 2H), 2.72 (m, 2H), 2.22 (s, 1H), 1.99 (m, 1H), 1.55 (m, 1H), 1.38 (m, 1H), 1.22 (m, 1H), 0.8 (d, 6H). H-MS (ESI) *m/z* calcd for $[C_{33}H_{36Br}N_3O_6S + H]^+$ 682.1581 (^{79}Br) and 684.1566 (^{81}Br); found 682.1589 (^{79}Br) and 684.1582 (^{81}Br).

5.6 References

1. J. Downward, *Nat. Rev. Cancer* **2003**, *1*, 11.
2. M. A. Morgan, A. Ganser, C.W. M. Reuter, *Curr. Drug Targets*, **2007**, *8*, 217.
3. P. J. Casey, P. A. Solski, C. J. Der, J. E. Buss, *Proc. Nat. Acad. Sci. U.S.A.* **1989**, *86*, 8323.
4. F. L. Zhang, P. J. Casey, *Annu. Rev. Biochem.* **1996**, *65*, 241.
5. D. B. Whyte, P. Kirschmeier, T. N. Hockenberry, *J. Biol. Chem*. **1997**, *272* , 14459.
6. J. B. Gibbs, A. Oliff, N. E. Kohl, *Cell* **1994**, *77*, 175.
7. R. A. Gibbs, *Curr. Opin. Drug Discovery Dev.* **2000**, *3*, 585.
8. N. M. G. M. Appels, J. H. Beijnen, J. H. M. Schellens, *The Oncologist* **2005**, *10*, 565.
9. Y. Qian, A. Vogt, A. Vasudevan, S. M. Sebti, A. D. Hamilton, *Bioorg. Med. Chem.* **1998**, *6*, 293.
10. K. M. Swanson, R. J. Hohl, *Curr. Cancer Drug Targets*, **2006**, *6*, 15.
11. E. C. Lerner, Y. Qian, A. D. Hamilton, S. M. Sebti, *J. Biol. Chem.* **1995**, *270*, 26770.

Bibliography

1. M. Goard, G. Aakalu, O. D. Fedoryak, C. Quinonez, J. St. Julien, S. J. Poteet, E. M. Schuman, T. M. Dore, *Chem. Biol*. **2005**, *12*, 685.

2. M. E. Vazquez, M. Nitz, J. Stehn, M. B. Yaffe, B. Imperiali, *J. Am. Chem. Soc.* **2003**, *125*, 10150.

3. M. C. Pirrung, S. J. Drabik, J. Ahamed, H. Ali, *Bioconjugate Chem*. **2000**, *11*, 679.

4. R. O. Schonleber, J. Bendig, V. Hagen, B. Giese, *Bioorg. Med. Chem*. **2002**, *10*, 97.

5. J. Gjerstad, E. C. Valen, D. Trotier, K. Doving, *Neuroscience* **2003**, *119*, 193.

6. J. Goedhart, T.W. J. Gadella, Jr., *Biochemistry* **2004**, *43*, 4263.

7. C. P. Salerno, D. Magde, A. P. Patron, *J. Org. Chem*. **2000**, 65, 3971.

8. S. Yagai, T. Karatsu, A. Kitamura, *Chem. Eur. J.* **2005**, *11*, 4054.

9. J. C. Cruz, M. Thomas, E. Wong, N. Ohgami, S. Sugii, T. Curphey, C. C. Y. Chang, T.-Y. Chang, *J. Lipid Res*. **2002**, *43*, 1341.

10. J. H. Kaplan, B. Forbush III, J. F. Hoffman, *Biochemistry* **1978**, *17*, 1929.

11. M. Goeldner, R. Givens, *Dynamic Studies in Biology*, Wiley-VCH, Weinheim, **2005**.

12. G. Marriott, *Methods in Enzymology*, Vol. *291*, Academic Press, San Diego, **1998**.

13. S. R. Adams, R. Y. Tsien, *Annu. Rev. Physiol*. **1993**, *55*, 755.

15. K. R. Gee, R. Wieboldt, G. P. Hess, *Proc. Natl. Acad. Sci. U. S. A.*, **1994**, *91*, 8752.

16. D. D. Young, A. Deiters, *Bioorg. Med. Chem. Lett*., **2006**, *16*, 2658.
17. T. Furuta, M. Iwamura, *Methods Enzymol*. **1998**, *291*, 50.
18. T. Furuta, S. S. H. Wang, J. L. Dantzker, T. M. Dore, W. J. Bybee, E. M. Callaway,W. Denk, R. Y. Tsien, *Proc. Natl. Acad. Sci. USA* **1999**, *96*, 1193.
19. R. S. Givens, C.-H. Park, Tetrahedron Lett. **1997**, *37*, 6259.
20. J. W. Wootton, D. R. Trentham, *NATO ASI Ser., Ser. C* **1989**, *272*, 277.
21. D. L. Pettit, S. S.-H. Wang, K. R. Gee, G. J. Augustine, *Neuron* **1997**, *19*, 465.
22. K. R. Gee, L. W. Kueper, J. Barnes, G. Dudley, R. S. Givens, *J. Org. Chem.* **1996**, *61*, 1228.
23. H. J. Montgomery, B. Perdicakis, D. Fishlock, G. A. Lajoie, E.Jervis, J. G. Guillemette, *Bioorg. Med. Chem*. **2002**, *10*, 1919.
24. B. Perdicakis, H. J. Montgomery, G. L. Abbott, D. Fishlock, G. A. Lajoie, J. G. Guillemette, E. Jervis, *Bioorg. Med. Chem*. **2005**, *13*, 47.
25. F. G. Cruz, J. T. Koh, K. H. Link, *J. Am. Chem. Soc.* **2000**, *122*, 8777.
26. D. D. Young, M. O. Lively, A. Deiters, *J. Am. Chem. Soc.* **2010**, *132* , 6183.
27. A. Blanc, C. G. Bochet, *J. Org. Chem*. **2003**, *68*, 1138 – 1141.
28. S. R. Adams, J. P. Y. J. Kao, R. Y. Tsien, *J. Am. Chem. Soc*. **1989**, *111*, 7957.
29. P. E. Dawson, S. B. H. Kent, *Annu. Rev. Biochem*. **2000**, *69*, 923.
30. N. Kotzur, B. Briand, M. Beyermann, V. Hagen *Chem. Commun*. **2009**, *172*, 3255.
31. A. Barth, S. R. Martin, J. E. T. Corrie, *Photochem. Photobiol. Sci*. **2006**, *5*, 107.
32. A. J. DeGraw, M. A. Hast, J. Xu, D. Mullen, L. S. Beese, G. Barany, M. D. Distefano, *Chem. Biol. Drug. Des*. **2008**, *72*, 171.

33. M. Ghosh, I. Ichetovkin, X. Song, J. S. Condeelis, D. S. Lawrence *J. Am. Chem. Soc.* **2002**, *124*, 2440.
34. C.-Y. Chang, T. Fernandez, R. Panchal, H. Bayley, *J. Am. Chem. Soc*. **1998**, *120*, 7661.
35. V. Hagen, B. Dekowski, N. Kotzur, R. Lechler, B. Wiesner, B. Briand, M. Beyermann *Chem. Eur. J.* **2008**, *14*, 1621.
36. N. Kotzur, B. Briand, M. Beyermann, and V. Hagen, *J. Am. Chem. Soc.* **2009**, *131*, 16927.
37. G. Arabaci, X.-C. Guo, K. D. Beebe, K. M. Coggeshall, D. Pei, *J. Am. Chem. Soc*. **1999**, *121*, 5085.
38. A. Specht, S. Loudwig, L. Peng, M. Goeldner, *Tetrahedron Lett.* **2002**, *43*, 8947.
39. M. C. Pirrung, J.-C. Bradley, *J. Org. Chem*. **1995**, *60*, 1116.
40. P. B. Jones, M. P. Pollastri, N. A. Porter, *J. Org. Chem*. **1996**, *61*, 9455.
41. A. P. Pelliccioli, J. Wirz, *Photochem. Photobiol. Sci.* **2002**, *1*, 441.
42. R. S. Givens, P. G. Conrad, II, A. L. Yousef, J.-I. Lee, *CRC Handb. Org. Photochem. Photobiol. (2nd Ed.)* **2004**, 691.
43. G. Mayer, A. Heckel, *Angew. Chem., Int. Ed.* **2006**, *45*, 4900.
44. G. C. R. Ellis-Davies, *Nat. Methods* **2007**, *4*, 619.
45. H.-M. Lee, D. R. Larson, D. S. Lawrence, *ACS Chem. Biol.* **2009**, *4*, 409.
46. A. Specht, F. Bolze, Z. Omran, J.-F. Nicoud, M. Goeldner, *HFSP J.* **2009**, *3*, 255.
47. C. W. Riggsbee, A. Deiters, *Trends Biotechnol.* **2010**, *28*, 468.
48. I. Schlichting, S. C. Almo, G. Rapp, K. Wilson, K. Petratos, A. Lentfer, A. Wittinghofer, W. Kabsch, E. F. Pai, et al., *Nature* **1990**, *345*, 309.
49. V. Hagen, J. Bendig, S. Frings, B. Wiesner, B. Schade, S. Helm, D. Lorenz, U. B. Kaupp, *J. Photochem. Photobiol., B* **1999**, *53*, 91.
50. D. D. Young, A. Deiters, *Angew. Chem., Int. Ed.* **2007**, *46*, 4290.
51. H. Li, J.-M. Hah, D. S. Lawrence, *J. Am. Chem. Soc.* **2008**, *130*, 10474.
52. A. Hall, *Current Opinion in Cell Biology* **1993**, *5*, 265.
53. P. J. Casey, P. A. Solski, C. J. Der, J. E. Buss, *Proc. Nat. Acad. Sci. U.S.A.* **1989**, *86*, 8323.
54. F. L. Zhang, P. J. Casey, *Annu. Rev. Biochem.* **1996**, *65*, 241.

55. N. E. Kohl, C. A. Omer, M. W. Conner, N. J. Anthony, J. P. Davide, S. J. deSolms, E. A. Giuliani, R. P. Gomez, S. L. Graham, K. Hamilton, *Nat Med* **1995**, *1*, 792.

56. L. Sepp-Lorenzino, Z. Ma, E. Rands, N. E. Kohl, J. B. Gibbs, A. Oliff, N. Rosen, *Cancer Res.* **1995**, *55*, 5302.

57. M. H. Gelb, L. Brunsveld, C. A. Hycyna, S. Michaelis, F. Tamanoi, W. C. Van Voorhis, H. Waldmann, *Nat. Chem. Biol.* **2006**, *2*, 518.

58. J. B. Gibbs, A. Oliff, N. E. Kohl, *Cell* **1994**, *77*, 175.

59. R. A. Gibbs, *Curr. Opin. Drug Discovery Dev.* **2000**, *3*, 585.

60. M. Schlitzer, M. Bohm, I. Sattler, H. M. Dahse, *Bioorg. Med. Chem.* **2000**, *8*, 1991.

61. S. M. Sebti, A. D. Hamilton, *Oncogene* **2000**, *19*, 6584.

62. R. J. Doll, P. Kirschmeier, W. R. Bishop, *Curr. Opin. Drug. Disc. Devel.* **2004**, *7*, 478.

63. S. F. Sousa, P. A. Fernandes, M. J. Ramos, *Curr. Med. Chem.* **2008**, *15*, 1478.

64. C. L. Strickland, W. T. Windsor, R. Syto, L. Wang, R. Bond, Z. Wu, J. Schwartz, H. V. Le, L. S. Beese, P. C. Weber, *Biochemistry* **1998**, *37*, 16601.

65. S. B. Long, P. J. Hancock, A. M. Kral, H. W. Hellinga, L. S. Beese, *Proc. Nat. Acad. Sci. USA* **2001**, *98*, 12948.

66. D. B. Rozema, S. T. Phillips, C. D. Poulter, *Org. Lett.* **1999**, *1*, 815.

67. C.-C. Huang, P. J. Casey, C. A. Fierke, *J. Biol. Chem.* **1997**, *272*, 20.

68. O. D. Fedoryak, T. M. Dore, *Org. Lett.* **2002**, *4*, 3419.

69. Y. Zhu, C. M. Pavlos, J. P. Toscano, T. M. Dore, *J. Am. Chem. Soc.* **2006**, *128*, 4267.

70. N. Kotzur, B. Briand, M. Beyermann, V. Hagen, *J. Am. Chem. Soc.* **2009**, *131*, 16927.

71. W. M. Kwok, H.-Y. An, C. Ma, A. C. Rea, J. L. Nganga, Y. Zhu, T. M. Dore, D. L. Phillips, *J. Phys. Chem. B* **2010**, Submitted.

72. J. B. Gibbs, D. L. Pompliano, S. D. Mosser, E. Rands, R. B. Lingham, S. B. Singh, E. M. Scolnick, N. E. Kohl, A. Oliff, *J. Biol. Chem.* **1993**, *268*, 7617.

73. N. E. Kohl, K. S. Koblan, C. A. Omer, A. Oliff, J. B. Gibbs, *Methods Mol. Biol.* **1998**, *84*, 283.
74. S. Kraus, R. Seger, *Methods Mol. Biol.* **2004**, *250*, 29.
75. E. Choy, V. K. Chiu, J. Silletti, M. Feoktistov, T. Morimoto, D. Michaelson, I. E. Ivanov, M. R. Philips, *Cell* **1999**, *98*, 69.
76. D. P. Walsh, Y.-T. Chang, *Chem. Rev.* **2006**, *106*, 2476.
77. X. Ouyang, J. K. Chen, *Chem. Biol.* **2010**, *17*, 590.
78. D. F. Underwood, D. A. Blank, *J. Phys. Chem. A* **2003**, *107*, 956.
79. A. Patchornik, B. Amit, R. B. Woodward, *J. Am. Chem. Soc*. **1970**, *92*, 6333.
80. K. Curley, D. S. Lawrence, *Pharmacol. Ther*. **1999**, *82*, 347.
81. G. Dorman, G. D. Prestwich, *Trends Biotechnol*. **2000**, *18*, 64.
82. C. G. J. Bochet, *J. Chem. Soc., Perkin Trans*. **2002**, *1*, 125.
83. C. Chou, D. D. Young, A. Deiters, *ChemBioChem* **2010**, *11*, 972.
84. E. Fino, R. Araya, D. S. Peterka, M. Salierno, R. Etchenique, R. Yuste, *Frontiers in Neural Circuits* **2009**, *3*, 1.
85. J. Downward, *Nat. Rev. Cancer* **2003**, *1*, 11.
86. T. M. Dore, Y. Zhu, K. G. Reddie, J. D. Lauderdale, (University of Georgia Research Foundation, Inc., USA). Application: US, **2010**, p. 46pp.
87. M. C. Pirrung, *Chem. Rev.* **1997**, *97*, 473-488.
88. S. Singh-Gasson, R. D. Green, Y. Yue, C. Nelson, F. Blattner, M. R. Sussman, F. Cerrina, *Nature Biotech*. **1999**, *17*, 974-978.
89. F. Guillier, D. Orain, M. Bradley, *Chem. Rev*. **2000**, *100*, 2091-2157.
90. G. Marriott, Ed. *Caged Compounds*; Academic Press: New York, 1998; Vol. 291.
91. J. E. T. Corrie, D. R. Trentham, In *Biological Applications of Photochemical Switches*; H. Morrison, Ed.; John Wiley & Sons: New York, 1993; pp 243-305.
92. J. M. Nerbonne, *Curr. Op. Neurobiol.* **1996**, *6*, 379-386.

93. W. T. Monroe, M. M. McQuain, M. S. Chang, J. S. Alexander, F. R. Haselton, *J. Biol. Chem.* **1999**, *274*, 20895-20900.

94. T. Furuta, H. Takeuchi, M. Isozaki, Y. Takahashi, M. Kanehara, M. Sugimoto, T. Watanabe, K. Noguchi, T. M. Dore, T. Kurahashi, M. Iwamura, R. Y. Tsien, *ChemBioChem* **2004**, *5*, 1119-1128.

95. S. Kantevari, M. Matsuzaki, Y. Kanemoto, H. Kasai, G. C. R. Ellis-Davies, *Nature Methods* **2009**, *7*, 123-125.

96. J. Ohkanda, D. B. Knowles, M. A. Blaskovich, S. M. Sebti, A. D. Hamilton, *Curr Top Med Chem* **2002**, *2*, 303-323.

97. J. H. Wosnick, M. S. Shoichet, *Chem. Matter.* **2008**, *20*, 55-60.

98. N. Kotzur, B. Briand, M. Beyermann, V. J. Hagen, *J. Am. Chem. Soc.* **2009**, *131*, 16927-16931.

99. M. A. Morgan, A. Ganser, C.W. M. Reuter, *Curr. Drug Targets*, **2007**, *8*, 217.

100. D. B. Whyte, P. Kirschmeier, T. N. Hockenberry, *J. Biol. Chem*. **1997**, *272* , 14459.

101. N. M. G. M. Appels, J. H. Beijnen, J. H. M. Schellens, *The Oncologist* **2005**, *10*, 565.

102. Y. Qian, A. Vogt, A. Vasudevan, S. M. Sebti, A. D. Hamilton, *Bioorg. Med. Chem.* **1998**, *6*, 293.

103. K. M. Swanson, R. J. Hohl, *Curr. Cancer Drug Targets*, **2006**, *6*, 15.

104. E. C. Lerner, Y. Qian, A. D. Hamilton, S. M. Sebti, *J. Biol. Chem.* **1995**, *270*, 26770.